NONLINEAR RESPONSE AND STABILITY ANALYSIS OF VESSEL ROLLING MOTION IN RANDOM WAVES USING STOCHASTIC DYNAMICAL SYSTEMS

A Dissertation

by

ZHIYONG SU

Submitted to the Office of Graduate Studies of
Texas A&M University
in partial fulfillment of the requirements for the degree of

DOCTOR OF PHILOSOPHY

August 2012

Major Subject: Ocean Engineering

NONLINEAR RESPONSE AND STABILITY ANALYSIS OF VESSEL ROLLING MOTION IN RANDOM WAVES USING STOCHASTIC DYNAMICAL SYSTEMS

A Dissertation

by

ZHIYONG SU

Submitted to the Office of Graduate Studies of
Texas A&M University
in partial fulfillment of the requirements for the degree of

DOCTOR OF PHILOSOPHY

Approved by:

Chair of Committee, Jeffrey M. Falzarano
Committee members, Loren D. Lutes
Richard Mercier
Moo-Hyun Kim
Alan Palazzolo
Head of Department, John Niedzwecki

August 2012

Major Subject: Ocean Engineering

ABSTRACT

Nonlinear Response and Stability Analysis of Vessel Rolling Motion in Random Waves Using Stochastic Dynamical Systems. (August 2012)

Zhiyong Su, B.S.; M.S., Shanghai Jiao Tong University

Chair of Advisory Committee: Dr. Jeffrey M. Falzarano

Response and stability of vessel rolling motion with strongly nonlinear softening stiffness will be studied in this dissertation using the methods of stochastic dynamical systems. As one of the most classic stability failure modes of vessel dynamics, large amplitude rolling motion in random beam waves has been studied in the past decades by many different research groups. Due to the strongly nonlinear softening stiffness and the stochastic excitation, there is still no general approach to predict the large amplitude rolling response and capsizing phenomena. We studied the rolling problem respectively using the shaping filter technique, stochastic averaging of the energy envelope and the stochastic Melnikov function. The shaping filter technique introduces some additional Gaussian filter variables to transform Gaussian white noise to colored noise in order to satisfy the Markov properties. In addition, we developed an automatic cumulant neglect tool to predict the response of the high dimensional dynamical system with higher order neglect. However, if the system has any jump phenomena, the cumulant neglect method may fail to predict the true response. The stochastic averaging of the energy envelope

and the Melnikov function both have been applied to the rolling problem before, it is our first attempt to apply both approaches to the same vessel and compare their efficiency and capability. The inverse of the mean first passage time based on Markov theory and rate of phase space flux based on the stochastic Melnikov function are defined as two different, but analogous capsizing criteria. The effects of linear and nonlinear damping and wave characteristic frequency are studied to compare these two criteria. Further investigation of the relationship between the Markov and Melnikov based method is needed to explain the difference and similarity between the two capsizing criteria.

ACKNOWLEDGMENTS

I firstly would like to express my sincere gratitude and special thanks to my advisor, Dr. Jeffrey Falzarano. This dissertation can never been done without his support, encouragement and guidance during my studies at Texas A&M University. I also would like to thank Dr. Loren Lutes for his continuous communication, discussions and support which always lead me to the right research direction. I greatly appreciate Dr. Mercier, Dr. Kim, and Dr. Palazzolo for their review and comments for my research topics and serving as committee members.

I am grateful to the librarians in the university library, for helping me get any research papers, reports and books around the world using "Get it for me" service.

The work has been funded by the Office of Naval Research (ONR) T-Craft Tools development program ONR Grant N00014-07-1-1067. I would like to thank the program manager Kelly Cooper for her support.

Lastly, and most importantly, I would like to thank my parents and all other family members for their continuous support and trust. Special thanks are expressed to my wife, Yusha, for her love, optimism, sacrifices and the wonderful gift, our baby girl.

TABLE OF CONTENTS

LIST OF FIGURES

LIST OF TABLES

CHAPTER I

INTRODUCTION

Static and Dynamic stability is one the most important safety features when designing floating offshore structures, especially for ship shaped structures. Insufficient stability could lead to large amplitude rolling motion or even capsizing. GM based static stability criterion were first developed back to nineteen century (Moseley, 1850), and this approach was further refined by Rahola in 1939 (Rahola, 1939). The first international intact stability resolutions IMO A.167 were approved by IMO in 1968 for ships less than 100m; this criterion was mostly based on Rahola's work (Rahola, 1939). The IMO intact stability (IS) code has been revised several times through the 1960s to now, but all of these codes are still based on the righting arm curve (GZ curve) in the calm water. The reason why dynamic stability has not been applied in the IS code is the difficulty of the nonlinear large amplitude rolling motion with the stochastic and probabilistic approach has not been applied completely and satisfactory. The numerical simulation in the time domain and model testing provides possible alternative ways to approach this complex stochastic failure event. However, both methods are not easy to apply and also require significant time and cost. Both numerical simulation and model testing are excellent for estimating structure response, but not for stability or long term

---

This dissertation follows the style and format of Ocean Engineering.

failure prediction. As the vessel capsizing failure is such a very rare event, analytical methods are still the most needed technique, which provides quick and accurate estimation of the system stability or failure. At present, International Maritime Organization (IMO) is working on the new regulations of intact stability based on the stochastic and probabilistic approach with dynamic effect. The sub-committee on Stability, Load Lines and on Fishing Vessels (SLF) of IMO is discussing the next generation of stability criterion during recent SLF meetings (SLF50/4, 2006; SLF51/4, 2008; SLF52/3, 2009) and proposed four main intact stability failure modes.

- Dead Ship Condition, i.e. ship without speed, exposed to environment
- Pure-loss of Stability
- Parametric Roll
- Surf-riding and Broaching to

Physical phenomena of the above failure modes are complex nonlinear dynamics. For research convenience and simplicity, all of the above dynamical motions are modeled as a single degree freedom system after decoupling from the other modes with some appropriate assumptions. Before studying vessel stability, it is necessary to explain the definition of an intact stability failure first. Basically, there are two types of intact stability failure as per the SLF documents, 1) Total Intact Stability failure - total loss of the vessel, which may be additionally combined with the loss of the lives. 2) Partial intact stability failure - the partial loss of the vessel's operational capabilities combined with the additional potential danger for people as well as for cargo and equipment. Capsizing is defined as the total intact stability failure and the capsizing is a

very rare event. Most capsizing accidents are related to the large angle rolling that leads to green water on deck or equipment shift. Large angle rolling is defined as the partial intact stability failure, which will not lead to capsizing. Only Dead Ship Condition with random beam waves will be considered in this dissertation.

1.1 Physical Fundamentals of Vessel Dynamics

The equations of motion describing a floating rigid body are nonlinear and coupled. The six degree of freedom equations of motion have been derived in variety of references (Abkowitz, 1969; Falzarano, 1990; Lewandowski, 2004). These Euler's equations of motions are as follows, derivations can be found in the Appendix A:

$$X = m[\dot{u} + qw - rv - x_G(q^2 + r^2) + z_G(pr + \dot{q})] \tag{1.1}$$

$$Y = m[\dot{v} + ru - pw + x_G(pq + \dot{r}) + z_G(qr - \dot{p})] \tag{1.2}$$

$$Z = m[\dot{w} + pv - qu + x_G(rp - \dot{q}) - z_G(p^2 + q^2)] \tag{1.3}$$

$$\begin{aligned} K = {} & I_{44}\dot{p} - (I_{55} - I_{66})qr - I_{64}(\dot{r} + pq) \\ & - mz_G(\dot{v} + ru - pw) \end{aligned} \tag{1.4}$$

$$\begin{aligned} M = {} & I_{55}\dot{q} - (I_{66} - I_{44})rp - I_{64}(r^2 - p^2) \\ & + mz_G(\dot{u} + qw - rv) - mx_G(\dot{w} + pv - qu) \end{aligned} \tag{1.5}$$

$$\begin{aligned} N = {} & I_{66}\dot{r} - (I_{44} - I_{55})pq - I_{64}(\dot{p} - qr) \\ & - mx_G(\dot{v} + ru - pw) \end{aligned} \tag{1.6}$$

where m is the mass of the ship, I_{44}, I_{55}, I_{66} and I_{64} are the moments and cross products of inertia in the body fixed system, which always put its origin at the mid-ship and design waterline, the subscripts represent respectively: 4=roll, 5=pitch, 6=yaw. u, v, w

are the velocity of the translational motions, surge, sway and heave; p q r are the angular velocity of the rotational motions, roll, pitch and yaw. x_G and z_G are the coordinates of ship center of gravity in the body fixed system. X, Y, Z, K, M, N are applied force and moments in the body fixed system, representing the hydrodynamic and hydrostatic forces and moments. The total hydrodynamic and static forces are assumed as the summation of various components: including Froude-Krylov forces, diffraction forces, and radiation forces, viscous nonlinear damping force and hydrostatic restoring force. These coupled nonlinear equations are difficult if not impossible to get analytical solution to, so approximation and assumption must be made for any real progress. Considering small motions, the Euler's equations of motions of equations (1.1) to (1.6) could be linearized to drop the nonlinear inertial terms. Following the derivations of Vugts (Vugts, 1970), the linearized equations of motions are as follows:

$$X = m[\dot{u} + z_G \dot{q}] \tag{1.7}$$

$$Y = m[\dot{v} + x_G \dot{r} - z_G \dot{p}] \tag{1.8}$$

$$Z = m[\dot{w} - x_G \dot{q}] \tag{1.9}$$

$$K = I_{44}\dot{p} - I_{64}\dot{r} - m z_G \dot{v} \tag{1.10}$$

$$M = I_{44}\dot{q} + m(z_G \dot{u} - x_G \dot{w}) \tag{1.11}$$

$$N = I_{66}\dot{r} - I_{64}\dot{p} + m x_G \dot{v} \tag{1.12}$$

Due to the port and starboard symmetry, the linearized equations have no inertial coupling terms between longitudinal (surge, heave and pitch) and lateral (sway, roll and yaw) modes. In order to better understand the complicated nonlinear dynamics of vessel

rolling motion, it is necessary to decouple the rolling mode from the other six degrees of freedom linearized equations.

In this dissertation, we consider beam waves only, so the yaw mode motion is small and negligible when considering the ship is fore-aft symmetric approximately, and therefore only the coupling between the sway and roll is considered. The linear two degree of freedom equations describing roll and sway:

$$\begin{bmatrix} m & -mz_G \\ -mz_G & I_{44} \end{bmatrix} \begin{bmatrix} \ddot{y} \\ \ddot{\phi} \end{bmatrix} = \begin{bmatrix} Y \\ K \end{bmatrix} \tag{1.13}$$

where y is the sway displacement and ϕ is the roll angle; $\dot{y} = v$ and $\dot{\phi} = p$; Note that the mass and moment inertial term m and I_{44} could also include the virtual mass and inertial. It is possible to find a new coordinate system that could remove the coupling term in the above equation. The two equations can be solved independently after the decoupling. The new coordinates are called principal coordinates or normal coordinates. Let us assume the distance between the new coordinate system x_N - y_N and the original system x - y is R_c . From the rigid body dynamics displayed in the Fig. 1, the relation involving the acceleration of the points on the body are given by below,

$$\begin{cases} \ddot{y} = \ddot{y}_N + R_c \ddot{\phi}_N \\ \ddot{\phi} = \ddot{\phi}_N \end{cases} \tag{1.14}$$

We also need to replace the forces and moments with equivalent force and moment in the new coordinate system,

$$\begin{cases} Y = Y_N \\ K = K_N - mR_c Y \end{cases} \tag{1.15}$$

By substituting the equations (1.14) and (1.15) back into (1.13), we get the decoupled equations with $R_c = z_G$,

$$\begin{bmatrix} m & 0 \\ 0 & I_{44N} \end{bmatrix} \begin{bmatrix} \ddot{y}_N \\ \ddot{\phi}_N \end{bmatrix} = \begin{bmatrix} Y_N \\ K_N \end{bmatrix} \tag{1.16}$$

where $I_{44N} = I_{44} - mz_G^2$;

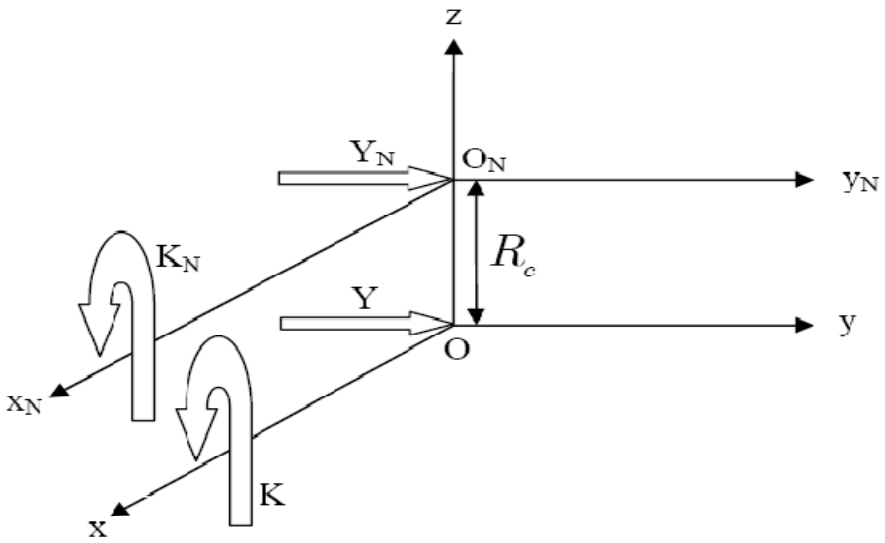

Fig. 1. Body fixed coordinate system x-y and principal system x_N - y_N

The decoupled single degree freedom roll equation (Lewis et al., 1989) is considered in this dissertation for response and stability analysis,

$$(I_{44N} + A_{44}(\omega))\ddot{\phi} + B_{44}(\omega)\dot{\phi} + B_{44q}(\omega)\dot{\phi}\left|\dot{\phi}\right| + \Delta(C_1\phi + C_3\phi^3 + ..) = f(t) \quad (1.17)$$

Linear added mass $A_{44}(\omega)$ and added damping $B_{44}(\omega)$ coefficients are from linear potential theory, which can be calculated by many hydrodynamic program, e.g., Strip Theory based SHIPMO (Beck and Troesch, 1990), or Three-Dimensional panel based WAMIT (Lee and Newman, 2009), AQWA (ANSYS, 2010), and MOSES (Ultramarine, 2010). We will use I_{44} to replace the notation I_{44N} in this dissertation for convenience. The constant Δ is the displacement of the vessel and C_1, C_3 are the linear and cubic nonlinear stiffness coefficients. B_{44q} is the quadratic viscous damping coefficients for roll motion, which is determined on a component basis (Falzarano, 1990) and is redefined and incorporated into SHIPMO. f is the external moment from wave excitation. The moment term in this dissertation is limited to linear excitation due to the limitation of available hydrodynamic code SHIPMO. However, the nonlinear part of the hydrodynamic force could also be considered for the large amplitude rolling motion (Kim, 2008). The damping moment, stiffness moment and external moment are part of K_N in equation (1.16). How to calculate the hydrodynamic forces and how to analyze the rigid body dynamics are the two major problems when studying the rolling motions.

1.2 Discussion of Intact Stability Failures Modes

The simplified and decoupled equation (1.17) is the generalized rolling math model. Based on the simple rolling model, the math modes for failure modes are described differently.

According to (Belenky et al., 2008), Pure-loss of stability and Parametric Roll both related to the variation of the restoring moment in waves. The restoring moment becomes larger in the wave trough and smaller on the wave crest due to the variation of hull geometry underwater. When the ship is sailing in the following or head seas and the wave length is comparable to the ship length, the variation of GZ is most evident. Pure loss of stability in waves means when the vessel spends enough time on the wave crest in the following or quartering waves, the stability becomes smaller and less than the heeling moments and then the vessel may experience capsize or large amplitude angle motion. Parametric roll or parametric roll resonance is a result of periodic changes of stability at some frequency related to the natural frequency of the rolling motion. The major approach researching parametric rolling is Mathieu equation and related Ince-Strutt diagram, which is a common approach in nonlinear dynamics to predict the stable and unstable zone for given parameters. Broaching to is also defined as a mode of intact stability failure, which is related to the maneuvering problem: surf-riding. Instead of researching the decoupled rolling equation for parametric rolling, the nonlinear math model for broaching is surge mode equation with resistance force and propeller force.

The most classic stability failure mode is considering the beam waves with constant restoring moment, the so called “Dead Ship Condition”. When a ship engine loses power during operation, the environment will turn the ship to the beam seas condition. How to analyze the vessel rolling dynamics in the beam waves is the main purpose of this dissertation. When considering regular beam wave excitation and neglecting the wind excitation, equation (1.17) with constant added mass, damping and

stiffness coefficients is a widely accepted mathematical model for large amplitude rolling motion or capsizing research. However, it has to be noted that the wave force is a stochastic or random process, which means the wave excitation cannot be modeled as a regular input and the time invariant system is questionable. For a single harmonic excitation, added mass and linear damping takes values at the input wave frequency. For excitation with narrow banded excitation, the values may be evaluated at the peak frequency of the input excitation. For wide band excitation, the values at the natural frequency may be a better approximation (Jiang et al., 2000).

Alternatively, the time domain model can overcome the variation of hydrodynamic coefficients in the frequency domain. Following (Ogilvie, 1964), the time domain ship rolling model that describes the realistic response in random waves is given as following with convolution integral:

$$\begin{aligned}&(I_{44}+A_{44}(\infty))\ddot{\phi}+\int_0^t K(t-\tau)\dot{\phi}(\tau)d\tau\\&+B_{44q}\dot{\phi}\left|\dot{\phi}\right|+\Delta(C_1\phi+C_3\phi^3+..)=f(t)\end{aligned} \tag{1.18}$$

where $A_{44}(\infty)$ is the added mass coefficient at infinite frequency, $K(t-\tau)$ is the retardation function or impulse response function (IRF) of velocity, which is determined by the geometry of the ship hull. The IRF and the frequency domain hydrodynamic coefficients are related by cosine or sine transform, see e.g. (Cummins, 1962; Ogilvie, 1964). The quadratic damping term B_{44q} is usually treated as approximately constant and independent of frequency.

The time domain equation (1.18) gives a more accurate representation of the dead ship condition stability model compared with the constant coefficients model equation

(1.17) for the study of rolling stability in random beam waves. However, the convolution integral also introduces additional difficulties when using traditional methods of stochastic dynamical system. The final goal of the rolling stability in the dead ship condition is to analytically calculate the response and the capsizing probability based on the decoupled time domain math model. As an initial stage research, we will first focus on the constant coefficients model.

1.3 Literature Review

Research on motions or dynamics of ships and offshore structures in random seas has been studied over the century. It is important to study the highly nonlinear large amplitude rolling motion of ship shaped structures, due to the its strong effect on the stability and safety, or even capsizing. Basically, there are two major obstacles to completely understand the highly nonlinear dynamics of offshore structures: hydrodynamic force computation and rigid body dynamics. The coefficients for the equations of rigid body dynamics and force excitation are determined from the hydrodynamics computations. Most current time domain commercial software for motion predications are based on numerical simulation of dynamical system after first determining the hydrodynamics coefficients. When considering the nonlinear effects on motions, e.g. nonlinear damping, nonlinear restoring force, or nonlinear excitation, etc; people have to be cautious when applying the direct numerical simulation, especially when the nonlinear effect is strong. Analytical methods are still the most needed

technique for understanding the nonlinear behavior of vessel motions, like the typical vessel rolling analysis.

Mathematical research models for vessel dynamics include both coupled multi degrees of freedom (Falzarano and Zhang, 1993; Zhang and Falzarano, 1994; Spyrou, 1996a; Spyrou, 1996b; Spyrou, 1997; Ibrahim and Grace, 2010) and also decoupled single degree freedom of system, especially rolling motion (Roberts, 1982; Roberts, 1982; Roberts and Spanos, 1986; Falzarano, 1990; Falzarano et al., 1992; Lin and Yim, 1995; Roberts and Vasta, 2000; Francescutto and Naito, 2004; Jamnongpipatkul et al., 2011; Su and Falzarano, 2011). Rolling motion is nonlinear and coupled with the other modes of motions: sway, yaw and pitch, etc. It is reasonable to model the rolling motion as a single degree of freedom equation (SDOF) in two special cases: one is the ship rolling in unidirectional head or following seas, which will lead to parametric rolling analysis using popular Mathieu chart or Hill chart. The other one is the ship rolling in unidirectional beam seas at low or zero speed, provided that we consider the coordinate origin to be located at a pseudo 'roll center' (Roberts and Vasta, 2000).

Analytical studies of rolling motion under beam sea were first initiated by Froude (Froude, 1861), he derived the SDOF rolling equation including nonlinear damping and restoring moment terms. Nonlinear terms in the roll equation may lead to very complicated behavior of the ship rolling response. Stability is the most important issue for naval architects and ocean engineers. Traditionally, the only static intact stability is considered for practical design purpose. More and more researchers have found that hydrodynamic induced damping, wave exciting force, initial conditions and green water

on deck are also important to ship stability. Due to the nonlinearity of the damping and stiffness, we are unable to find the analytical solution for even the single degree freedom system of the general second order ordinary differential equation, even when the excitation force is only harmonic.

The response of nonlinear rolling motion in regular waves is a nonlinear dynamics problem with harmonic excitation, which may generate super harmonic, sub harmonic (Cardo, 1981; Cardo et al., 1984),or even chaos phenomena (Thompson, 1990; Thompson, 1992). Cardo and Francescutto applied harmonic excitation to the SDOF rolling motion and investigated three different mechanisms for the onset of super and sub harmonics phenomenon. Thompson (Thompson, 1990) proposed the conception of safe basin and basin erosion with harmonic direct and parametric excitation and introduced that the transient motions induced capsize should be paid more attention than steady state conditions. Different initial conditions under harmonic excitation will be attracted to different steady state oscillations or divergent solutions. The safe basin is defined as the area of initial conditions which are attracted to the bounded steady state solutions. With the increasing direct or parametric excitation, the erosion of safe basin will reduce the safe area significantly. Also the frequency of excitation close to the natural frequency of rolling is found to be the worst excitation scenario. Virgin (Virgin, 1987) studied the chaotic rolling motions in regular beam waves for SDOF rolling model using a semi empirical roll model. Qualitative prediction techniques for the possibility of capsizing were utilized using dynamical system theory. Nayfeh (Nayfeh, 1986a;

Nayfeh, 1986b; Nayfeh, 1990) applied Floquet and bifurcation theory to study the local stability of the dynamical system with steady state solutions.

It is more accurate to consider the randomness of the excitation force than just considering harmonic force for vessel motions in realistic waves. How to understand the possibility of capsizing of ships in realistic waves is a very challenging research topic even only considering the SDOF rolling model. The math model for the SDOF rolling model with random forces is a nonlinear random vibration problem. Many different research groups have made contributions to analyzing the rolling stability in the sense of random waves. Roberts (Roberts, 1982; Roberts, 1982; Roberts and Spanos, 1986; Roberts et al., 1994; Roberts and Vasta, 2000) have studied the rolling problem for more than two decades using stochastic averaging technique. By modeling the energy envelope of system response as a continuous Markov process, the one dimensional energy process satisfies the Fokker Planck Equation, which will be introduced in the next chapter. The drift and diffusion coefficients could be evaluated by the two state variable rolling equation's system parameters. The issue of the stochastic averaging of the energy envelope is limited to the light damping. However, the statistics of first passage time to approach the critical boundary can be evaluated from the one dimensional Markov process and the associated Fokker Planck Equation.

Since the rolling response satisfies the Fokker Planck Equation, which is a partial differential equation (PDE), many researchers also have contributed to numerically solving the PDE. The path integral method is the most popular numerical tool for the analysis of random rolling response. The research group of Yim (Lin and Yim, 1995;

Yim et al., 2005) first applied the path integral method to a harmonic plus white noise excited rolling system and then to a filtered white noise excited roll-heave coupled system. The application of the path integral method to the stochastic rolling process can be also found from different authors (Liqin and Yougang, 2007; Cottone et al., 2009; Jamnongpipatkul et al., 2011). Instead of the numerical solution, Francescutto (Francescutto and Naito, 2004) utilized moment equations to study a six dimensional stochastic system with four Gaussian filter variables using the Gaussian cumulant neglect method. The author investigated the effect of linear and nonlinear damping, and righting moment effect on the statistics of the rolling response. There is no limitation on the damping and force magnitudes for both moment equations and path integral methods. The difficulty for the filtered system is the high dimension, which is always to be avoided by researchers when dealing with stochastic systems.

Geometric methods have been applied to many nonlinear systems, especially to the nonlinear ship rolling model. Instead of directly studying the stochastic differential equation, the geometric methods try to analyze the problem in the sense of phase space for qualitative behavior. The Melnikov method was initially introduced into Naval Architecture by Falzarano (Falzarano, 1990; Falzarano et al., 1992) for harmonic excitations. And the conception of phase space flux rate with random excitation was applied to dynamical systems by Frey and Simiu (Frey and Simiu, 1993). Then the Michigan research group continued to extend the Melnikov method with stochastic excitation to large amplitude rolling motion with both constant coefficients (Hsieh et al., 1994) and a time domain memory included model (Jiang et al., 2000). The dynamical

system with memory or a convolution term is a high dimensional system when extending the convolution integral into a linear state space model (Holappa and Falzarano, 1999). High dimensional stochastic problems are difficult and challenging question in random vibration. Jiang successfully applied the Melnikov method to understand the stability of stochastic system without extending the convolution term to extended state space model. Considering periodic excitation with random white noise disturbance, Lin and Yim (Lin and Yim, 1995) developed a generalized Melnikov method to predict upper bound of potential chaotic roll motion and further capsizing possibility. Chen and Shaw (Chen, 1999) introduced a systematic approach to modeling multi degree freedom ship motions with regular excitation input. Bikdash (Bikdash et al., 1994) studied different damping models for rolling dynamics and derived a condition that linear-plus-cubic and linear-plus-quadratic model yields the same Melnikov predictions. Huang (Huang, 2003; Huang, 2004) presented the safe basin erosion in random waves with energy based Melnikov methods. He also considered the stochastic averaging method developed by Robert to relate the capsizing phenomena and Melnikov function. Wu (Wu and McCue, 2008) used the extended Melnikov method to two rolling model in regular seas without the constraint of small damping.

As the analytical methods for large amplitude rolling motion and capsizing analysis have to resort to many assumptions, e.g., decoupling, low damping, low excitation, constant hydrodynamics coefficients, etc, one of the possible solutions might be developing numerical simulation tool considering all nonlinear hydrodynamic effect. Belenky (Belenky and Sevastianov, 2007; Belenky et al., 2011) combining the analytical

method and Large Amplitude Motion Program (LAMP) to evaluate the probability of the rare event capsizing.

1.4 Methods and Procedure

When the vessel is excited by random beam waves, the response and capsizing problem are governed approximately by the single DOF dynamical system, equation (1.17). The most direct method to study the response and the stability of the rolling motion is the numerical simulation, or so called Monte Carlo simulation. As capsizing is such a rare event, the numerical simulation provides no improvement for the practical vessel design. Analytical methods are still the most needed technique for vessel rolling analysis. We will study three different methods to understand the rolling response and stability problems separately by,

- Increasing the dimension—Shaping filter technique
- Decreasing the dimension—Stochastic averaging of energy envelope
- Maintain the dimension—Melnikov Method

The fundamentals of stochastic dynamics are introduced in the Chapter II, with a focus on Brownian motion, Markov processes, stochastic differential equations, and the Fokker Planck Equation.

In Chapter III, the random excitation force is reproduced by using a linear filter, i.e., the so called shaping filter technique. This method introduces some additional Gaussian filter variables to transform the Gaussian white noise to colored noise in order to apply

the Markov properties. There is no limitation on the damping or excitation magnitude for the shaping filter technique. We will introduce the automatic cumulant neglect tool to analyze the statistical response of the high dimensional rolling model and also discuss the limitation of the cumulant neglect application to non Gaussian response.

In Chapter IV, the stochastic averaging of the energy of envelope decreases the two dimension rolling system to a one dimensional energy process, which satisfies the Markov process property under the small damping and excitation assumptions. Compared with the Markov method, the Melnikov method analyzes the rolling capsizing problem from the view of the phase space flux. This dissertation initially compares the efficiency, capacity and difference of the three methods and discusses their advantages and disadvantages respectively.

The work is summarized and future research directions are presented in Chapter V. Finally the derivation of nonlinear coupled equation of motion and stochastic averaging of energy envelope is given in the Appendix.

CHAPTER II

FUNDAMENTALS OF STOCHASTIC DYNAMICS

Probabilistic or stochastic domain methods, which are different from the traditional frequency domain and time domain method in the offshore industry, are getting more and more attentions in the modern analysis of dynamical system, especially when designing new concept structures with nonlinear aspects. The loading of marine structures due to wind and wave, are always stochastic in nature. Therefore the probabilistic or stochastic methods are important to accurately estimate the response. A major concern in stability problems is estimating the extreme values and the upcrossing rate, while the probability density function (PDF) of the response signal can give the superior results, if the response PDF is known accurately. The demand for precise estimation of the response has motivated research on nonlinear stochastic dynamical systems. In order to understand the whole probabilistic domain method, application for the analysis of the stochastic dynamical systems, we first introduce the fundamentals of stochastic dynamics.

2.1 Introduction to Stochastic Dynamics Systems

Stochastic dynamical systems or random dynamical systems are a theoretical formulation of a dynamical system with some elements of randomness or uncertainty. It consists of noise excitation and state variables. Analysis of stochastic dynamical systems

is a challenging field which has attracted many researchers for more than a century. The theory of stochastic dynamics in general began in the nineteenth century (Fuller, 1969), when physicists were trying to show that the heat in a medium is essentially a random motion of the molecules. Robert Maxwell (Maxwell, 1860; Maxwell, 1867) developed the steady state probability density function for the individual molecules. Later Ludwig Boltzmann (Boltzmann, 1868) generalized Maxwell's result to include the conservative force field. The probability density function given as an exponential function of total energy, which is known as Maxwell-Boltzmann distribution. They laid the foundation of stochastic dynamics, even the systems they considered were conservative and autonomous, and only initial conditions were random. Around the end of nineteenth century, Rayleigh (Rayleigh, 1880) was the first to treat a random walk in physics and obtained a partial differential equation for the probability density function of the displacement. Moreover, he applied a similar technique to the theory of gas and arrived at a PDE governing probability density function of the velocity of the gas molecules (Rayleigh, 1891). The PDE is the first example of what was later defined as the Fokker Planck Equation. Bachelier (Bachelier, 1900) obtained a simple Fokker Planck Equation describing the French stock exchange. Later (1910, 1912) he studied the gambler's ruin which led to a moderately general Fokker Planck equation. The work developed by Rayleigh and Bachelier have been largely unnoticed (Fuller, 1969).

In 1905, Albert Einstein (Einstein, 1905) brought the Maxwell-Boltzman theory and the random walk method together in a paper on Brownian motion. The definition of Brownian motion will be defined in the next section. Langevin interpreted the random

disturbances as an additional forcing function, which is the initiation of the stochastic differential equations (SDE). Fokker (Fokker, 1913; Fokker, 1914) treated a first order system with state dependent white noise. Planck (Planck, 1917) studied a n-th order system with state dependent white noise and also generalized Fokker's equation. And Kolmogorov (Kolmogoroff, 1931) made the Fokker Planck Equation more general and abstract. He also assumed the process to be a Markov process. FPE is also called Fokker Planck Kolmogorov (FPK) or Kolmogorov's second equation to honor his contribution. Additionally, he also named Kolmogorov's first equation, also known as backward Kolmogorov equation, which is adjoint of the second equation. In 1933, Kolmogorov (Kolmogorov, 1933) extended the theory to the vector process and also discussed the uniqueness of the solution of the FPE.

Other early useful references to understanding the progress and history of stochastic dynamics and the Fokker Planck Equation can be found in (Uhlenbeck and Ornstein, 1930; Wang and Uhlenbeck, 1945), (Caughey and Dienes, 1961; Caughey, 1963a)and (Crandall and Mark, 1963). Recent developments in the analysis of stochastic dynamics, are mostly based on the early development of Brownian motion. Analysis method for FPE and stochastic differential equations, include statistical linearization (Caughey, 1963b; Roberts and Spanos, 1990), statistical nonlinearization (Lutes, 1970), stochastic averaging (Roberts and Spanos, 1986; Zhu, 1988), moments closure, exponential polynomial closure method (Er, 1998), etc. More conclusive work can be found in classic textbooks (Soong and Grigoriu, 1993; To, 2000; Lutes and Sarkani, 2004; Ibrahim, 2007). Stochastic differential equations and FPE have been applied to many

engineering and science fields, such as particle physics, structural dynamics, aerodynamics, hydrodynamics, stock market, etc.

2.2 Brownian Motion and Markov Process

Brownian motion is named after an English botanist Robert Brown to describe the random drift of particles in a fluid or the mathematical model used to describe such random motions. In mathematics, Brownian motion B_t , also called Wiener Process in honor of Norbert Wiener, is characterized by following properties for the unit process;

- $B_0 = 0$
- B_t has independent increments with $dB = B_t - B_s \sim N(0, \sigma(t-s))$ for $0 \leq s \leq t$
- $E(B_t) = 0$, and $E(B_t, B_s) = \sigma^2 \min(t, s)$

$N(\mu, \sigma^2)$ denotes the Gaussian distribution with mean value μ and variance σ^2. E represents the expectation operation. The process is continuous everywhere but differential nowhere. Gaussian white noise W_t is defined as the increment of the Wiener process. From the property of the Wiener process, the increments are independent and Gaussian distributed. So variables W_t are uncorrelated for each time t. Hence the spectrum will be a flat curve, which means Gaussian 'white' noise. The mathematical relationship is given by:

$$dX_t = W_t dt = W(t)dt \tag{2.1}$$

$W(t)$ is Gaussian white noise, when numerically integrated the above equation, the response X_t is the Wiener process. Therefore we related the white noise and Wiener process by,

$$dB_t = W_t dt \tag{2.2}$$

Given a stationary Gaussian white noise with power spectrum density (PSD) s_0, $S_{WW}(\omega) = s_0$. The autocorrelation is given by,

$$R_{WW}(\tau) = 2\pi s_0 \delta(\tau) \tag{2.3}$$

where $R_{WW}(\tau) = E(W(t)W(t+\tau))$ is the correlation function. Also notice that s_0 is the value for two side spectrum density. If we consider the one sided PSD, then $S_{WW}(\omega) = 2s_0$. The relation of autocorrelation and spectral density function can be given by following Fourier transforms pairs,

$$S_{XX}(\omega) = \frac{1}{2\pi}\int_{-\infty}^{+\infty} R_{XX}(\tau)e^{-i\omega\tau}d\tau \tag{2.4}$$

and

$$R_{XX}(\tau) = \int_{-\infty}^{+\infty} S_{XX}(\omega)e^{i\omega\tau}d\omega \tag{2.5}$$

The constant spectral density of white noise implies that the energy of the random process in uniformly distributed over whole frequency range and the autocorrelation function with Dirac delta function means that the Gaussian white noise has infinite variance. Such a process with infinite variance does not exist in reality, but it is a good

approximation to model wide band noise with very short correlation time, which is defined as,

$$\tau_c = \int_0^\infty \frac{\left|R_{XX}(\tau)\right|}{R_{XX}(0)} d\tau \tag{2.6}$$

where $R_{XX}(\tau) = E(X(t)X(t+\tau))$. In the study of stochastic differential equations and stochastic systems, Gaussian white noise is a most important concept. The response of any linear or nonlinear system driven by white noise constitutes a Markov Process and therefore the system can be analyzed by using Markov methods.

The Markov process, named after the Russian mathematician Andrey Markov, is a stochastic process with the Markov property, and very limited memory, namely the process has only one step memory given below mathematically,

$$p(x_{t_n} \left| x_{t_{n-1}}, x_{t_{n-2}}, ..., x_{t_0}\right.) = p(x_{t_n} \left| x_{t_{n-1}}\right.) \tag{2.7}$$

where $t_n > t_{n-1} > t_{n-2} ... > t_0$ and $p(\bullet \left| \bullet \right.)$ designates the conditional probability density function (PDF) and x_{t_n} represent the state value at time step t_n. The above equation means that the future state x_{t_n} depends only on current state $x_{t_{n-1}}$ and does not depend on any other past state values.

The well known Smoluchowski-Chapman-Kolmogorov (SCK) equation, which is very useful when understanding the derivation of FPE, can be derived based on equation(2.7),

$$p(x_{t_n} \left| x_{t_{n-1}}\right.) = \int_{-\infty}^{+\infty} p(x_{t_n} \left| x_t\right.).p(x_t \left| x_{t_{n-1}}\right.) dx_t \tag{2.8}$$

where $t_n > t > t_{n-1}$. The probability of the random variable x arriving at x_{t_n} at time t_n, given that the process started at the value of $x_{t_{n-1}}$ at time t_{n-1}, is the summation of probability of arriving there by passing through all the possible intermediate values x_t. Fig. 2 helps to interpret the SCK equation.

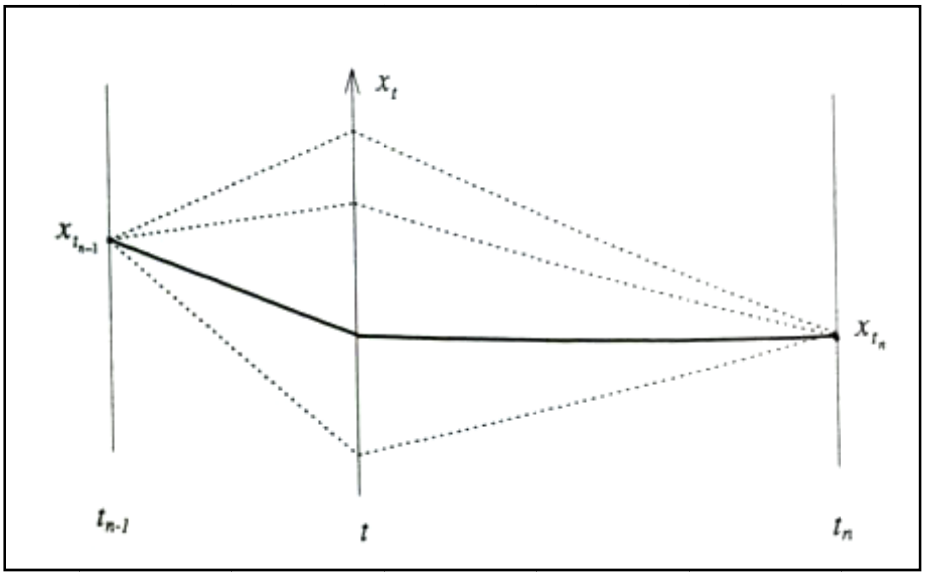

Fig. 2. Illustration of the SCK equation (2.8) (Moe, 1997)

2.3 Stochastic Differential Equations - SDE

A stochastic differential equation is an ordinary differential equation governing the motion or response of the dynamical structures with one or more of the terms is a stochastic process, e.g. white noise or other type of noise. To apply the Markov process assumption, the random term in the SDE has to be white noise. In case of colored noise

excitation, the limitation of white noise term can be eliminated by using a shaping filter technique to be introduced in the next chapter. Generally, the stochastic differential equation can be expressed with a stochastic white noise term $W(t)$ as below,

$$\frac{dX}{dt} = F(X,t) + G(X,t)W(t) \tag{2.9}$$

where X is the vector of stochastic process, $F(X,t)$ is defined as drift coefficient vector, and $G(X,t)$ is the diffusion coefficient matrix of the dynamical system. F and G both have deterministic function forms with nonlinear terms if the related dynamical system is nonlinear. The SDE above is equivalent to the general integration:

$$X_t = X_{t_0} + \int_{t_0}^{t} F(X,\tau)d\tau + \int_{t_0}^{t} G(X,\tau)dB \tag{2.10}$$

where t_0 is the initial time and X_{t_0} represent initial condition of the stochastic process. The first integral at RHS of the equation is an ordinary mean square Riemann-Stieltjes integral, but the second integral is not. Here we discuss the one dimensional problem only, however, all these results can be generalized to higher dimensions. The Riemann-Stieltjes integration of X_t with respect to a variable R_t is given by

$$\int_{t_1}^{t_2} X_t dR_t \approx \sum_{i=1}^{m-1} X_{\tilde{\tau}_i}(R_{\tau_{i+1}} - R_{\tau_i}) \tag{2.11}$$

where $\tau_i \le \tilde{\tau}_i \le \tau_{i+1}$ and $t_1 = \tau_1 < \tau_2 < .... < \tau_M = t_2$, when $m \to +\infty$, the right hand side will converge to the unique integral. For the second integration of (2.10) including the Wiener process dB, the limit of the Rimann-Stieltjes integration depends

on evaluation point of $\tilde{\tau}_i$ is chosen. Basically, there are two different commonly used integral evaluation methods, namely the Itô integral, if $\tilde{\tau}_i = \tau_i$, and the Stratonovich integral, if $\tilde{\tau}_i = (\tau_{i+1} + \tau_i)/2$.

The Itô, equation (2.12), and Stratonovich, equation (2.13) integral of the second term of equation (2.10) are written by,

$$\int_{t_1}^{t_2} G_t dB_t \approx \sum_{i=1}^{m-1} G(\tau_i)(B_{\tau_{i+1}} - B_{\tau_i}) \tag{2.12}$$

$$\int_{t_1}^{t_2} G_t dB_t \approx \sum_{i=1}^{m-1} G(\frac{\tau_i + \tau_{i+1}}{2})(B_{\tau_{i+1}} - B_{\tau_i}) \tag{2.13}$$

The Stratonovich integral satisfies all the formal rules of classical calculus and therefore it is a better choice for SDE. However, the Itô integrals are martingales and have more advantages for computational purposes (To, 2000). The Stratonovich integral SDE becomes equivalent to the Itô SDE by adding a modified drift term,

$$dX = (F + \frac{1}{2} G \frac{\partial G}{\partial X})dt + GdB \tag{2.14}$$

in which G is a matrix, the differentiation term in the parentheses is not appropriate. Thus, above SDE can be written more explicitly,

$$dx_i = (F_i + \frac{1}{2}\sum_{j=1}^{n}\sum_{k=1}^{n} G_{kj} \frac{\partial G_{ij}}{\partial x_k})dt + \sum_{j=1}^{n} G_{ij} dB_j, \quad i = 1,2,3,4.... \tag{2.15}$$

So the methodology for solving an Itô SDE is adapted for solving a Stratonovich SDE. The correction term $\frac{1}{2} G \frac{\partial G}{\partial X}$ is well known as Wong-Zakai or Stratonovich correction

term. Note that the Itô and Stratonovich SDEs are equivalent in the case of additive noise, that is *G* is just a constant or constant vector, $\frac{\partial G}{\partial X}$=0. For a system with parametric excitation, the correction term is necessary regardless of whether the Gaussian white noise excitation $W(t)$ is ideal or physical.

2.4 The Derivation of Fokker Planck Equation from the SDE

The key to the Markov process modeling is the derivation of the Fokker Planck Equation, which governs the transient probability density of the Markov process. Although the derivation of the FPE from the stochastic dynamic system can be found in many textbooks and papers, see e.g. (Fuller, 1969; Risken, 1996; Lin and Cai, 2004) , it may not be obvious for Naval Architects and Ocean Engineers. For this dissertation to be self-contained, we first derive the FPE for the simplest case and then extend it to more general case following Fuller (Fuller, 1969). At the end of this section, we will also discuss the initial and boundary conditions for the FPE.

2.4.1 The derivation of the FPE from the one dimensional SDE

The simplest case of a SDE is a scalar process $x(t)$ obtained by integrating white noise $w(t)$; the SDE for $x(t)$ is given by,

$$\frac{dx}{dt} = w(t) \tag{2.16}$$

Following the formal integral rule,

$$x(t) = x(0) + \int_0^t w(\tau)\tau \tag{2.17}$$

The increment of $x(t)$ is independent of its past value and time, hence $x(t)$ is a Markov process. Applying the Smoluchowski-Chapman-Kolmogorov (SCK) equation(2.8) to $x(t)$,

$$p(x_3, t+\delta t) = \int_{-\infty}^{\infty} p(x_3, t+\delta t \,|\, x_2, t) p(x_2, t) dx_2 \tag{2.18}$$

Considering x_2 is a fixed value, and by defining the change of x during the time δt as z, $z = x_3 - x_2$,

$$p(x_3, t+\delta t \,|\, x_2, t) dx_3 = q(z, \delta t \,|\, x_2, t) dz \tag{2.19}$$

where $q(z, \delta t \,|\, x_2, t)$ is the transition probability density. Here we assume the variable increment z is independent of past value x_2, so the equation (2.19) can be simplified to

$$p(x_3, t+\delta t \,|\, x_2, t) dx_3 = q(z, \delta t \,|\, x_2, t) dz = q(z, \delta t) dz \tag{2.20}$$

From equation (2.20) , equation (2.18) may be written as,

$$p(x, t+\delta t) = \int_{-\infty}^{\infty} q(z, \delta t) p(x - z, t) dz \tag{2.21}$$

It is notable that we have dropped the subscript of x_3. Equation (2.21) states the property of the Markov Process. The increments are independent of past value and time. The probability of the system at x is equal to the product of the transition probability of the change z and the variable value at the past time step $x - z$, with integration over all possible change z. We assume that the time step δt is very small, so the probability of a

large change z is very small. The transition probability density $q(z,\delta t)$ in the integral of equation (2.21) has considerable magnitude only when z is close to zero. By expanding $p(x-z,t)$ and $p(x,t+\delta t)$ at x and t respectively by Taylor series and retain the first few terms, equation (2.21) becomes

$$\begin{aligned} p(x,t)+\delta t\frac{\partial p(x,t)}{\partial t}+\ldots = p(x,t)\int_{-\infty}^{\infty} q(z,\delta t)dz-\frac{\partial p(x,t)}{\partial x}\int_{-\infty}^{\infty} zq(z,\delta t)dz \\ +\frac{1}{2!}\frac{\partial p^2(x,t)}{\partial x^2}\int_{-\infty}^{\infty} z^2q(z,\delta t)dz-\frac{1}{3!}\frac{\partial p^3(x,t)}{\partial x^3}\int_{-\infty}^{\infty} z^3q(z,\delta t)dz+\ldots \end{aligned} \tag{2.22}$$

The first integral on the RHS is unity, therefore it cancels the first term on the LHS; and the second integral on the RHS is zero considering the mean of the z is zero. The fourth term on RHS is a third order term of z, so it is negligible compared with the second order. The equation (2.22) may be simplified to the standard Fokker Planck Equation (FPE),

$$\frac{\partial p(x,t)}{\partial t}=\frac{b}{2}\frac{\partial p^2(x,t)}{\partial x^2} \tag{2.23}$$

where $E[W(t)W^T(t+\tau)]=\mathrm{Q}\delta(\tau)$ is the intensity of the white noise and given by the formula below,

$$b=\lim_{\delta t\to 0}\frac{1}{\delta t}\int_{-\infty}^{\infty} z^2q(z,\delta t)dz \tag{2.24}$$

The derivation of the above FPE is based on many assumptions which lack the strict mathematical justification, but it is still very helpful and intuitive to understand the FPE for the beginners.

2.4.2 Derivation of FPE from general SDE

Most dynamical systems have more than two variables, the associated FPE therefore become a high dimensional partial differential equation (PDE). It is challenging to analyze a high dimensional PDE. The general SDE has N dimensional variables and may be written in a standard differential equation format,

$$\frac{dx_i}{dt} = F_i(x_1, x_2, ..., x_N, t) + w_i(t) \quad (i = 1, 2, ..., N) \tag{2.25}$$

Similar to the derivation in the simple case, the generalized SCK equation may be written as,

$$p(X, t + \delta t) = \int_{-\infty}^{\infty} q(Z, \delta t \,|\, X - Z, t) p(X - Z, t) dZ \tag{2.26}$$

Unlike the assumption in equation (2.20), we did not assume that the increment Z is independent of the past value $X - Z$. Compared with equation (2.21), the variable X and the changes Z are both vectors, the probability density p and transition probability density q are scalars and $dZ = dz_1 dz_2 ... dz_N$ is a hyper volume differential elements. Assuming the time step X is small, so that the probability of large changes Z is very small. Only values Z close to zero contributes considerable to the integral in (2.26). Expanding the $X - Z$ term by Taylor Series with respect to X, the integral in (2.26) becomes,

$$
\begin{aligned}
q(Z,\delta t\big|X-Z,t)p(X-Z,t) = {} & q(Z,\delta t\big|X,t)p(X,t) \\
& -\sum_{i=1}^{N} z_i \frac{\partial}{\partial x_i} q(Z,\delta t\big|X,t)p(X,t) \\
& +\frac{1}{2!}\sum_{i=1}^{N}\sum_{j=1}^{N} z_i z_j \frac{\partial^2}{\partial x_i \partial x_j} q(Z,\delta t\big|X,t)p(X,t) \\
& -\frac{1}{3!}\sum_{i=1}^{N}\sum_{j=1}^{N}\sum_{k=1}^{N} z_i z_j z_k \frac{\partial^3}{\partial x_i \partial x_j \partial x_{ki}} q(Z,\delta t\big|X,t)p(X,t) \\
& +.....
\end{aligned}
\tag{2.27}
$$

Substituting the above equation back into equation (2.26) and expanding the LHS of (2.26) by Taylor Series,

$$
\begin{aligned}
p(X,t)+\delta t\frac{\partial p(X,t)}{\partial t}+... = {} & \int_{-\infty}^{\infty} q(Z,\delta t\big|X,t)dZp(X,t) \\
& -\sum_{i=1}^{N}\frac{\partial}{\partial x_i}\left[\int_{-\infty}^{\infty} z_i q(Z,\delta t\big|X,t)dZp(X,t)\right] \\
& +\frac{1}{2!}\sum_{i=1}^{N}\sum_{j=1}^{N}\frac{\partial^2}{\partial x_i \partial x_j}\left[\int_{-\infty}^{\infty} z_i z_j q(Z,\delta t\big|X,t)dZp(X,t)\right] \\
& +.....
\end{aligned}
\tag{2.28}
$$

The first integral on the RHS is unity and cancels the first term on the LHS. With the assumption that the changes of variables Z, we neglect the third and higher order terms on the RHS. When $\delta t \to 0$, we postulate some ratios to be constant as below,

$$
\lim_{\delta t\to 0}\frac{\int_{-\infty}^{\infty} z_i q(Z,\delta t\big|X,t)dZ}{\delta t} = a_i(X,t) \tag{2.29}
$$

and

$$
\lim_{\delta t\to 0}\frac{\int_{-\infty}^{\infty} z_i z_j q(Z,\delta t\big|X,t)dZ}{\delta t} = b_{ij}(X,t) \tag{2.30}
$$

Then we reach the Kolmogorov version of Fokker Planck Equation

$$\begin{aligned}\frac{\partial p(X,t)}{\partial t} = &-\sum_{i=1}^{N}\frac{\partial}{\partial x_i}\big[a_i(X,t)p(X,t)\big] \\ &+\frac{1}{2!}\sum_{i=1}^{N}\sum_{j=1}^{N}\frac{\partial^2}{\partial x_i \partial x_j}\big[b_{ij}(X,t)p(X,t)\big]\end{aligned} \tag{2.31}$$

The coefficients $a_i(X,t)$ and $b_i(X,t)$ are called moments rates. Recall equation (2.25), we have,

$$z_i = x_i(t+\delta t) - x_i(t) = \int_t^{t+\delta t} F_i(X,\tau)d\tau + \int_t^{t+\delta t} w_i(\tau)d\tau \qquad (i = 1,2....N) \tag{2.32}$$

when $\delta t \to 0$, the mean of increment z_i yields

$$\overline{z_i} = F_i(X,t)\delta t + \overline{\Delta w_i} \qquad (i = 1,2....N) \tag{2.33}$$

The overbar of variables represents taking the mean value of its ensemble; the mean of white noise increments is zero by definition, so the first moment rate can be found by

$$a_i(X,t) = \frac{\overline{z_i}}{\delta t} = F_i(X,t) \qquad (i = 1,2....N) \tag{2.34}$$

Following the same method, the second moment rate $b_i(X,t)$ yields

$$\begin{aligned}\overline{z_i z_j} &= F_i F_j(\delta t)^2 + F_i\overline{\Delta w_j}\delta t + F_j\overline{\Delta w_i}\delta t + \overline{\Delta w_i}\,\overline{\Delta w_j} \\ &\approx \overline{\Delta w_i}\,\overline{\Delta w_j} \qquad (i = 1,2....N;\ j = 1,2....N)\end{aligned} \tag{2.35}$$

From (2.30) and (2.35),

$$b_{ij} = \lim_{\delta t \to 0}\frac{\overline{\Delta w_i}\,\overline{\Delta w_j}}{\delta t} \quad (i = 1,2....N;\ j = 1,2....N) \tag{2.36}$$

The second moment's rates are related with the properties of the white noise intensity. More details of derivation can be found in (Fuller, 1969)

2.4.3 Discussion of the Fokker Planck equation

We have derived the Fokker Planck Equation for one dimensional and higher dimensional dynamical systems. The FPE transforms the stochastic dynamical equation governing the displacement and velocity into a partial differential equation governing the probability density function, which includes the higher order error term from the Taylor series expansion cut off. The approximate solution for the Fokker Planck Equation, especially the higher dimensional FPE, is a very difficult work. Even if we have an excellent numerical solution for the FPE, it is noted the solution is still an approximation to the original stochastic dynamical systems. When the theory is applied to practical problems in stochastic dynamics, the associated FPE may be solved numerically with suitable initial condition and boundary conditions. The appropriate initial condition associated with the parabolic differential equations FPE are:

$$p(X,t\,|\,X_0,t_0) = \delta(X - X_0) \tag{2.37}$$

$\delta(X - X_0)$ is a Dirac's delta function. Note that both conditional probability density function $p(X,t\,|\,X_0,t_0)$ and unconditional probability density function $p(X,t)$ satisfy the FPE.

The boundary conditions of the FPE are defined at infinity, which always indicates that the probability flow must vanish at the infinity:

$$p(\infty,t) = 0 \quad t \geq 0 \tag{2.38}$$

In addition to the initial and boundary conditions, $p(X,t\,|\,X_0,t_0)$ should also fulfill the positivity and normalization constraints:

$$p(X,t) \geq 0 \quad t \geq 0 \tag{2.39}$$

$$\int_{-\infty}^{\infty} p(X,t)dX = 1 \quad t \geq 0 \tag{2.40}$$

CHAPTER III

THE CUMULANT NEGLECT METHOD APPLICATION TO THE NONLINEAR ROLLING RESPONSE

Rolling motions of ships in random beam seas may cause stability issues and affect the ability of cargo handling, helicopter landing and missile launching, etc. Prediction of ship rolling dynamics is very important for practical application. Due to the randomness of realistic waves in the ocean, rolling motions are always considered as a stochastic process. For the marine and offshore industry, the nonlinear effect of loads and responses lead to many complicated phenomena, e.g., bifurcation, chaos, non-Gaussian statistics, etc. There are two different types of nonlinearity, i.e., forcing nonlinearity, such as the 100 or 1000 year return period storm conditions and the other one is the system nonlinearity, e.g. stiffness and damping nonlinearity, the most typical case of which is the ship rolling equation which can be decoupled from other modes. The responses of linear systems with Gaussian input are always Gaussian. All higher order statistics can be derived from the second order moments. However, nonlinear system will have non-Gaussian response; large amplitude rolling motion with nonlinear damping and strong nonlinear stiffness needs more advanced technique to analyze the higher order response statistical moments and capture the non-Gaussian effects.

Large amplitude ship rolling motion under random beam sea has been approached several times by different research groups, the analysis methods include Markov methods and non- Markov methods. Non-Markov methods include statistical equivalent linearization(Roberts and Spanos, 2003), perturbation methods, Monte Carlo methods, Melnikov methods(Falzarano et al., 1992; Hsieh et al., 1994; Jiang et al., 1996; Jiang et al., 2000) and Vakakis methods (Vishnubhotla et al., 2000; Falzarano et al., 2004; Falzarano et al., 2005; Vishnubhotla and Falzarano, 2009). Statistical equivalent linearization is widely used for nonlinear problems in the non-Markov methods. Linearization methods introduce some linear terms to replace nonlinear terms based on energy conservation. With linearization, the response has to be assumed Gaussian, losing any non-Gaussian effect.

The Markov assumption of the ship rolling process is the most popular procedure for random nonlinear dynamical analysis. Markov methods include the stochastic averaging method (Roberts and Vasta, 2000), moment closure methods (Francescutto and Naito, 2004) and also the direct solution of the Fokker-Planck-Kolmogorov (FPK) equation(Naess and Moe, 2000). The FPK equation is limited to the Markov assumption and ideal white noise excitation or filtered white noise. Wave excitation is the most typical forcing for ocean structures. Since wave excitation spectra normally have a central peak and limited bandwidth, a method of transformation between ideal white noise and color noise has been developed using filter technology. Using linear filters, any type of excitation can be handled by the Fokker-Planck-Kolmogorov equation. As we know, analytical solutions of the FPK equations are limited to linear systems and

some special nonlinear dynamical system with stationary responses (Soize, 1994). The numerical solution procedures mainly focus on three branches: finite element methods (Spencer and Bergman, 1993), finite difference methods (Kumar and Narayanan, 2006) and path integral method(Naess and Moe, 2000). With all these numerical methods, the FPK solution suffers from problems due to high dimensions, the so-called "curse of dimension". With an increased number state dimensions, the finite element method and finite difference method require very large amounts of computer memory and may experience numerical stability issues.

Alternatively, moment closure methods have been applied in many fields. In this method, the differential equations governing the response process are first determined. The Itô differential rule is then applied to the governing equations to obtain moment equations. If the system has nonlinear terms, the moment equations up to Nth order will include N+1, N+2 order and higher order moments, which is called the infinite hierarchy. Higher order moments have to be closed by some closure method. The closure methods include the moment neglect, the cumulant neglect, the Hermite moment closure (Ness et al., 1989), etc. The cumulant neglect method which discards cumulants higher than a particular order N is adopted in this dissertation to close the moment equations. If N equals 2, then the method is defined as Gaussian closure, which is the equivalent of statistical linearization, otherwise the method is non-Gaussian closure. By setting the higher order cumulants to zero, the higher order moment can be expressed by the lower order moments to form the closed form equations. The response moments can be further used to generate the probability density function by Fourier transforming its

characteristic function (Wojtkiewicz, 2000),maximum entropy (Sobczyk and Trcebicki, 1999). For the ship rolling problems, most previous papers about moment equations only consider Gaussian cumulant closure due to the difficulty in tracking the higher order closure (Francescutto, 1990; Francescutto and Naito, 2004). This is especially true for higher order systems which may include a linear filter. The cumulant neglect method becomes tedious and untraceable when increasing the neglect order. This tedium is the motivation to develop an automatic tool to address the difficulty to handle the higher dimensional state space stochastic models and higher order closure levels. Ship rolling responses with strong nonlinear terms result in non-Gaussian effects. The higher order cumulant neglect method will help to analyze higher order moment effects, such as skewness and kurtosis, or even higher statistical moments. In this dissertation, we extend the neglect order to fourth order by developing an automatic tool. Higher order moments response will benefit from our understanding of the non-Gaussian effect of nonlinear ship rolling motion and further understanding of ship capsizing.

3.1 Modeling of Rolling Motion with Filter Application

3.1.1 Modeling of ship rolling

The second order ordinary differential equation describing the single degree freedom ship rolling motion is recalled in this section:

$$(I_{44} + A_{44}(\omega))\ddot{\phi} + B_{44}(\omega)\dot{\phi} + B_{44_q}(\omega)\dot{\phi}\left|\dot{\phi}\right| + \Delta(C_1\phi + C_3\phi^3 + ..) = f(t) \quad (3.1)$$

where ϕ represent the roll angle and $\dot{\phi}$ is the roll velocity. I_{44} and $A_{44}(\omega)$ represent the roll inertia and added inertia of vessel respectively. $B_{44}(\omega)$ and $B_{44_q}(\omega)$ are the linear and

quadratic damping coefficients from the hydrodynamic and viscous effects respectively. Δ is the displacement of the vessel, C_1 and C_3 are the linear and nonlinear restoring force coefficients. $f(t)$ represents the random wave excitation. If $f(t)$ is only some harmonic moment, all frequency dependent parameters are constant. If the excitation force is not purely harmonic, say, random force, $A_{44}(\omega)$ and $B_{44}(\omega)$ will no longer be constant any more. Then equation (3.1) with constant coefficients becomes an approximation for the rolling motion. For wide banded forcing spectrum, values at natural frequency are recommended; for narrow banded forcing, peak frequency values are more reasonable (Jiang et al., 2000). Here the non linear damping term is not in the polynomial form, which is required by the moment closure methods. An equivalent nonlinear polynomial form will be constructed by the least square method (Dalzell, 1978). All hydrodynamic coefficients can be calculated using a strip theory hydrodynamics program (Beck and Troesch, 1990). 'T-AGOS', an ocean surveillance ship, was analyzed by using strip theory and the parameters are shown in Table 1. Plots of the hydrodynamic force coefficient can be found in Fig. 3 to Fig. 6.

Dividing by the inertia and added inertia, Equation (3.1) is rewritten as follows:

$$\begin{cases} \dot{x}_1 = x_2 \\ \dot{x}_2 = -2\mu x_2 - \delta {x_2}^3 - \omega_0^2 x_1 - \alpha_3 {x_1}^3 + \varepsilon f(t) \end{cases} \tag{3.2}$$

where $x_1 = \phi, x_2 = \dot{\phi}$, $f(t)$ represents the external roll excitation. In linear hydrodynamics theory, the magnitude of the external force can be calculated by multiplying the RAO by the wave height. The spectrum of the external moment can be represented as follows:

$$S_{ff}(\omega) = S_{\eta\eta}(\omega)\left|F_{rolling}(\omega)\right|^2 \tag{3.3}$$

where: $S_{ff}(\omega)$ is the external exciting spectrum; $F_{rolling}(\omega)$ is the rolling moment amplitude per unit wave height, also defined as the force RAO of rolling motion; and $S_{\eta\eta}(\omega)$ is the wave spectrum. The wave amplitude is irregular and always described as a stationary, ergodic and Gaussian stochastic process. For simplicity, we adopt a one-parameter Pierson-Moskowitz spectrum described by equation(3.4).

Table 1. 'T-AGOS' dimensional parameters

Parameter	Dimensional Value	Parameter	Dimensional Value
$I_{44}+A_{44}(\omega)$	5.540 X 10^7 kg m^2	Δ	2.017 X 10^7 N
$B_{44}(\omega)$	5.266 X 10^6 kg m^2s^{-1}	$B_{44q}(\omega)$	2.877 X 10^6 kg m^2
C_1	3.168 m	C_3	-2.513 m

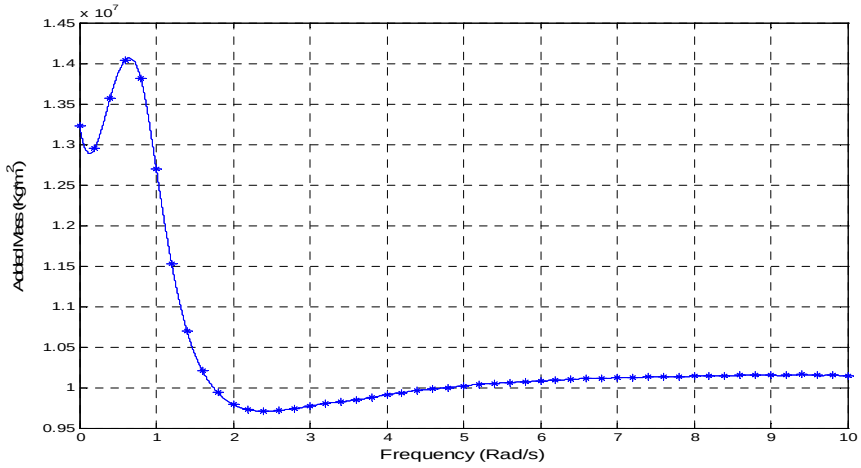

Fig. 3. Added mass of T-AGOS

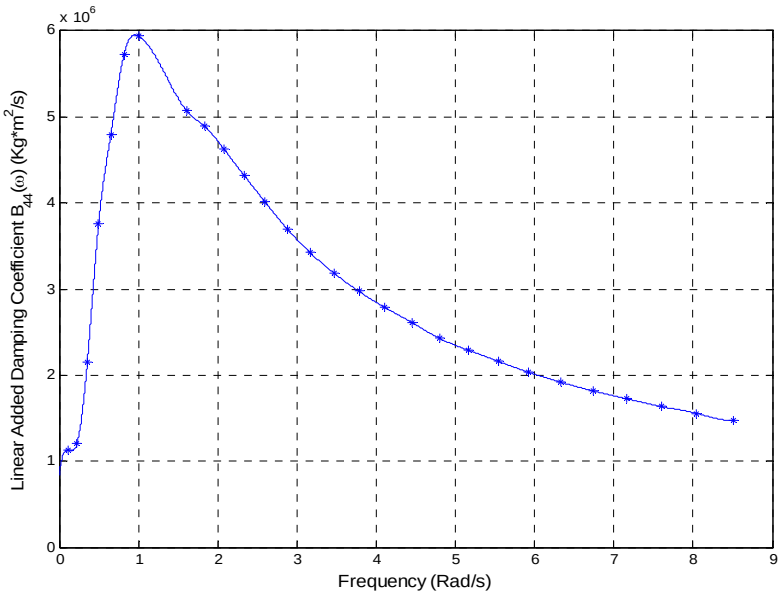

Fig. 4. Linear added damping coefficient

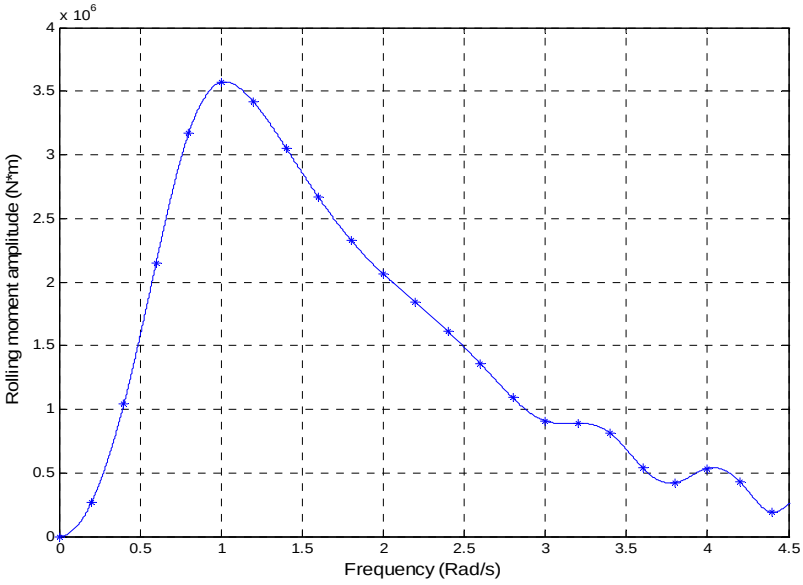

Fig. 5. Rolling moment amplitude per unit wave height

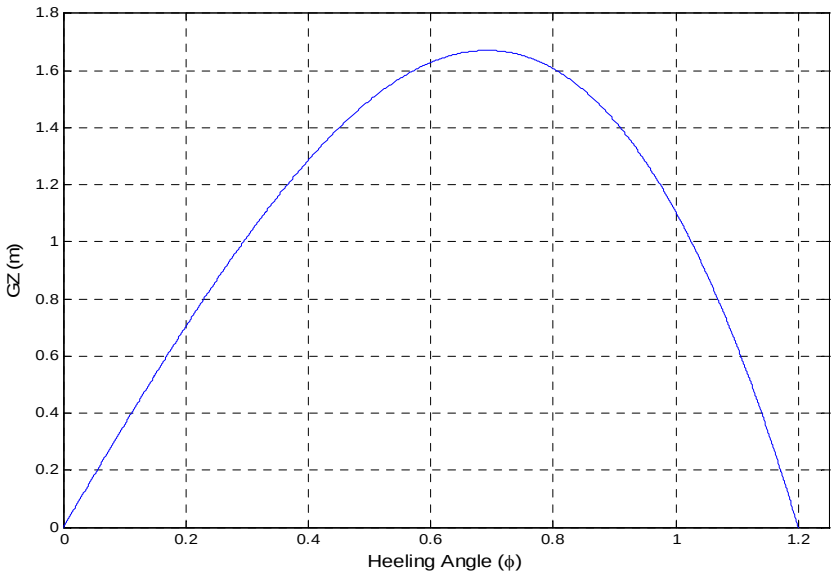

Fig. 6. GZ curve of T-AGOS (C1=3.618m,C3=-2.513m)

$$S_{\eta\eta}(\omega) = \frac{A}{\omega^5} \cdot \exp(-\frac{4A}{h_s^{\,2}\omega^4}) \tag{3.4}$$

where $\mathrm{A} = 0.0081 g^2$, g is the gravitational acceleration. The significant wave height h_s is the only parameter in this formula.

3.1.2 Modeling of rolling excitation moment

Since the moment equations are derived from the Fokker Planck equation, which is based on the theory of diffusion process. The excitation force for the Itô system has to be pure white noise. However, the random excitation term of rolling motion in equation (3.1) cannot be modeled as white noise. One method to handle the non white excitation is using a shaping filter, which is driven by white noise. Filter techniques are usually

performed by a linear ordinary differential equation. The response of linear differential equation, which has white noise as its excitation input, may represent a realistic excitation for the dynamical system. Analog filters designed for simulation of wave elevation and wave kinematics were introduced by Spanos (Spanos, 1983; Spanos, 1986). Definitions of different types of filters, e.g. Auto-Regressive Algorithm (AR), Moving Average (MA), and Autoregressive Moving Average Algorithms (ARMA) can be found in any time series textbook.

For a Linear constant-coefficient differential equation (LCCDE system) as follows (Stark and Woods, 2002):

$$\begin{aligned} &a_N Y^N(t) + a_{N-1} Y^{N-1}(t) + ... + a_0 Y^0(t) = b_M X^M(t) \\ &+b_{M-1} X^{M-1}(t) + ... + b_0 X^0(t) \qquad -\infty < t < +\infty \end{aligned} \tag{3.5}$$

where N and M are the order of derivation to time, the frequency response function or transfer function for this linear system above is:

$$H(\omega) = B(\omega) \,/\, A(\omega), \quad with\, a_0 \neq 0 \tag{3.6}$$

where $B(\omega) = \sum_{m=0}^{M} b_m (j\omega)^m$

$$A(\omega) = \sum_{n=0}^{N} a_n (j\omega)^n$$

where j represent the imaginary unit, and the relationship between input excitation X (t) and output response Y (t) spectrums:

$$S_{YY}(\omega) = \left|H(\omega)\right|^2 S_{XX}(\omega) \tag{3.7}$$

General methods for filter design are available only for the case of stationary stochastic processes (Thampi and Niedzwecki, 1992). We can design lots of different filters following equation (3.5). Three filters will be introduced in this dissertation(Francescutto and Naito, 2004). They are frequently used in the analysis of stochastic nonlinear problems. Bandwidth, characteristic frequency, etc, can be easily adjusted by changing the coefficient of the linear filter.

1) The simplest filter will be a second order linear differential equation:

$$\ddot{Y}(t) + \alpha_1 \dot{Y}(t) + \beta_1 Y(t) = \gamma_1 W(t) \tag{3.8}$$

where $W(t)$ is the Gaussian white noise input or excitation of the dynamical system with unit one side spectral density $S_{WW}(\omega) = 1$ and $Y(t)$ is the response of this linear dynamical system. The response of this filter system is actually the input excitation to the ship roll system. Frequency response function is defined by equation (3.6), as followed:

$$H(\omega) = \frac{\gamma_1}{(j\omega)^2 + \alpha_1(j\omega) + \beta_1} = \frac{\gamma_1}{(\beta_1 - \omega^2) + j\alpha_1\omega} \tag{3.9}$$

$$S_{YY}(\omega) = \left|H(\omega)\right|^2 S_{WW}(\omega) = \frac{{\gamma_1}^2}{(\beta_1 - \omega^2)^2 + (\alpha_1\omega)^2} \tag{3.10}$$

2) The second order linear filter with differentiation to white noise:

$$\ddot{Y}(t) + \alpha_2 \dot{Y}(t) + \beta_2 Y(t) = \gamma_2 \dot{W}(t) \tag{3.11}$$

$$H(\omega) = \frac{j\gamma_2\omega}{(j\omega)^2 + \alpha_1(j\omega) + \beta_1} = \frac{j\gamma_2\omega}{(\beta_1 - \omega^2) + j\alpha_1\omega} \tag{3.12}$$

$$S_{YY}(\omega) = \left|H(\omega)\right|^2 S_{WW}(\omega) = \frac{{\gamma_2}^2\omega^2}{(\beta_2 - \omega^2)^2 + (\alpha_2\omega)^2} \tag{3.13}$$

3) Fourth order linear differential equation could be designed as a higher order filter. This filter is also viewed as cascade of two linear filters (Spanos, 1983; Francescutto and Naito, 2004).

$$\dddot{Y}(t) + \lambda_3\ddot{Y}(t) + \lambda_2\ddot{Y}(t) + \lambda_1\dot{Y}(t) + \lambda_0 Y(t) = \gamma_3\ddot{W}(t) \tag{3.14}$$

$$H(\omega) = \frac{-\gamma_3\omega^2}{(j\omega)^4 + \lambda_3(j\omega)^3 + \lambda_2(j\omega)^2 + \lambda_1(j\omega) + \lambda_0} \tag{3.15}$$

$$\begin{aligned} S_{YY}(\omega) = \left|H(\omega)\right|^2 S_{WW}(\omega) &= \frac{{\gamma_3}^2\omega^4}{(\omega^4 - \lambda_2\omega^2 + \lambda_0)^2 + (\lambda_1\omega - \lambda_3\omega^3)^2} \\ &= \frac{{\gamma_3}^2\omega^4}{[(\beta_1 - \omega^2)^2 + (\alpha_1\omega)^2][(\beta_2 - \omega^2)^2 + (\alpha_2\omega)^2]} \end{aligned} \tag{3.16}$$

where $\lambda_3 = \alpha_1 + \alpha_2, \lambda_2 = \beta_1 + \beta_2 + \alpha_1\alpha_2, \lambda_1 = \alpha_1\beta_2 + \alpha_2\beta_1, \lambda_0 = \beta_1\beta_2$;

Generally, it is not allowed to take the derivative of the Gaussian white noise mathematically. However, the state space format of variables will avoid taking derivative, see example in equation (3.17). We set rolling moment excitation $f(t)$ as the output of equation (3.8), (3.11)and (3.14) respectively. Random excitation force can be reproduced from these three filters from white noise. All coefficients of the filter are determined through non linear curve fittings methods after setting $S_{ff} = S_{YY}$, where definition of S_{ff} can be found in equation(3.3). Fitting results are show in Fig. 7 . The original curve represent the target spectrum S_{ff} ,and filter1, filter2, filter3 represents S_{YY} using various fitting coefficients of equations (3.8), (3.11)and (3.14). The plots in

Fig. 7 shows that filter 1 produces too large value e in the low frequency range and a non zero value at zero frequency. Filter 2 and filter 3 both provide better approximation of the original spectrum. Filter 3 performs best. Similar results can be found in (Francescutto and Naito, 2004).

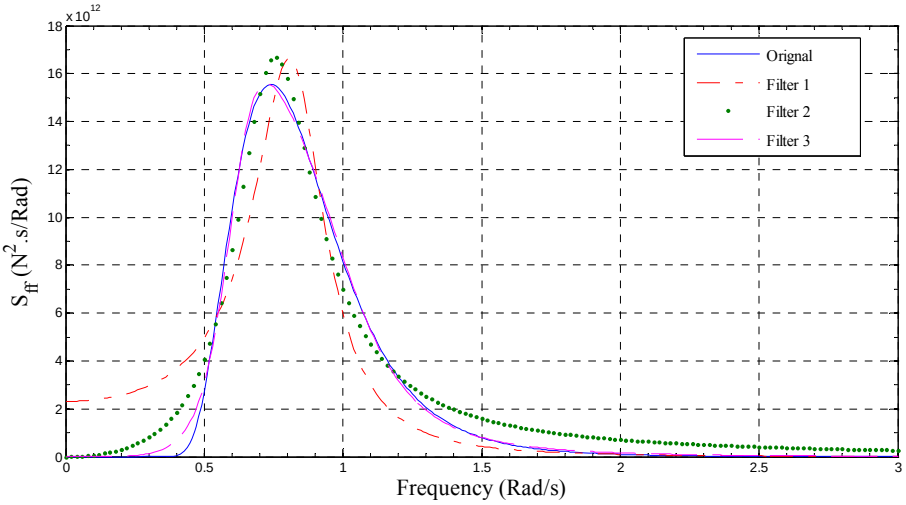

Fig. 7. Comparison of original force spectrum with filtered spectrum

3.1.3 State space formation of rolling motion

By combining the rolling equation of motion (3.2) and the filter equations (3.14), the rolling motion in random seas can be modeled in a state space form. Any excitation spectrum can be reproduced by some filter designed as explained above.

$$\begin{cases} \dot{x}_1 = x_2 \\ \dot{x}_2 = -2\mu x_2 - \delta {x_2}^3 - \omega_0^2 x_1 - \alpha_3 {x_1}^3 + \varepsilon x_3(t) \\ \dot{x}_3 = x_4 - \lambda_3 x_3 \\ \dot{x}_4 = x_5 - \lambda_2 x_3 + \gamma_3 W(t) \\ \dot{x}_5 = x_6 - \lambda_1 x_3 \\ \dot{x}_6 = -\lambda_0 x_3 \end{cases} \tag{3.17}$$

where $x_3 = f$ and $W(t)$represents white noise. With the Markov assumption, equation (3.17) forms Itô's differential equations:

$$dX = F(X,t)dt + G(X,t)dB \tag{3.18}$$

$\frac{dB}{dt} = W(t)$ and $W(t)$ is the white noise excitation. $B(t)$ is defined as Wiener process or Brownian motion. And $F(X,t)$ is defined as the drift coefficient, $G(X,t)$ is the diffusion coefficient for the dynamical system. $F(X,t)$ is a Nx1 matrix, N is the dimension of equation(3.17); $G(X,t)$ is N x M matrix, here N=6, M=1. In equation, F, G and X are listed below:

$$F(X,t) = \begin{Bmatrix} x_2 \\ -2\mu x_2 - \delta {x_2}^3 - \omega_0^2 x_1 - \alpha_3 {x_1}^3 + \varepsilon x_3(t) \\ x_4 - \lambda_3 x_3 \\ x_5 - \lambda_2 x_3 \\ x_6 - \lambda_1 x_3 \\ -\lambda_0 x_3 \end{Bmatrix} = \begin{Bmatrix} F^{(1)} \\ F^{(2)} \\ F^{(3)} \\ F^{(4)} \\ F^{(5)} \\ F^{(6)} \end{Bmatrix} \quad and \; G = \begin{Bmatrix} 0 \\ 0 \\ 0 \\ \gamma_3 \\ 0 \\ 0 \end{Bmatrix} \tag{3.19}$$

For the beam sea condition, γ_3 is defined as a constant number, which means γ_3 is not coupled to any state space variable or time. This Markov system has only additive white noise. If G(X, t) is coupled with the state space variable x and time, the system will become a random parametric problem (e.g. random stiffness, random damping, or random inertia). Parametric rolling is induced by random stiffness. The Itô differential equation will involve the Wong-Zakai (Wong and Zakai, 1964) correction term. The Fokker Planck Equation (FPE) is defined by the transition probability density function $P(X,t\,|\,X_0,t_0)$.

$$\frac{\partial P(X,t\,|\,X_0,t_0)}{\partial t} = -\sum_{i=1}^{N}\frac{\partial(F^{(i)}P)}{\partial x_i} + \frac{1}{2}\sum_{i=1}^{N}\sum_{j=1}^{N}\frac{\partial^2((GQG^T)_{ij}P)}{\partial x_i \partial x_j} \tag{3.20}$$

$E[W(t)W^T(t+\tau)] = Q\delta(\tau)$, Q is the intensity of white noise and $\delta(\cdot)$ is the Dirac delta function. If we have Q =2π, spectrum density of two side white noise is unit in this way, $P(X,t\,|\,X_0,t_0)$ is transition probability density function at X at time step t, given the initial state value X_0 at time t_0.

3.2 The Cumulant Neglect Closure Method

Equation(3.20), which governs the probability density function of the diffusion process, is a high dimensional partial differential equation. The numerical solution of this high dimensional PDE will involve many stability and accuracy issues. Alternatively, the Moment equation, which governs the response of statistical moments, can be solved after some reasonable assumption and closure technique. For the N-dimensional Itô differential equations, N(N+1)(N+2)…(N+M-1)/M! moment equations could be generated for Mth order moment. Six 1st order, 21 second order, 56 third order and 126 fourth order moment equations could be generated from equation(3.17). In the Gaussian Cumulant neglect method, the algorithm will analyze order up to two, and all higher order moments can be estimated by second and lower order moments. The Itô's differential rule can be used to generate moment equations governing the response of stochastic dynamical system. Let us set φ to be a scalar valued real function and $\varphi = x_1^{k_1}x_2^{k_2}\cdots x_n^{k_n}$, where $X = [x_1, x_2, \cdots x_n]^T$ is the state space vector in equation (3.17).

$E(\varphi)$ represents the expectation of the combination φ. Following the Itô's differential rule (Itô, 1951), the moment equations for φ are formed in equation(3.21).

$$\frac{\partial E(\varphi)}{\partial t} = E(\sum_{i=1}^{N} F^{(i)} \frac{\partial \varphi}{\partial x_i}) + \frac{1}{2}\sum_{i=1}^{N}\sum_{j=1}^{N} E((GQG^T)_{ij} \frac{\partial^2 \varphi}{\partial x_i \partial x_j}) \tag{3.21}$$

It is clear that the moment equations will not be closed due to the nonlinear term in the dynamical system. The second order moment equations will include third, fourth or even higher order unknown moments. When higher order moment equations are derived, even higher order moments will be introduced into the equations, this is the so called infinite hierarchy. Therefore, moment closure must be used to approximate the higher statistical moments. If we simply neglect moments higher then 2, then all the nonlinear effect will be lost. Here the cumulant neglect method was adopted. Cumulant of order higher than some particular order N will be neglected and all higher moments can be expressed as a function of the lower order moment. The moment equations will form a closed system of equations after application of the closure of the cumulant. The C Cumulant neglect, or Cumulant discard method was first applied to turbulence theory(Beran, 1965). More details can be found in the books of Lin(Lin and Cai, 2004), Lutes(Lutes and Sarkani, 2004) and Ibrahim(Ibrahim, 2007).

3.2.1 Gaussian cumulant neglect method without automatic neglect tool

To apply the Gaussian Cumulant neglect method to the rolling problem, moment up to second order will be derived below. For the Itô type equation (3.17) , moments equations are listed separately for first order in equation (3.22) and second order in equation (3.23) and(3.24),

$$\begin{cases} \dfrac{dE(x_1)}{dt} = E(x_2) \\ \dfrac{dE(x_2)}{dt} = -2\mu E(x_2) - \delta E(x_2^{\,3}) - \omega_0^{\,2} E(x_1) - \alpha_3 E(x_1^{\,3}) + \varepsilon E(x_3) \\ \dfrac{dE(x_3)}{dt} = E(x_4) - \lambda_3 E(x_3) \\ \dfrac{dE(x_4)}{dt} = E(x_5) - \lambda_2 E(x_3) \\ \dfrac{dE(x_5)}{dt} = E(x_6) - \lambda_1 E(x_3) \\ \dfrac{dE(x_6)}{dt} = -\lambda_0 E(x_3) \end{cases} \tag{3.22}$$

$$\begin{cases} \dfrac{dE(x_1^{\,2})}{dt} = 2E(x_1 x_2) \\ \dfrac{dE(x_2^{\,2})}{dt} = -4\mu E(x_2^{\,2}) - 2\delta E(x_2^{\,4}) - 2\omega_0^{\,2} E(x_1 x_2) - 2\alpha_3 E(x_1^{\,3} x_2) + 2\varepsilon E(x_2 x_3) \\ \dfrac{dE(x_3^{\,2})}{dt} = 2E(x_3 x_4) - 2\lambda_3 E(x_3^{\,2}) \\ \dfrac{dE(x_4^{\,2})}{dt} = 2E(x_4 x_5) - 2\lambda_2 E(x_3 x_4) + 2\pi\gamma_3^{\,2} \\ \dfrac{dE(x_5^{\,2})}{dt} = 2E(x_5 x_6) - 2\lambda_1 E(x_3 x_5) \\ \dfrac{dE(x_6^{\,2})}{dt} = -2\lambda_0 E(x_3 x_6) \end{cases} \tag{3.23}$$

$$
\begin{cases}
\frac{dE(x_1x_2)}{dt} = E(x_2^{\,2}) - 2\mu E(x_1x_2) - 2\delta E(x_1x_2^{\,3}) - \omega_0^{\,2}E(x_1^{\,2}) - \alpha_3 E(x_1^{\,4}) + \varepsilon E(x_1x_3) \\
\frac{dE(x_1x_3)}{dt} = E(x_2x_3) + E(x_1x_4) - \lambda_3 E(x_1x_3) \\
\frac{dE(x_1x_4)}{dt} = E(x_2x_4) + E(x_1x_5) - \lambda_2 E(x_1x_3) \\
\frac{dE(x_1x_5)}{dt} = E(x_2x_5) + E(x_1x_6) - \lambda_1 E(x_1x_3) \\
\frac{dE(x_1x_6)}{dt} = E(x_2x_6) - \lambda_0 E(x_1x_3) \\
\frac{dE(x_2x_3)}{dt} = E(x_2x_4) - (\lambda_3 + 2\mu)E(x_2x_3) - \delta E(x_2^{\,3}x_3) - \omega_0^{\,2}E(x_1x_3) - \alpha_3 E(x_1^{\,3}x_3) + \varepsilon E(x_3^{\,2}) \\
\frac{dE(x_2x_4)}{dt} = -2\mu E(x_2x_4) - \delta E(x_2^{\,3}x_4) - \omega_0^{\,2}E(x_1x_4) - \alpha_3 E(x_1^{\,3}x_4) \\
\qquad\qquad +\varepsilon E(x_3x_4) + E(x_2x_5) - \lambda_2 E(x_2x_3) \\
\frac{dE(x_2x_5)}{dt} = \text{-}2\mu E(x_2x_5) - \delta E(x_2^{\,3}x_5) - \omega_0^{\,2}E(x_1x_5) - \alpha_3 E(x_1^{\,3}x_5) + \varepsilon E(x_3x_5) \\
\qquad\qquad + E(x_2x_6) - \lambda_1 E(x_2x_3) \\
\frac{dE(x_2x_6)}{dt} = \text{-}\lambda_0 E(x_2x_3) - 2\mu E(x_2x_6) - \delta E(x_2^{\,3}x_6) - \omega_0^{\,2}E(x_1x_6) \\
\qquad\qquad - \alpha_3 E(x_1^{\,3}x_6) + \varepsilon E(x_3x_6) \\
\frac{dE(x_3x_4)}{dt} = E(x_3x_5) - \lambda_2 E(x_3^{\,2}) + E(x_4^{\,2}) - \lambda_3 E(x_3x_4) \\
\frac{dE(x_3x_5)}{dt} = E(x_3x_6) - \lambda_1 E(x_3^{\,2}) + E(x_4x_5) - \lambda_3 E(x_3x_5) \\
\frac{dE(x_3x_6)}{dt} = -\lambda_0 E(x_3^{\,2}) + E(x_4x_6) - \lambda_3 E(x_3x_6) \\
\frac{dE(x_4x_5)}{dt} = E(x_4x_6) - \lambda_1 E(x_3x_4) + E(x_5^{\,2}) - \lambda_2 E(x_3x_5) \\
\frac{dE(x_4x_6)}{dt} = -\lambda_0 E(x_3x_4) + E(x_5x_6) - \lambda_2 E(x_3x_6) \\
\frac{dE(x_5x_6)}{dt} = -\lambda_0 E(x_3x_5) + E(x_6^{\,2}) - \lambda_1 E(x_3x_6)
\end{cases}
\tag{3.24}
$$

27 moment equations up to second order are derived above. Clearly, these 27 moment equations up to second order are not closed due to the higher order moment terms. If these higher moments are directly neglected, all nonlinearities of the equation are ignored. The Cumulant neglect method can close the equations without neglecting any nonlinearity of dynamical system. These 27 moment equations can be solved after closure of the higher order moments by the cumulant neglect method. The Cumulant neglect method includes both Gaussian and Non Gaussian methods. The cumulants are related to the statistical moments as follows (Stratonovich, 1963).

$$\begin{cases} E(x_j) = \kappa_1(x_j) \\ E(x_j x_k) = \kappa_2(x_j, x_k) + \kappa_1(x_j)\kappa_1(x_k) \\ E(x_j x_k x_l) = \kappa_3(x_j, x_k, x_l) + 3\{\kappa_1(x_j)\kappa_2(x_k, x_l)\}_s + \kappa_1(x_j)\kappa_1(x_k)\kappa_1(x_l) \\ E(x_j x_k x_l x_m) = \kappa_4(x_j, x_k, x_l, x_m) + 3\{\kappa_2(x_j, x_k)\kappa_2(x_l, x_m)\}_s + 4\{\kappa_1(x_j)\kappa_3(x_k, x_l, x_m)\}_s \\ \qquad\qquad + 6\{\kappa_1(x_j)\kappa_1(x_k)\kappa_2(x_l, x_m)\}_s + \kappa_1(x_j)\kappa_1(x_k)\kappa_1(x_l)\kappa_1(x_m) \end{cases} \tag{3.25}$$

where κ_i is the ith order cumulant of variable, $\{\bullet\}_s$ means a symmetrizing operation with respect to its all arguments and takes the arithmetic mean of different permuted terms similar to the one within the braces. For example,

$$\{\kappa_1(x_j)\kappa_2(x_k, x_l)\}_s = \frac{1}{3}\{\kappa_1(x_j)\kappa_2(x_k, x_l) + \kappa_1(x_k)\kappa_2(x_j, x_l) + \kappa_1(x_l)\kappa_2(x_j, x_k)\} \tag{3.26}$$

In the sense of Gaussian cumulant approximation, third and higher order cumulants are set to be zero. Equation (3.27) is substituted into the moment equations to close the moment equation system.

$$\begin{cases} E(x_i^3) = 0 \\ E(x_i^4) = 3E(x_i^2)^2 \\ E(x_i x_j^3) = 3E(x_i x_j)E(x_j^2) \end{cases} \tag{3.27}$$

Fig. 8 and Fig. 9 show the transient response of the root mean square rolling angle and rolling velocity. Both displacement and velocity will come to some stationary state under appropriate initial condition. Here since we did not give a divergence result; the system may not converge to the stationary state, which depends on the coefficients of the dynamical system and the initial conditions of the moment equations.

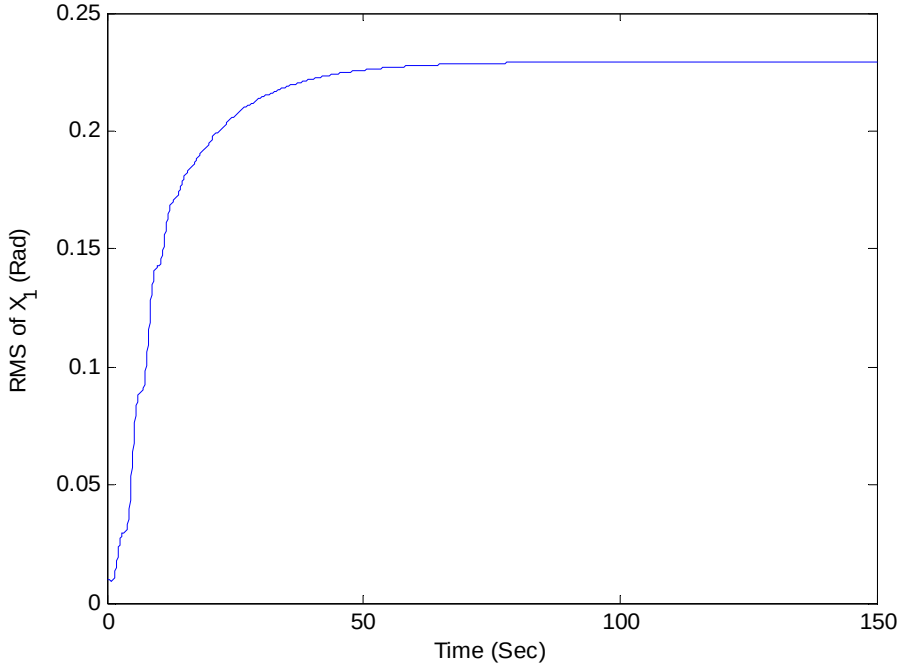

Fig. 8. Transient response of root mean square of rolling angle

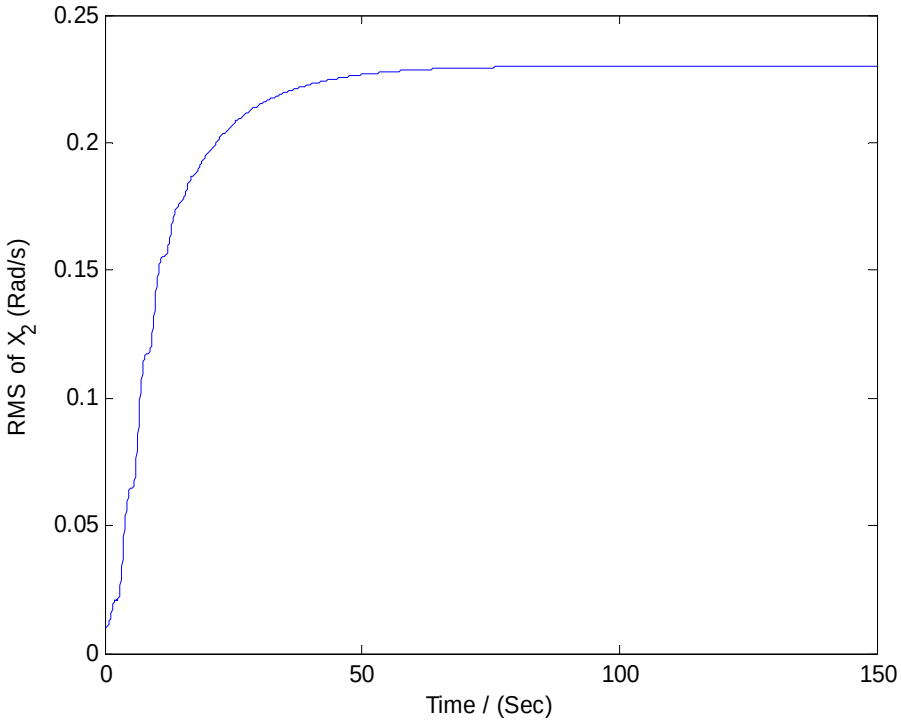

Fig. 9. Transient response of root mean square of rolling velocity

Fig. 10, Fig. 11 and Fig. 12 express the effect of the nonlinear damping coefficient, nonlinear stiffness and linear damping on the rolling response. Horizontal coordinates represent natural frequency of this dynamical system and vertical coordinates represent stationary response of root mean square of rolling displacement.

Bending direction of the curves does not appear reasonable compared with some conventional response amplitude curve with negative nonlinear stiffness, which bends to the left. Some of the curves even have more than two values with respect to same frequency, which is defined as a bifurcation phenomenon caused by nonlinearity of

dynamical system. Here we use ω_0 (the undamped natural frequency of the dynamical system)as the horizontal coordinate, and traditional amplitude curves are given by ω / ω_0, where ω represent the frequency of the harmonic excitation force and ω_0 is denominator there. So the stochastic response curves are still reasonable.

In Fig. 10, four different values of nonlinear damping coefficients were used. It is expected that the response of the dynamical system should decrease with increasing nonlinear damping. From Fig. 7, the excitation force spectrum has a peak frequency close to 1.0 Rad/s. The maximum of response in Fig. 10 also appears in that range. This can be viewed as a kind of 'resonance'. The difference of response is limited when the natural frequency ω_0 is far from the peak frequency of excitation force or excitation wave. Fig. 11 also adopts four different values of the nonlinear stiffness coefficient to analyze the response, including the zero case and three negative values. There is a significant difference in the low natural frequency range (left part of plot), compared to Fig. 10, but limited difference in the high natural frequency domain. Fig. 12 shows the effect of linear damping coefficient on the response curves. This result demonstrates one peak value at some special frequency. Linear damping seems more important than the nonlinear damping or stiffness coefficient comparing Fig. 10 and Fig. 11. By inspecting the 27 moment equations up to second order, it seems impossible to analyze the stochastic system by moment equation to above second order. There are 209 moment equations for up to fourth order moments. In order to handle this difficulty, an automatic neglect tool was designed and applied to the ship rolling motion to capture the response of Non-Gaussian effect.

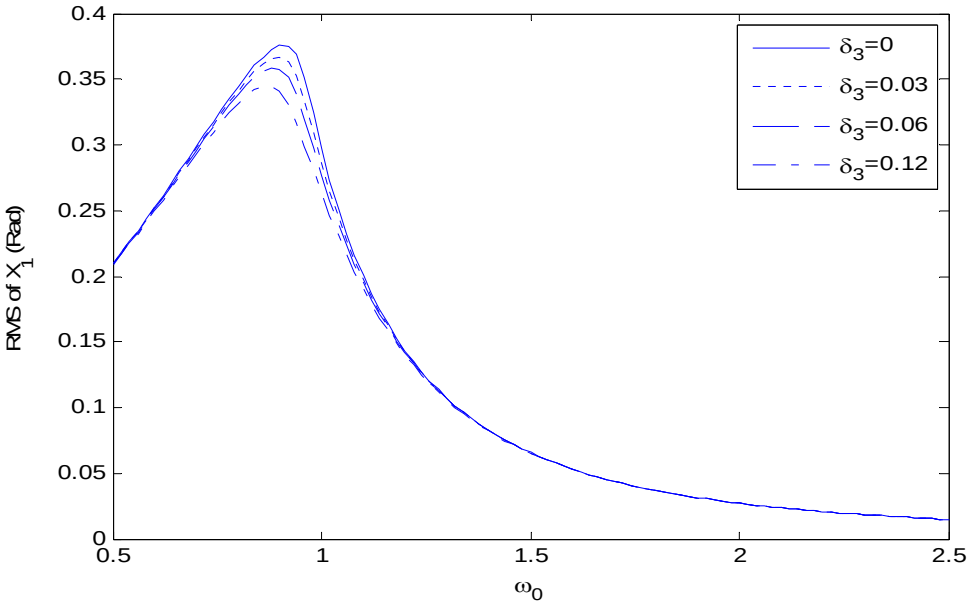

Fig. 10. Effect of nonlinear damping coefficient
on the root mean square (RMS) of rolling displacement

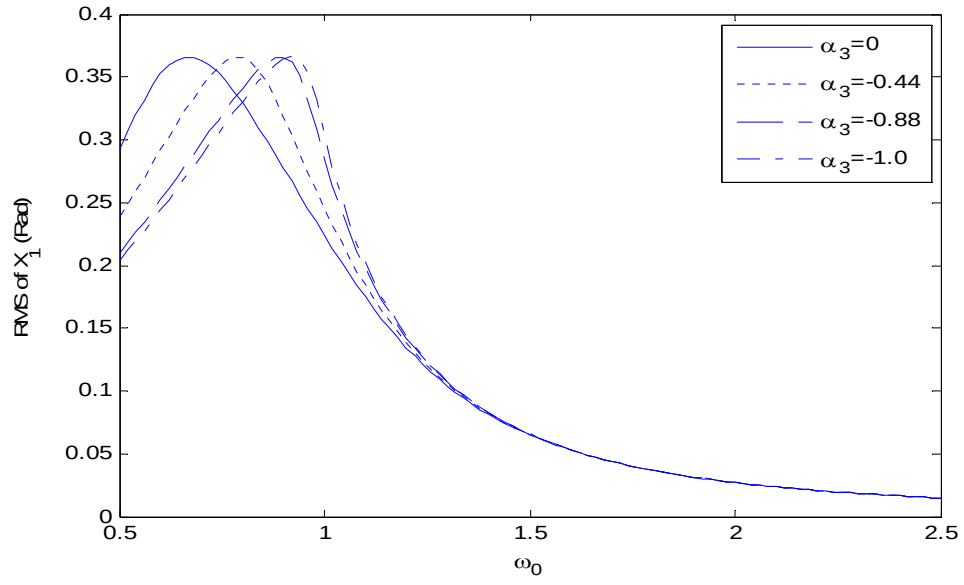

Fig. 11. Effect of nonlinear stiffness coefficient
on the root mean square (RMS) of rolling displacement

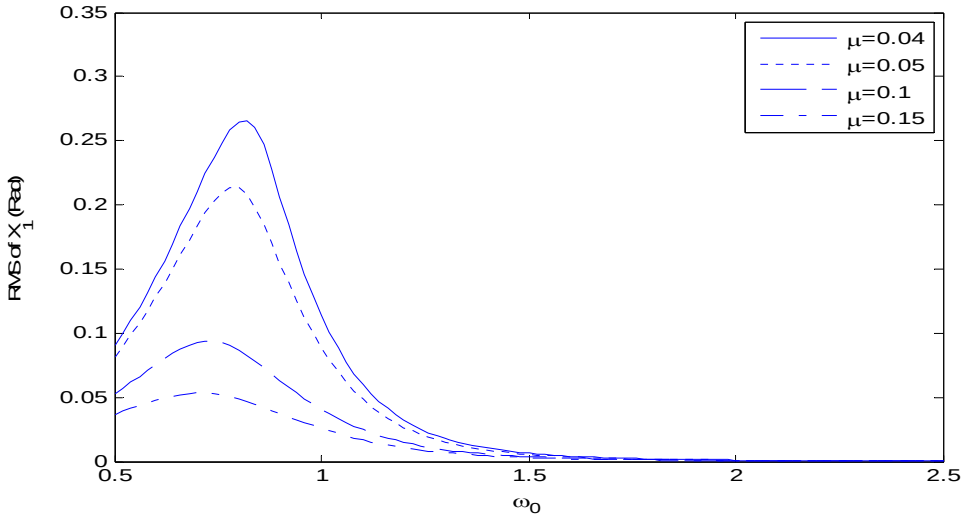

Fig. 12. Effect of linear stiffness coefficient
on the root mean square (RMS) of rolling displacement

3.2.2 The higher order cumulant neglect method with automatic neglect tool

In the cumulant closure technique, the response cumulants which are higher than some closure level are assumed to be smaller in comparison to those cumulants below the closure order and then can be neglected. To establish the relation between cumulants and ordinary moments, we consider the random vector $X^T = [x_1, x_1 \ldots\ldots x_n]$ with characteristic function(Soong and Grigoriu, 1993) as follows.

$$\phi(u_1, \cdots, u_n) = E\{\exp[j\sum_{i=1}^{n} u_i x_i]\} \tag{3.28}$$

where $j = \sqrt{-1}$, n is the dimension of the state space in the diffusion process, e.g. in equation (3.17), n=6. It can be expanded by Taylor series expansion in terms of ordinary moments $E\{x_i x_j \cdots\}$ or cumulants $\kappa\{x_i, x_j \cdots\}$. The expansion has two forms as follows

$$\phi_1(u_1,\cdots,u_n)=\exp\left\{j\sum_{i=1}^{n}u_i\kappa(x_i)+\frac{j^2}{2!}\sum_{i=1}^{n}\sum_{j=1}^{n}u_iu_j\kappa(x_i,x_j)+\cdots+\frac{j^C}{C!}\sum_{i=1}^{n}\cdots\sum_{C=1}^{n}u_i\cdots u_C\kappa(x_i,\cdots,x_C)+\cdots\right\} \tag{3.29}$$

$$\phi_2(u_1,\cdots,u_n)=1+j\sum_{i=1}^{n}u_iE(x_i)+\frac{j^2}{2!}\sum_{i=1}^{n}\sum_{j=1}^{n}u_iu_jE(x_ix_j)+\cdots+\frac{j^C}{C!}\sum_{i=1}^{n}\cdots\sum_{C=1}^{n}u_iu_j\cdots u_CE(x_ix_j\cdots x_C)+\cdots \tag{3.30}$$

here 'C' in equation (3.29)and (3.30) is the closure level and is a constant number. ϕ_1 and ϕ_2 are the same function with different expressions. Moments and cumulants can thus be found through the characteristic functions.

$$E(x_1^{k_1}\cdots x_n^{k_n})=\frac{1}{j^k}\frac{\partial^k\phi_1}{\partial u_1^{k_1}\cdots\partial u_n^{k_n}}\bigg|_{u_1=\cdots u_n=0} \tag{3.31}$$

$$\kappa(x_1^{k_1},\cdots,x_n^{k_n})=\frac{1}{j^k}\frac{\partial^k\ln\phi_2}{\partial u_1^{k_1}\cdots\partial u_n^{k_n}}\bigg|_{u_1=\cdots u_n=0} \tag{3.32}$$

where $k=k_1+k_2+\cdots k_n$. Cumulants of order higher than the closure order 'C' can be set equal to zero and moments higher than that closure order will be written in terms of moments of order less than or equal to that closure level. The stochastic system equation (3.17) has 6 state space variables, so n=6 in the characteristic function ϕ_1 and ϕ_2. The non-Gaussian cumulant neglect method up to fourth order will involve 209 equations, which is an extremely large, complex and nearly impossible system to find a solution to by hand. The automatic procedure algorithm is described in Fig. 13. Compared with the algorithm process in Wojtkiewicz's dissertation (Wojtkiewicz, 2000), the algorithm

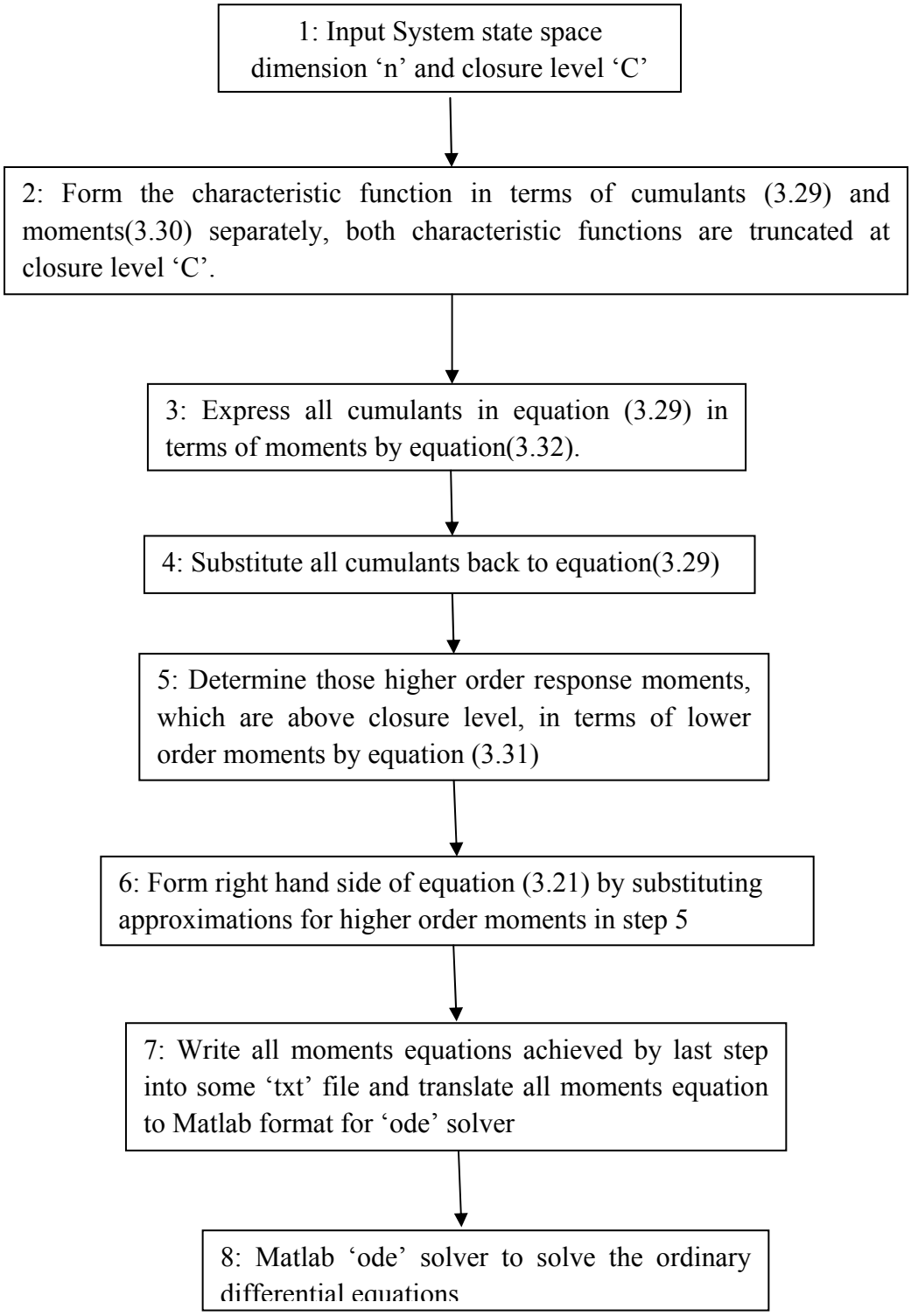

Fig. 13. Automatic Cumulant Neglect Tool procedure

developed here takes advantage of two different expansions for the characteristic function, i.e., equation (3.29) and (3.30). This avoids the difficulty of substitution between the cumulants and the moments. Steps 1 to 7 generate the closed moment equations using MAPLE and all moment equations are written into a 'txt' file and then translated to the MATLAB format for the 'ode' solver in MATLAB. Step 8 takes advantages of the efficiency and convenience of the MATLAB ordinary differential equation solver.

3.2.2.1 Application to Stochastic Dynamical Systems with Analytical Solutions

Several precautions should be taken to the algorithm before programming the tools in MAPLE and MATLAB. To reduce memory load and computational speed, the symmetry of moments and cumulants require consideration to avoid repeating them. For example, $E(x_1x_2)$ and $E(x_2x_1)$ are equivalent mathematically. In step 4, after substituting all cumulants back into equation(3.29), the characteristic function ϕ_1 is in terms of moments with order less than or equal to closure level 'C'.

Case 1

A simple Duffing oscillator with white noise excitation and nonlinear hardening stiffness (Wojtkiewicz, 2000) is first analyzed to validate the accuracy of the automatic neglect tool.

$$\begin{cases} \dot{x}_1 = x_2 \\ \dot{x}_2 = -2\zeta\omega_0 x_2 - \omega_0^2 \mathrm{x}_1 - \varepsilon\omega_0^2 \mathrm{x}_1^{\,3} + W(t) \end{cases} \tag{3.33}$$

where $W(t)$ is a Gaussian white noise with zero mean and correlation:

$$E[W(t_1)W(t_2)] = 2D\delta(\tau), \quad \tau = t_2 - t_1 \tag{3.34}$$

Parameters of the system are given by

$$\varepsilon = 0.1,\ D = 0.4,\ \zeta{=}0.2,\ \omega_0 = 1 \tag{3.35}$$

An analytical solution exists for the stationary probability density function of the system defined in(3.33), which is given by

$$p(x_1, x_2) = C_0 \exp(-\frac{2\zeta\omega_0}{D}(\frac{x_2^2}{2} + \frac{\omega_0^2 x_1^2}{2} + \frac{\varepsilon\omega_0^2 x_1^4}{4})) \tag{3.36}$$

and C_0 is the normalization constant, response moment can be easily calculated from this analytical function. Fig. 14 indicates that the response has only one peak, as does a Gaussian response.

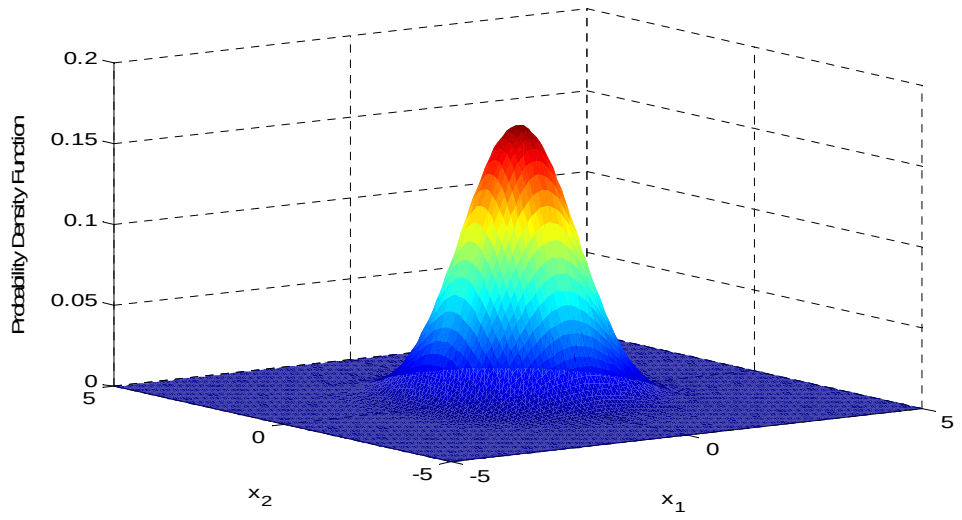

Fig. 14. Analytical probability density function of unimodal Duffing oscillator

To verify the automatic neglect tool developed above, the mean square of displacement is calculated and compared with the exact result from equation (3.36) and the numerical

result from the reference(Wojtkiewicz, 2000). With the Itô differential rule, moment equations are given by,

$$\begin{aligned}\frac{dE(p,q)}{dt} &= pE(p-1,q+1)-\omega^2 qE(p+1,q-1)-\varepsilon\omega^2 qE(p+3,q-1)\\ &\quad -2\zeta\omega qE(p,q)+Dq(q-1)E(p,q-2)\end{aligned} \tag{3.37}$$

where $E(x_1^p x_2^q)=E(p,q)$. The moment term $E(p+3,q-1)$ is a higher order moment, which needs to be approximated by the lower order moments through the cumulant neglect method. Transient and stationary response of displacement and velocity are given in Fig. 15 and Fig. 16. Table 2 lists the computational result by the algorithm developed above, results from the reference (Wojtkiewicz, 2000) and the exact result. The comparison indicates the accuracy of the automatic neglect tool. Here we just computed the response up to 8th order; the automatic tool can provide even higher order.

For the stationary displacement statistics, second order cumulant neglect, which is Gaussian closure and equivalent to the method of statistical linearization, underestimates the true response about 15%. However there is only 0.1% error left when increasing the neglect order to four. Even more accurate result can be achieved when applying the 6th and 8th order. Velocity x_2 is a Gaussian variable, therefore all closure order provides exact stationary statistical response, which is unity and shown in Fig. 16.

With the analytical solution, it seems that we easily investigated the accuracy of the closure method. But it is necessary to mention that the response of this dynamical system is close to Gaussian, which means that the response probability density function has a unimodal peak, that is bell shaped and close to the Gaussian distribution. We will now apply the cumulant to more systems for better understanding.

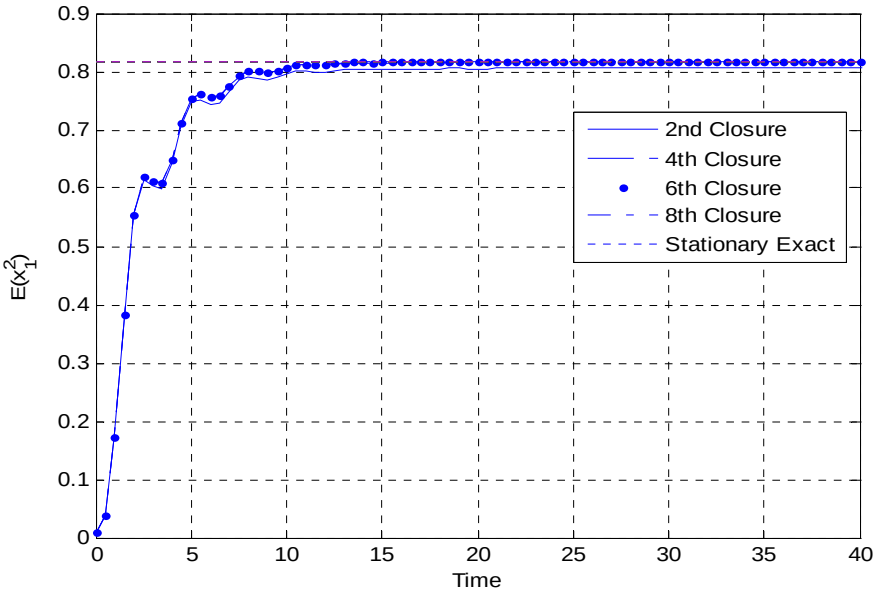

Fig. 15. Mean square of displacement with different cumulant neglect order

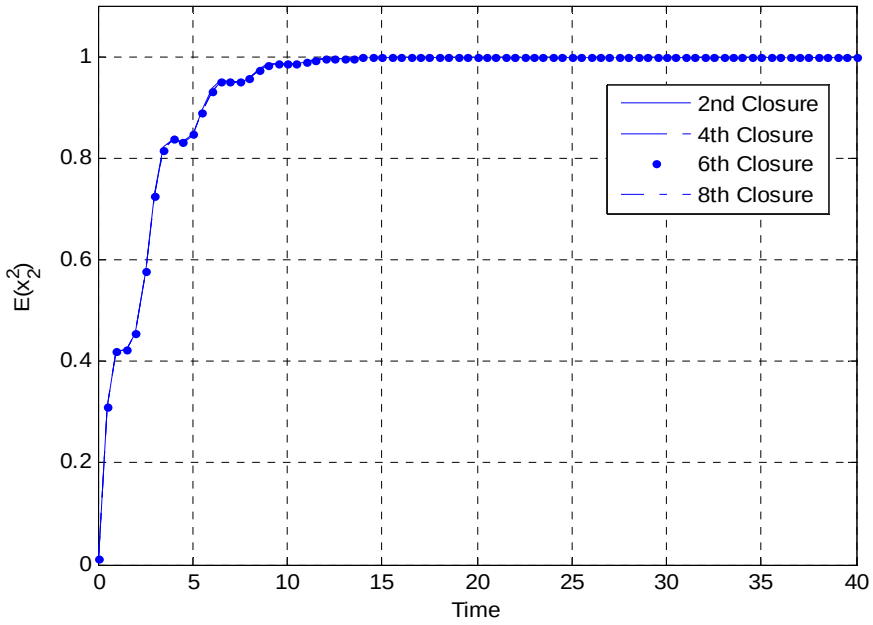

Fig. 16. Mean square of velocity with different cumulant neglect order

Table 2. Comparison of stationary mean square displacement of the unimodal Duffing 0scillator

Closure Level	$E(x_1^2)$			
	Result by Fig. 13	Result from (Wojtkiewicz, 2000)	Error for E(x1^2)	Exact
Second Order Cumulant Neglect	0.805401	0.8054	1.49%	0.81756
Fourth Order Cumulant Neglect	0.816497	0.8165	0.13%	
Six Order Cumulant Neglect	0.817374	0.8174	0.02%	
Eighth Order Cumulant Neglect	0.817511	0.8175	0.01%	

Case 2

To further investigate the application of the cumulant neglect method, we applied the automatic tool to a four dimensional dynamical system(Er, 2000b), which will also have a near Gaussian response with an analytical probability density function. It is expected that the accuracy of response will increase with increasing of the closure order. The four dimensional dynamical system is given by a two degree of freedom system:

$$\begin{cases} \ddot{Y}_1 + \frac{1}{2}a_1(s_{11}\dot{Y}_1 + 2a_2 s_{12}\dot{Y}_2) + 2a_3 Y_1 + 4a_4 Y_1^3 + 6a_5 Y_1^5 = W_1(t) \\ \ddot{Y}_2 + \frac{1}{2}a_1[2(1-a_2)s_{12}\dot{Y}_1 + s_{22}\dot{Y}_2] + 2a_6 Y_2 + 4a_7 Y_2^3 + 6a_8 Y_2^5 = W_2(t) \end{cases} \tag{3.38}$$

where $a_1, a_2, a_3, \ldots a_8$ are constant numbers and the white noises are defined by,

$$E[W_i(t_1)W_j(t_2)] = s_{ij}\delta(\tau), \quad \tau = t_2 - t_1 \text{ and } i, j = 1,2 \tag{3.39}$$

The system is written in state space format as following:

$$\begin{cases} \dot{x}_1 = x_2 \\ \dot{x}_2 = -\frac{1}{2}a_1(s_{11}x_2 + 2a_2 s_{12}x_4) - 2a_3 x_1 - 4a_4 x_1^3 - 6a_5 x_1^5 + W_1(t) \\ \dot{x}_3 = x_4 \\ \dot{x}_4 = -\frac{1}{2}a_1[2(1-a_2)s_{12}x_2 + s_{22}x_4] - 2a_6 x_3 - 4a_7 x_3^3 - 6a_8 x_3^5 + W_2(t) \end{cases} \tag{3.40}$$

where $Y_1 = x_1, \ \dot{Y}_1 = x_2, \ Y_2 = x_3, \ \dot{Y}_2 = x_4,$

Parameters are given as below,

$$\begin{aligned} &\mathrm{a}_1 = 1; \mathrm{a}_3 = 1; \mathrm{a}_4 = 1; \mathrm{a}_5 = 0.5; \mathrm{a}_7 = 0.5; \mathrm{a}_6 = 1.5; \mathrm{a}_8 = 0.2; \\ &\mathrm{s}_{11} = 2; \mathrm{s}_{22} = 2; \ \ \mathrm{s}_{12}, \ \ \mathrm{a}_2 = \textit{arbitrary number} \end{aligned} \tag{3.41}$$

The analytical probability density function is given by (Scheurkogel and Elishakoff, 1988) with normalization constant.

$$\begin{aligned} p(x_1, x_2, x_3, x_4) = C \exp\{-a_1[\frac{1}{2}(x_2^2 + x_4^2) + a_3 x_1^2 + a_4 x_1^4 \\ + a_5 x_1^6 + a_6 x_3^2 + a_7 x_3^4 + a_8 x_3^6]\} \end{aligned} \tag{3.42}$$

The analytical equation (3.42) could be verified by substituting the PDF formula back to the associated Fokker Planck Equation, equation(3.43),

$$\begin{aligned} \frac{\partial p}{\partial t} = &-\frac{\partial[x_2 p]}{\partial x_1} - \frac{\partial[[-\frac{1}{2}a_1(s_{11}x_2 + 2a_2 s_{12}x_4) - 2a_3 x_1 - 4a_4 x_1^3 - 6a_5 x_1^5]p]}{\partial x_2} \\ &-\frac{\partial[x_4 p]}{\partial x_3} - \frac{\partial[[-\frac{1}{2}a_1[2(1-a_2)s_{12}x_2 + s_{22}x_4] - 2a_6 x_3 - 4a_7 x_3^3 - 6a_8 x_3^5]p]}{\partial x_4} \\ &+\frac{1}{2}s_{11}\frac{\partial^2 p}{\partial x_2^2} + \frac{1}{2}s_{22}\frac{\partial^2 p}{\partial x_4^2} + s_{12}\frac{\partial^2 p}{\partial x_2 \partial x_4} \end{aligned} \tag{3.43}$$

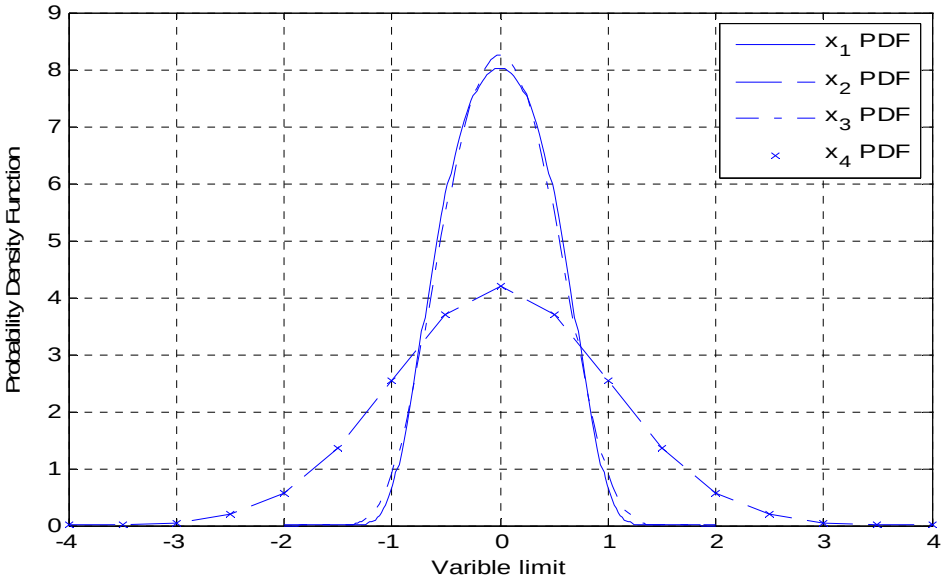

Fig. 17. Analytical probability density function of x_1 x_2 x_3 and x_4

The probability density function plots in Fig. 17 all have bell shaped curves for each variable, which indicates that variables in this dynamical system may have Gaussian or near Gaussian response. With the Itô differential rule, the moment equation is given by,

$$\begin{aligned} \mathrm{d}E(\mathrm{p},\,\mathrm{q},\,\mathrm{r},\,\mathrm{s}) = {} & \mathrm{p}E(\mathrm{p}\text{-}1,\,\mathrm{q}+1,\,\mathrm{r},\,\mathrm{s}) + \mathrm{q}(-(1/2)\mathrm{a}_1\mathrm{s}_{11}E(\mathrm{p},\,\mathrm{q},\,\mathrm{r},\,\mathrm{s}) \\ & -\mathrm{a}_1\mathrm{a}_2\mathrm{s}_{12}E(\mathrm{p},\,\mathrm{q}\text{-}1,\,\mathrm{r},\,\mathrm{s}+1) - 2\mathrm{a}_3E(\mathrm{p}+1,\,\mathrm{q}\text{-}1,\,\mathrm{r},\,\mathrm{s}) \\ & -4\mathrm{a}_4E(\mathrm{p}+3,\,\mathrm{q}\text{-}1,\,\mathrm{r},\,\mathrm{s}) - 6\mathrm{a}_5E(\mathrm{p}+5,\,\mathrm{q}\text{-}1,\,\mathrm{r},\,\mathrm{s})) \\ & +\mathrm{r}E(\mathrm{p},\,\mathrm{q},\,\mathrm{r}\text{-}1,\,\mathrm{s}+1) + \mathrm{s}(-\mathrm{a}_1(1-\mathrm{a}_2)\mathrm{s}_{12}E(\mathrm{p},\,\mathrm{q}+1,\,\mathrm{r},\,\mathrm{s}\text{-}1) \\ & -(1/2)\mathrm{a}_1\mathrm{s}_{22}E(\mathrm{p},\,\mathrm{q},\,\mathrm{r},\,\mathrm{s}) - 2\mathrm{a}_6E(\mathrm{p},\,\mathrm{q},\,\mathrm{r}+1,\,\mathrm{s}\text{-}1) \\ & -4\mathrm{a}_7E(\mathrm{p},\,\mathrm{q},\,\mathrm{r}+3,\,\mathrm{s}\text{-}1) - 6\mathrm{a}_8E(\mathrm{p},\,\mathrm{q},\,\mathrm{r}+5,\,\mathrm{s}\text{-}1)) \\ & +(1/2)\mathrm{s}_{11}\mathrm{q}(\mathrm{q}\text{-}1)E(\mathrm{p},\,\mathrm{q}\text{-}2,\,\mathrm{r},\,\mathrm{s}) \\ & +(1/2)\mathrm{s}_{22}\mathrm{s}(\mathrm{s}\text{-}1)E(\mathrm{p},\,\mathrm{q},\,\mathrm{r},\,\mathrm{s}\text{-}2) + \mathrm{s}_{12}\mathrm{q}\mathrm{s}E(\mathrm{p},\,\mathrm{q}\text{-}1,\,\mathrm{r},\,\mathrm{s}\text{-}1) \end{aligned} \tag{3.44}$$

where $E(\mathrm{p},\,\mathrm{q},\,\mathrm{r},\,\mathrm{s}) = E(x_1^p x_2^p x_3^r x_4^s)$, there are four moments in the right hand side of equation (3.44) which might need to be approximated by the cumulant neglect method

when the order is higher than the closure level, including $E(\mathrm{p+3},\ \mathrm{q\text{-}1},\ \mathrm{r},\ \mathrm{s})$, $E(\mathrm{p+5},\ \mathrm{q\text{-}1},\ \mathrm{r},\ \mathrm{s})$, $E(\mathrm{p},\ \mathrm{q},\ \mathrm{r+3},\ \mathrm{s\text{-}1})$, $E(\mathrm{p},\ \mathrm{q},\ \mathrm{r+5},\ \mathrm{s\text{-}1})$. As expected, the cumulant neglect methods and moment equations successfully increase the accuracy of statistics of the non Gaussian variables x_1 and x_3 by increasing the closure order in Fig. 18 and Fig. 19. Table 3 lists the error associated with the different closure level. We conclude that the fourth order cumulant neglect method greatly reduces the error compared with the Gaussian closure. Fig. 20 and Fig. 21 are the variances for velocities x_2 , x_4 , there is no difference with increasing closure level, as the velocity variables are Gaussian distributed.

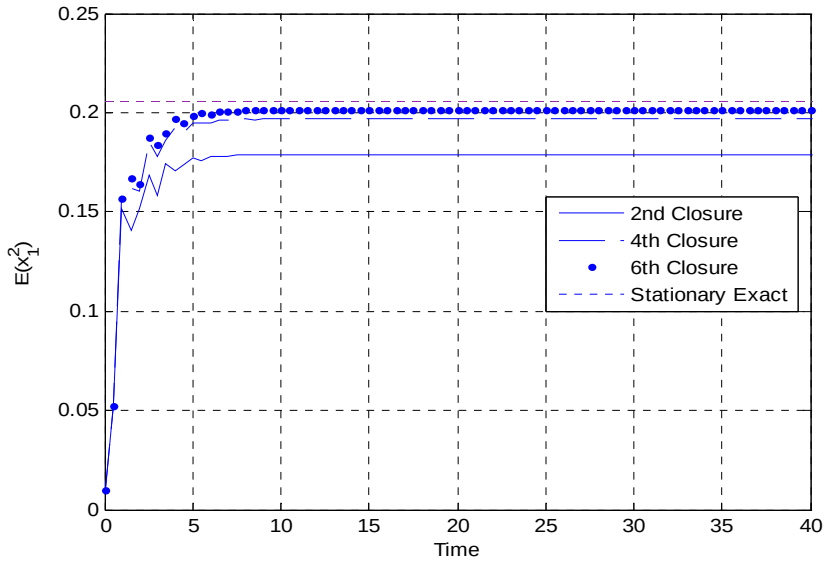

Fig. 18. Mean square of x_1 with different cumulant neglect order and exact solution

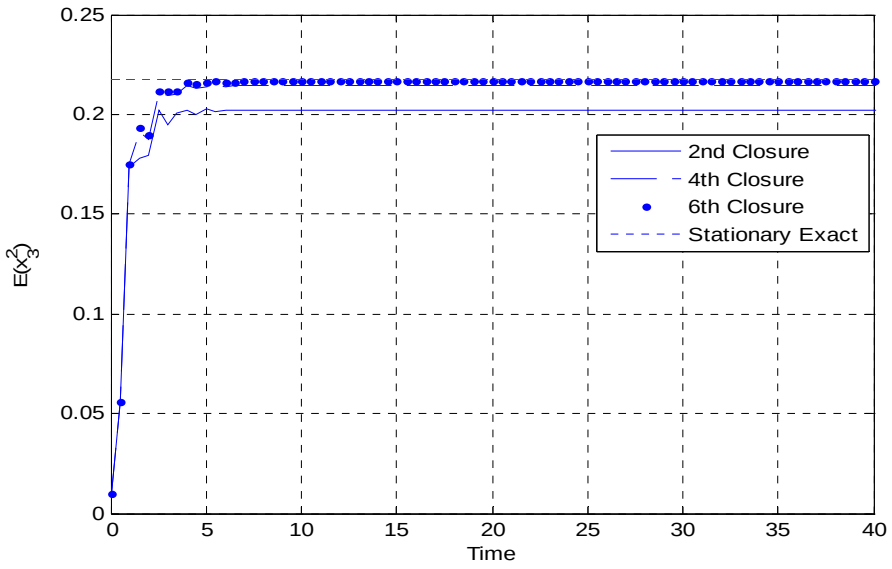

Fig. 19. Mean square of x_3 with different cumulant neglect order and exact solution

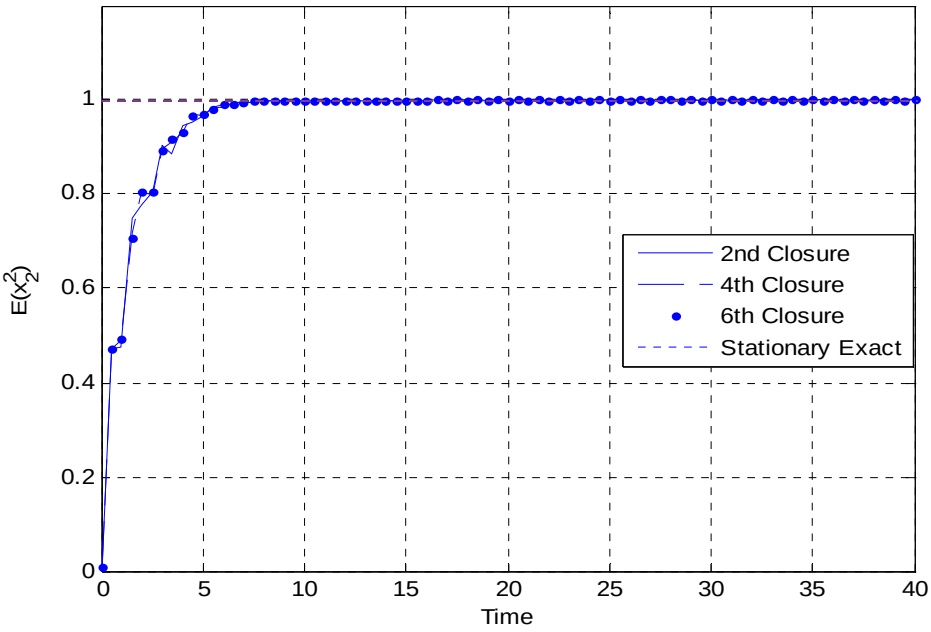

Fig. 20. Mean square of x_2 with different cumulant neglect order and exact solution

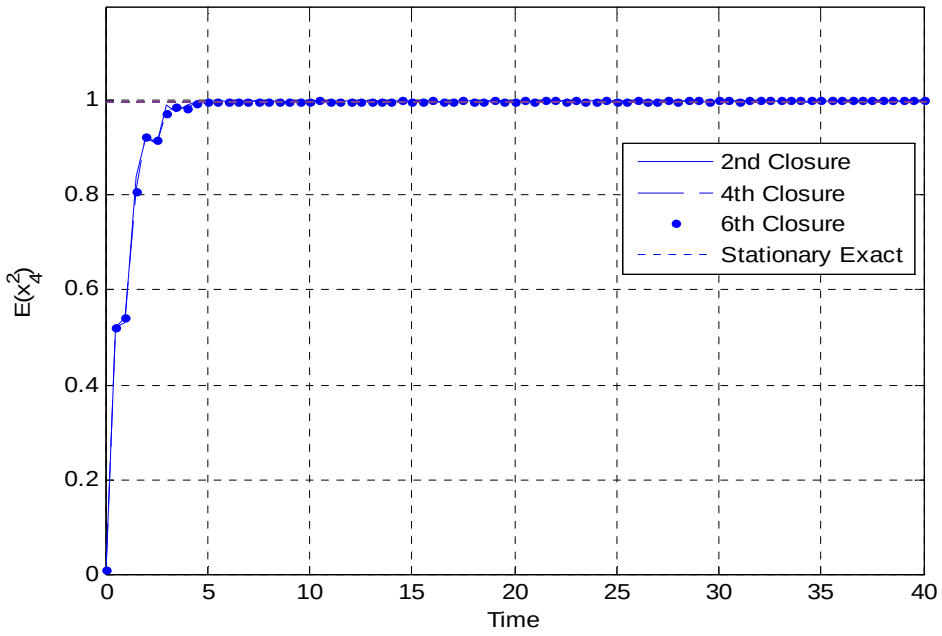

Fig. 21. Mean square of x_4 with different cumulant neglect order and exact solution

Table 3. Comparison of stationary mean square of state variables with different closure level and exact stationary value

Closure Level	Stationary $E(x_1^2)$	Error for $E(x_1^2)$	Stationary $E(x_2^2)$	Stationary $E(x_3^2)$	Error for $E(x_3^2)$	Stationary $E(x_4^2)$
2nd Order	0.1789	12.99%	1.00	0.2021	7.34%	1.00
4th Order	0.1968	4.28%	1.00	0.2143	1.41%	1.00
6th Order	0.2014	2.04%	1.00	0.2164	0.39%	1.00
Exact	0.2056		1.00	0.2172		1.00

Case3

Both analytical solutions for case 1 and case 2 are close to the Gaussian distribution, and cumulant neglect and moment equations perform excellently. In case 3, we will test a simple one dimensional dynamical system with obvious non-Gaussian behavior.

Considering the following stochastic differential equation with only additive noise (Er, 2000a):

$$\dot{z} = (z - z^3 - \alpha z^5) / 2 + W(t) \tag{3.45}$$

where α is a constant and the Gaussian white noise is defined as $E[W(t)W(t+\tau)] = q\delta(\tau)$ and q is also a constant. The analytical stationary PDF of z is known to be

$$p(z) = c\exp[\frac{1}{2q}(z^2 - \frac{z^4}{2} - \alpha\frac{z^6}{3})] \tag{3.46}$$

where c is the normalization constant. For α=0.05, q=2, the PDF is given in Fig. 22, and the plot indicates that z is a non-Gaussian variable.

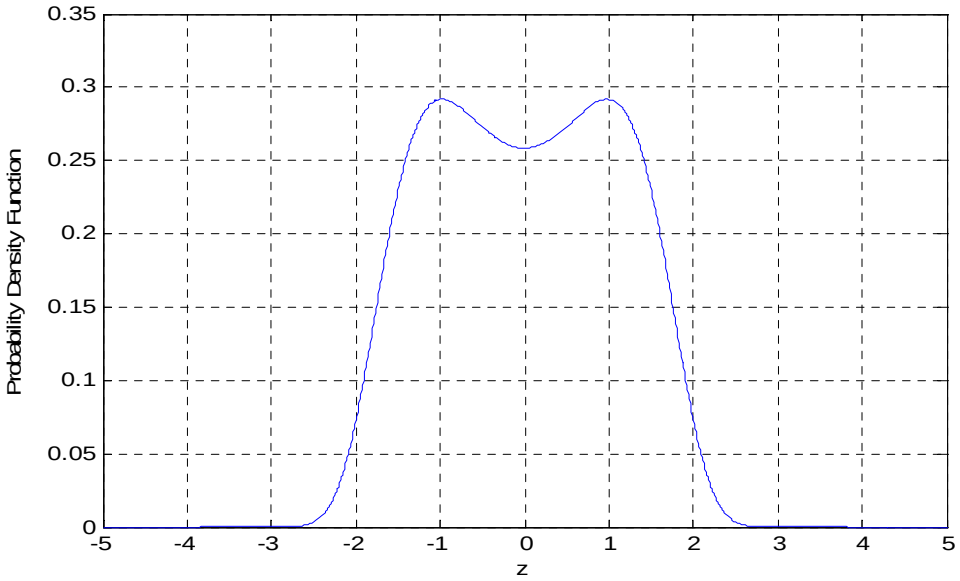

Fig. 22. Analytical probability density function of z

The moment equations for the one dimensional system are derived following the Itô differential rule, with $E(z^p) = E(p)$,

$$\frac{dE(p)}{dt} = \frac{1}{2}p[E(p) - E(p+2) - \alpha E(p+4)] + \frac{1}{2}qp(p-1)E(p-2) \qquad (3.47)$$

The transient and stationary response of variance of z with different closure level is in given Fig. 23 and Table 4 shows that there is still 7.98% difference even with 10th order cumulant neglect method, which could be explained by the plot in Fig. 22. The true stationary response does not have a bell-shaped PDF, but two peaks.

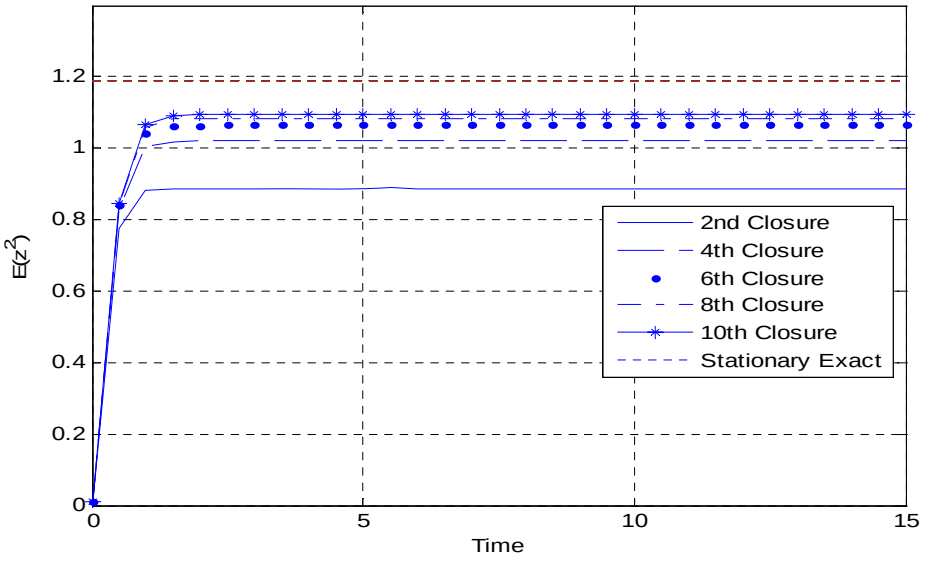

Fig. 23. Mean square of z with different cumulant neglect order and exact solution

Table 4. Comparison of stationary mean square of z with different closure level and exact stationary value

Closure Level	Stationary E(z^2)	Error for E(z^2)
2nd Order	0.8883	25.32%
4th Order	1.0199	14.25%
6th Order	1.0645	10.50%
8th Order	1.0843	8.84%
10th Order	1.0945	7.98%
Exact	1.1894	

Case4

Case1, case2 and case3 only have additive excitation. We consider a dynamical system with both multiplicative and additive stochastic noise, given in the following equation,

$$\ddot{x} + \alpha\dot{x} + \eta(x + \gamma\dot{x})^2\dot{x} + \lambda x^5 = (ax + b\dot{x})W_1(t) + W_2(t) \tag{3.48}$$

where $\alpha > 0, \eta > 0$ and $ab > 0$ Gaussian white noise $W_1(t)$ and $W_2(t)$ are independent with correlation function $E[W_i(t)W_i(t+\tau)] = 2\pi K_{ii}\delta(\tau)\ \ (i = 1,2)$. The system belongs to the generalized stationary potential when the following conditions are satisfied (Lin and Cai, 2004):

$$\gamma = \frac{b}{a}, \qquad \eta = \frac{K_{11}}{K_{22}}a^2(\alpha + \pi K_{11}b^2) \tag{3.49}$$

The stationary joint probability density function is given by equation (3.50) and the marginal PDF is given in Fig. 24,

$$p(x_1, x_2) = c\exp\{-\frac{\alpha + \pi K_{11} b^2}{2\pi K_{22}}[x_2^2 + \pi K_{11} a b x_1^2 + \lambda \frac{x_1^6}{3}]\} \tag{3.50}$$

where c is the normalization constant, and $x = x_1, \dot{x} = x_2$. It is noted that the term $\pi K_{11} a b x_1^2$ in the PDF equation is from the Wong-Zakai correction term due to the parametric excitation. We assume $K_{11} = K_{22} = 1/(2\pi)$, $\eta = 1.5$, $\gamma = \alpha = a = b = \lambda = 1$ for the computation.

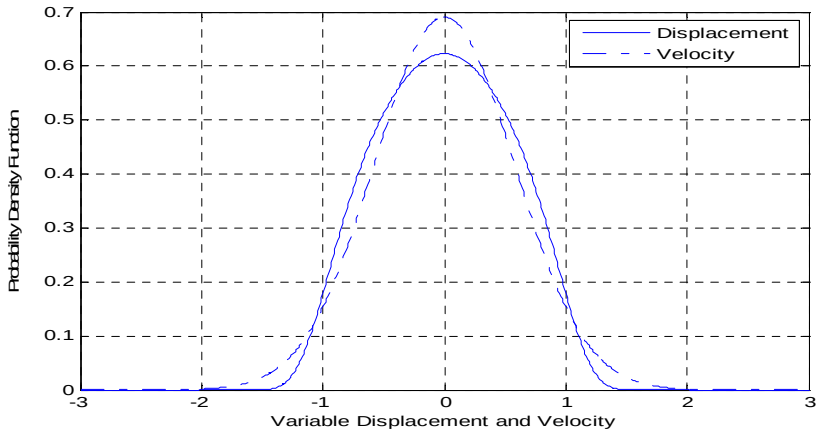

Fig. 24. Analytical probability density function of x and $\dot{x}$

The moment equations for the two dimensional system with multiplicative and additive noise are derived following the Itô differential rule with Wong-Zakai correction terms,

$$\begin{aligned} dE(p,q) = {} & pE(p-1,q+1) + q(-\alpha E(p,q) - \eta(E(p+2,q) \\ & + \gamma^2 E(p,q+2) + 2\gamma E(p+1,q+1) - \lambda E(p+5,q-1) \\ & + \pi K_{11}(a^2 E(p+1,q-1) + b^2 E(p,q))) + \pi K_{11} q(q-1)(a^2 E(p+2,q-2) \\ & + b^2 E(p,q) + 2abE(p+1,q-1) + \pi K_{22} q(q-1)E(p,q-2)) \end{aligned} \tag{3.51}$$

where $E(\mathrm{p},\ \mathrm{q})=E(x_1^p x_2^p)$ The marginal PDF of displacement and velocity in Fig. 24 have Gaussian or nearly Gaussian response, it is expected that cumulant neglect method with moment equation will give more accurate solution with neglect order increasing. Second to sixth order closure are applied to the parametric system, Fig. 25 and Fig. 26 display the evolution to stationary statistics for both displacement and velocity. As discussed in the previous cases, the velocity variable is Gaussian distributed, so all different closure gives same solution. While the displacement is a non Gaussian variable, the higher order closure predicts a better estimation. However, instability happens when increasing the closure order to eight as shown in Fig. 27 and Fig. 28. The question is whether this instability is just a mathematical error or mistakes from the methodology. Further research is necessary to address this problem.

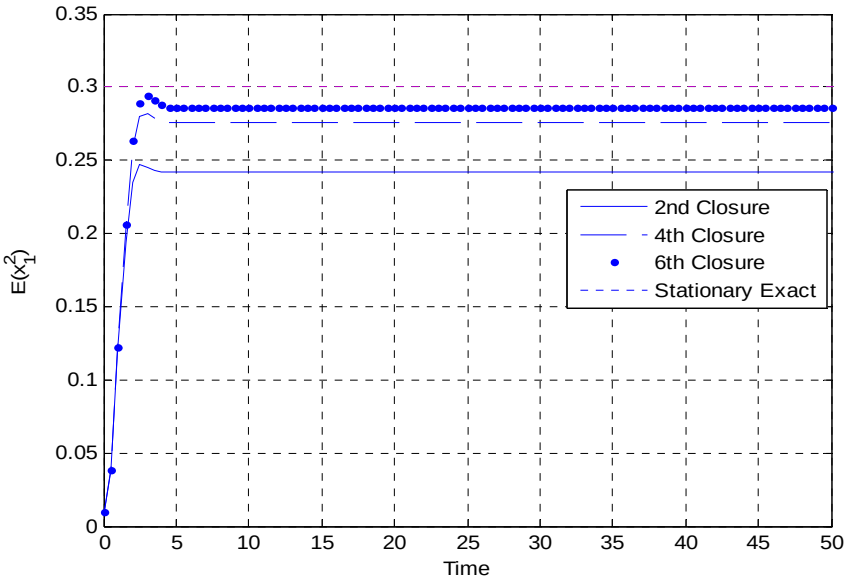

Fig. 25. Mean square of x_1 with different cumulant neglect order and exact solution

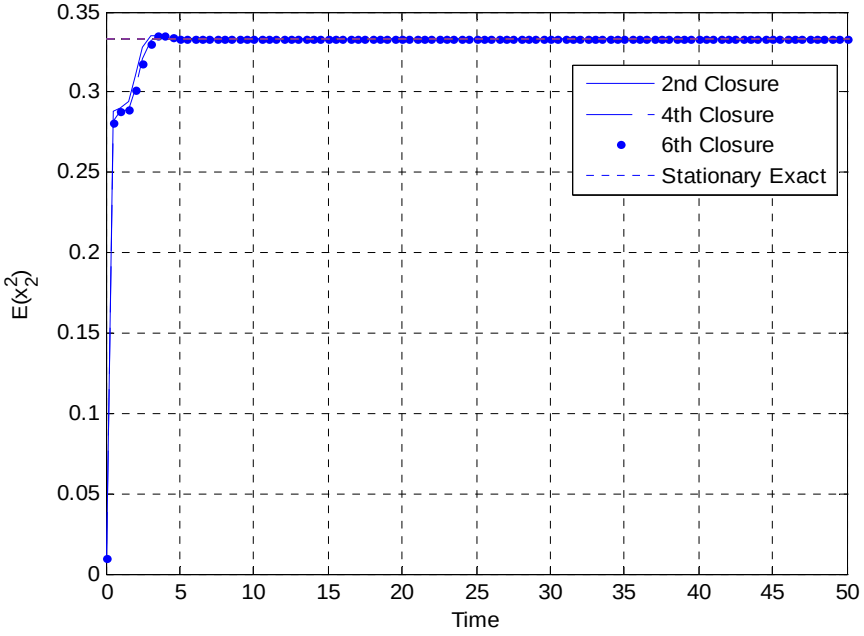

Fig. 26. Mean square of x_2 with different cumulant neglect order and exact solution

Table 5. Comparison of stationary mean square of x_1 and x_2 with different closure level and exact stationary value

Closure Level	Stationary E(x1^2)	Error for E(x1^2)	Stationary E(x2^2)	Error for E(x2^2)
2nd Order	0.2419	19.34%	0.3333	0.00%
4th Order	0.2758	8.04%	0.3333	0.00%
6th Order	0.2865	4.47%	0.3333	0.00%
Exact	0.2999		0.3333	

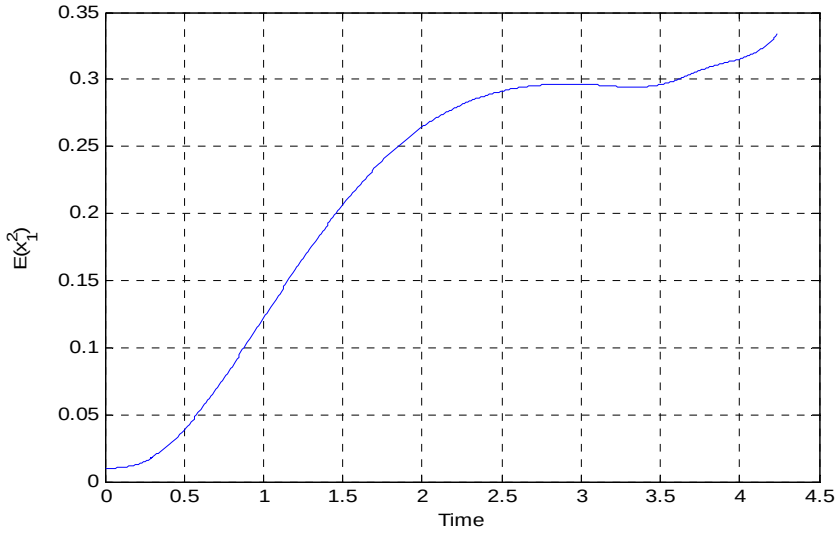

Fig. 27. Instability of cumulant neglect method with 8th order closure for mean square of x_1

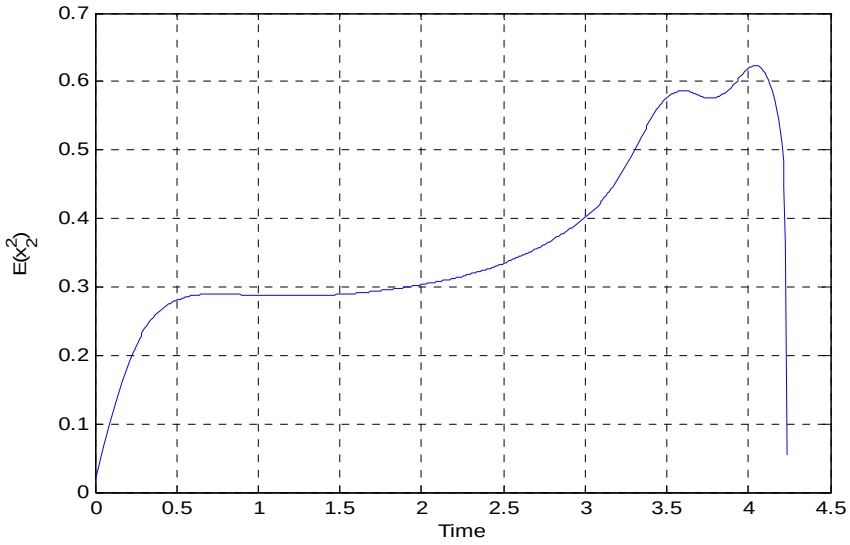

Fig. 28. Instability of cumulant neglect method with 8th order closure for mean square of x_2

Case5

The bimodal Duffing oscillator was considered to investigate the limitation of cumulant neglect method (Wojtkiewicz, 2000). The stochastic dynamical system is given by

$$\begin{cases} \dot{x}_1 = x_2 \\ \dot{x}_2 = -2\zeta\omega_0 x_2 + \omega_0^2 \mathrm{x}_1 - \varepsilon\omega_0^2 \mathrm{x}_1^{\ 3} + W(t) \end{cases} \tag{3.52}$$

The only difference from *case1* is the negative linear stiffness. All parameters are same with the dynamical system defined in equation(3.33). Analytical joint probability density function is given by below equation and plotted in Fig. 29 and Fig. 30, which indicates that the response has obviously double peaks, thus non-Gaussian behavior,

$$p(x_1, x_2) = C_0 \exp(-\frac{2\zeta\omega_0}{D}(\frac{x_2^2}{2} - \frac{\omega_0^2 x_1^2}{2} + \frac{\varepsilon\omega_0^2 x_1^4}{4})) \tag{3.53}$$

The cumulant neglect applications with different closure order (2nd to 6th order) are displayed in Fig. 31, Fig. 32 and Table 6. Since velocity is a Gaussian variable, all level closure provides the exact result. But the accuracy for displacement variable is much less attractive; there is very limited progress with higher order neglect method. The performance of 8th order neglect method is same as the previous example; further research is needed to understand the instability of the algorithm.

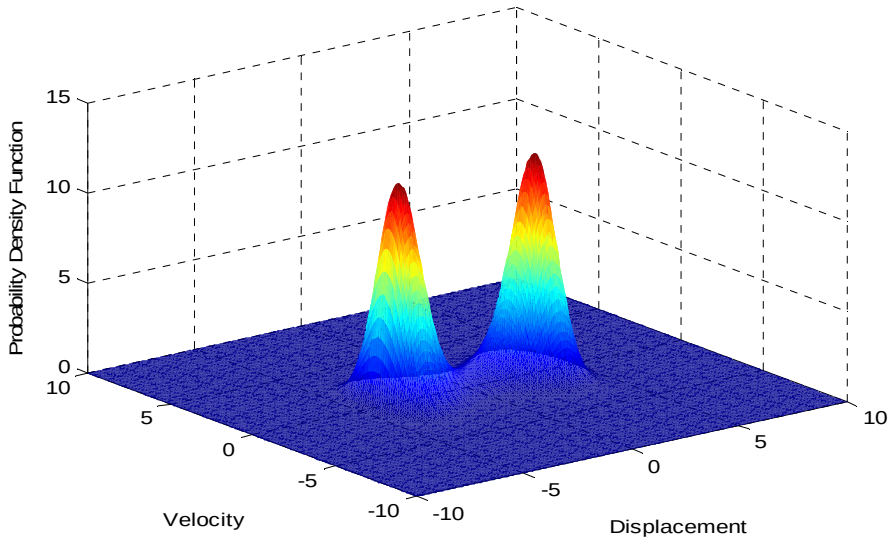

Fig. 29. Analytical probability density function of bimodal Duffing oscillator

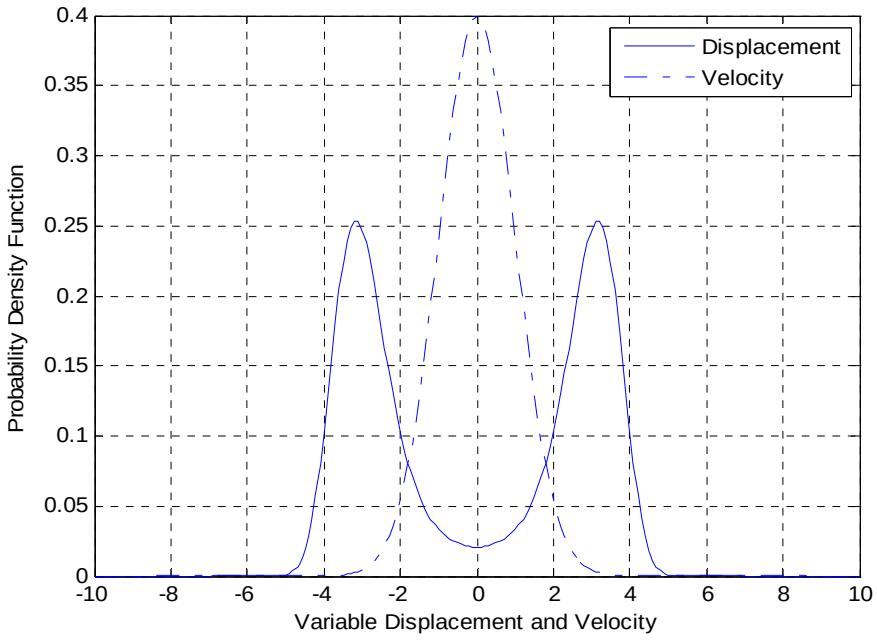

Fig. 30. Marginal probability density function of Duffing oscillator

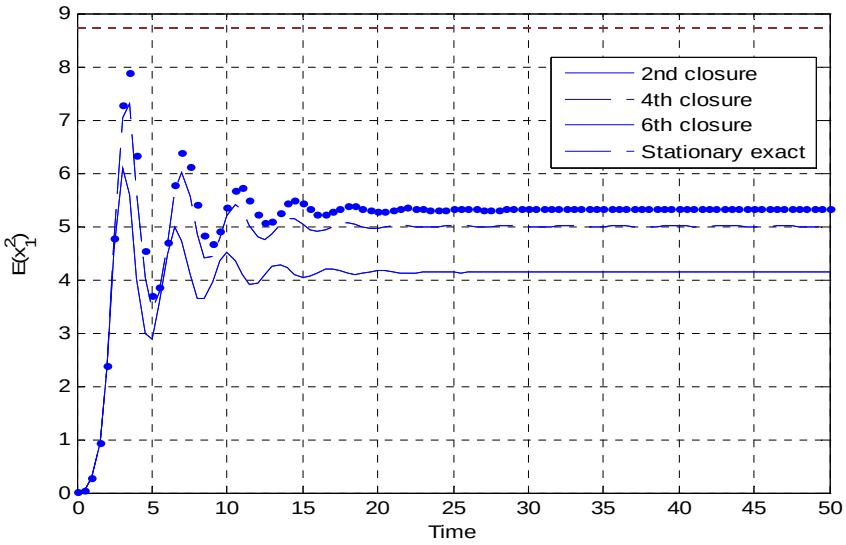

Fig. 31. Mean square of x_1 with different cumulant neglect order and exact solution

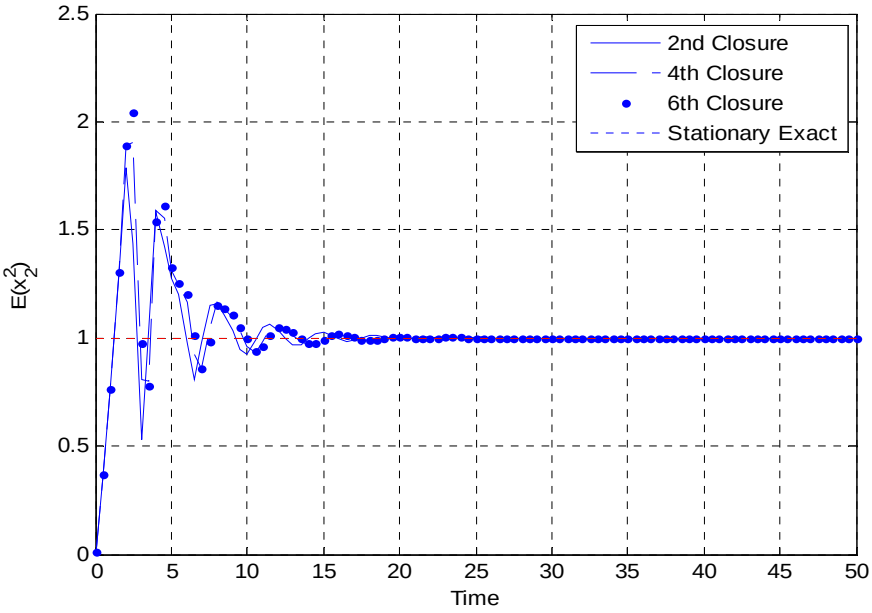

Fig. 32. Mean square of x_2 with different cumulant neglect order and exact solution

Table 6. Comparison of stationary mean square of x_1 and x_2 with different closure level and exact stationary value for bimodal Duffing oscillator

Closure Level	Stationary E(x1^2)	Result from (Wojtkiewicz, 2000)	Error for E(x1^2)	Stationary E(x2^2)	Error for E(x2^2)
2nd Order	4.1387	4.1387	52.50%	1.000	0.00%
4th Order	5.0000	5.0000	42.62%	1.000	0.00%
6th Order	5.3195	5.3196	38.95%	1.000	0.00%
Exact	8.7136			1.000	

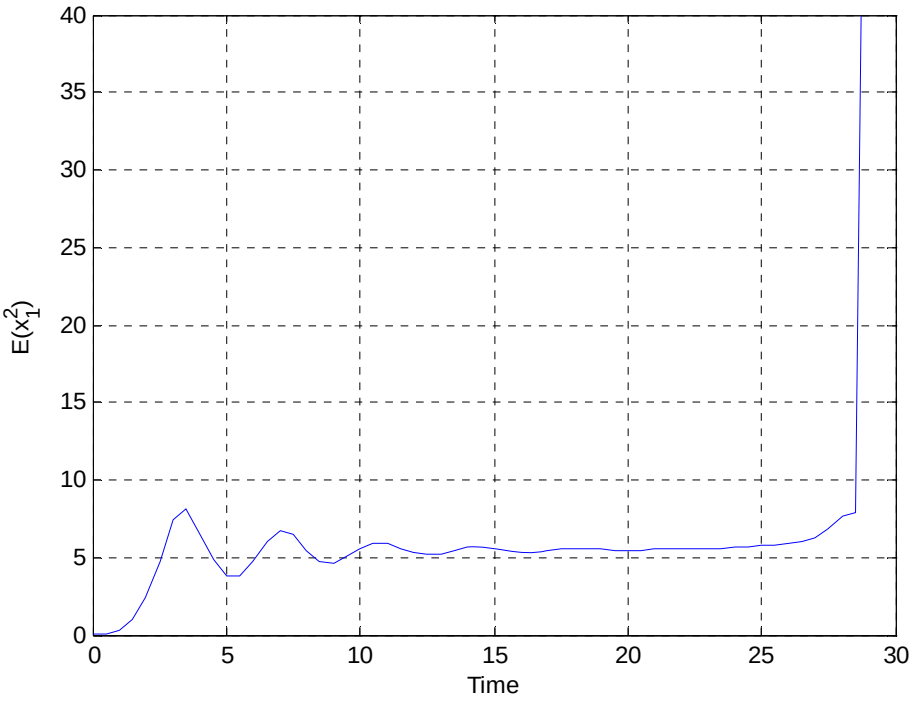

Fig. 33. Instability of cumulant neglect method with 8th order closure for mean square of x_1

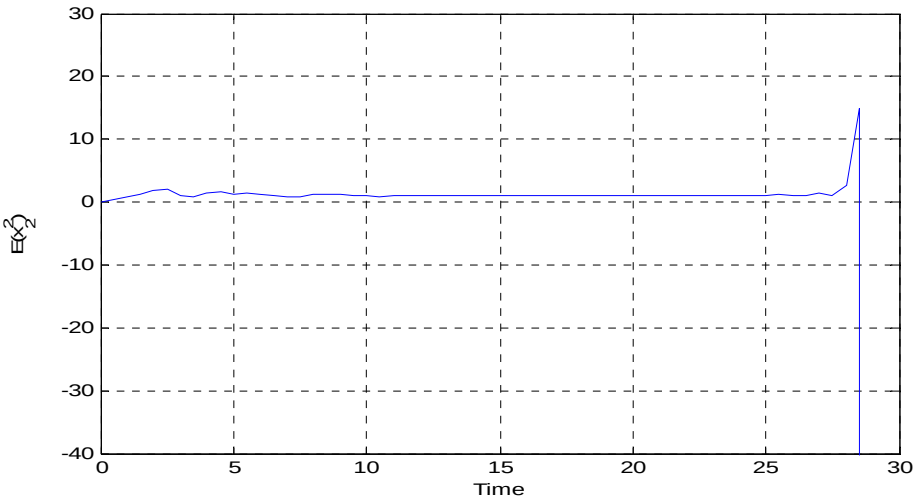

Fig. 34. Instability of cumulant neglect method with 8th order closure for mean square of x_2

3.2.2.2 Application to Rolling motion with Filter

By applying the automatic cumulant neglect tool, the moment equations for the stochastic system (3.17) up to fourth order have been computed to compare with Gaussian neglect result in last section. The moment equation is derived as below,

$$\begin{aligned} dE(p,q,r,s,t,m) = {} & pE(p-1,q+1,r,s,t,m) - (2\mu q + \lambda_3 r)E(p,q,r,s,t,m) \\ & - \delta qE(p,q+2,r,s,t,m) - \omega_0^2 qE(p+1,q-1,r,s,t,m) \\ & - \alpha_3 qE(p+3,q-1,r,s,t,m) + \varepsilon qE(p,q-1,r+1,s,t,m) \\ & + rE(p,q,r-1,s+1,t,m) + sE(p,q,r,s-1,t+1,m) \\ & - \lambda_2 sE(p,q,r+1,s-1,t,m) + tE(p,q,r,s,t-1,m+1) \\ & - \lambda_1 tE(p,q,r+1,s,t-1,m) - \lambda_0 mE(p,q,r+1,s,t,m-1) \\ & + \pi {\gamma_3}^2 s(s-1)E(p,q,r,s-2,t,m) \end{aligned} \tag{3.54}$$

Fig. 35 and Fig. 36 show the evolutions of root square of displacement and velocity respectively. The Second order cumulant neglect closure (Gaussian Closure) performs as good as the fourth order neglect closure at the transient phase. However, the Gaussian closure underestimates the stationary response moments as compared to the fourth order cumulant neglect result for both displacement and velocity.

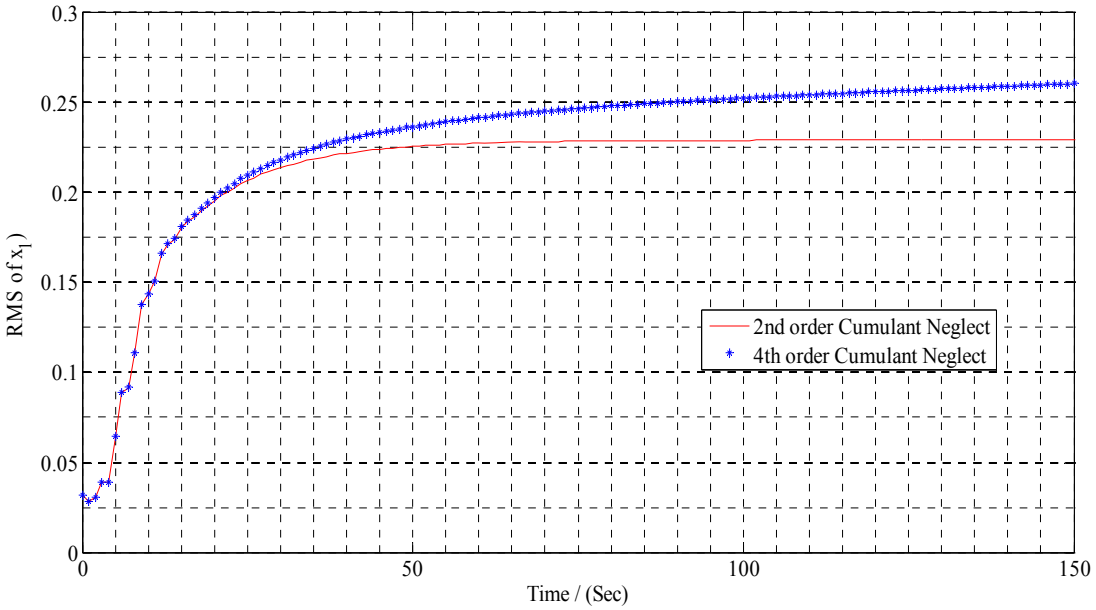

Fig. 35. Evolution of the root mean square of the rolling displacement

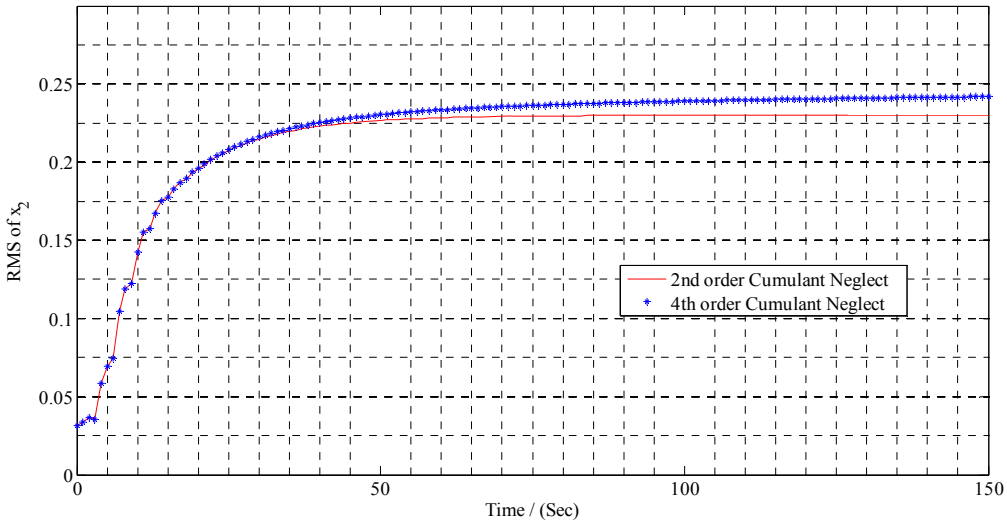

Fig. 36. Evolution of the root mean square of the rolling velocity

3.3 Discussions of the Moment Equations

Due to the complications of higher dimensional stochastic systems, this dissertation develops a convenient method of analyzing these higher dimensional systems. The higher order moment equations are solved with a cumulant neglect method with an automatic neglect tool. This algorithm will greatly assist in analyzing higher dimensional stochastic dynamical systems at any closure level. And kurtosis could be verified larger than 3 by checking fourth order moments, which shows non Gaussian effect of rolling motion response and soft spring effect (Winterstein, 1988).

As analyzed in the case 4, a system with parametric stochastic excitation (multiplication noise) can be analyzed as well as external stochastic excitation (additive noise) without loss of generality. The mathematical model for ship rolling here is an approximate frequency domain equation. Constant coefficients are used for the added

mass and added damping. All these coefficients are selected with respect to the peak frequency of the excitation force and within frequency domain analysis. Following Ogilvie (Ogilvie, 1964), the modified time domain rolling equation with impulse response function is derived and analyzed using an extended state space method (Holappa and Falzarano, 1999). Instead of numerical simulation, the extended state space system can be studied in a stochastic conception. With the extended state space, time domain state space model will become more complicated, but the automatic tool developed in this dissertation will be able to handle the high dimensional stochastic system without difficulty. Additionally, all linear filter variables and extended state space variables (if extended by linear system) are all Gaussian variables, thus only Gaussian cumulant neglect method (second order) is needed to cut off those variables associated moment equations. This will largely reduce the amount of moment equations.

With the automatic cumulant neglect tool, we should be able to calculate the response moment with arbitrary number of states and closed at any closure level theoretically. However, the cumulant neglect method provides good approximation only when the response of systems is close to Gaussian behavior. If the system posses any jump behavior, e.g. bimodal oscillator in case 5, the cumulant neglect method is not capable to capture the true displacement moments. Also the higher order moment equations involves many ordinary differential equations even for the low dimensional dynamical system, time domain simulation of those closed moment equations is necessary for stationary statistics. Therefore it is difficult to find any moment jump phenomena.

CHAPTER IV

MARKOV AND MELNIKOV BASED APPROACHES FOR STABILITY ANALYSIS

Vessel stability or capsizing analysis in random beam sea has been approached using different analytical methods in the past decades. However, due to the strong softening nonlinear stiffness and stochastic excitation, there is still no general method of dealing with capsizing prediction in a random sea. The Fokker-Planck Equation (FPE) based on the continuous Markov process model and the phase space flux rate based on Melnikov function are two of the most attractive analytical approaches which provide different views of the capsizing criteria. In this chapter, both methods have been applied to the same vessel model to compare its capabilities and efficiencies and also discussed their limitations and advantages for capsizing criterion development. In the Markov based portion, both the shaping filter method and the stochastic averaging of energy envelope are applied to the SDOF freedom rolling equation. The rate of phase transport flux based on the Melnikov function and the mean first passage rate based on FPE are compared for capsizing prediction. The relationship, i.e., similarities and differences between the two is then demonstrated through various parameter studies.

4.1 Introduction

Stochastic analysis of nonlinear marine structures is used to examine the random response and stability of the ocean system. Ship rolling is the most typical strong nonlinear phenomena in ocean engineering. All our cases are based on the ship rolling problem in the beam seas. However all methods mentioned and studied here could be applied to other nonlinear stochastic problems without loss of generality. Two different approaches are applied to the dead ship (zero speed) condition with random beam waves, the so called Markov and the Melnikov based method.

A random process can be recognized as a Markov process if its future probability depends only on its most recent values. The Fokker Planck equation (FPE) is the related equation governing probability density function of the system response distribution of a Markov process. The FPE is a partial differential equation with appropriate initial and boundary condition discussed in the second Chapter. When the system is excited by purely Gaussian white noise, the response will be a Markov process and the probability density function is governed by the FPE. Unfortunately, the wave excitation is described by a non-white spectrum or even a narrow banded spectrum. The FPE cannot be applied to the rolling motion directly. Basically, researchers found two different ways to overcome this difficulty by using a shaping filter (Francescutto and Naito, 2004; Su and Falzarano, 2011) or stochastic averaging of energy envelope of response (Roberts, 1982; Roberts and Vasta, 2000). By applying the shaping filter technique, any wave excitation spectrum can be generated from the designed filter. When the dynamical system with filter variables are written into the Itô type differential equation, the related FPE

equation gives the transition probability density function with higher dimensions. The difficulty is solving the higher dimensional FPE. It should be noted that many researchers are still working on solving the higher dimensional FPE (Naess and Moe, 2000; Di Paola and Sofi, 2002; Kumar et al., 2010; Er, 2011; Martens and Wagner, 2011). The solution to the FPE is the transition probability density function of the response. The first passage type failure could be easily solved by defining the reliability function with transient probability density function. In this chapter, we do not focus on solving the FPE numerically due to its difficulty and efficiency. The Automatic neglect cumulant neglect tools was developed in the Chapter three to analyze the higher dimensional stochastic dynamical system approximately, but it is still far from satisfactory for capsizing analysis. Alternatively, stochastic averaging of the energy envelope was applied to analyze rolling motion by Roberts (Roberts, 1982; Roberts and Vasta, 2000). By reducing the dimension of the dynamical system to one dimension, the first passage time could be derived from the well-known Pontryagin equation (Andronov et al., 1933). And the first passage time is defined as the capsizing criterion based on the Markov method. The limitation of the stochastic averaging method is that the input spectrum bandwidth has to be much wider than the output spectrum bandwidth. Only when the damping is very light, can this condition be met.

As a global geometric method, the Melnikov method was introduced to naval architecture, ship rolling in harmonic waves by Falzarano (Falzarano, 1990; Falzarano et al., 1992). The method has already been applied to the rolling problems with stochastic excitation (Hsieh et al., 1994; Jiang et al., 2000; Vishnubhotla et al., 2000; Falzarano et

al., 2010). Ship capsizing is described in the phase space plane by the escape of a trajectory from the safe basin or potential well to the unsafe area under random excitation. The normalized phase transport rate or phase flux rate was defined as a criterion for vessel capsizing analysis.

We applied both the Markov and the Melnikov method to the same vessel parameters in this chapter to compare their relative efficiency and discuss their advantages and disadvantages.

4.2 Markov Modeling for Capsizing Analysis

Markov modeling of the stochastic dynamical system is based on the diffusion process. The general theory requires that the excitation force has to be a pure white noise process, while the random wave excitation spectrum normally has a limited bandwidth and a peak value. Basically, there are two different ways to deal with this problem. The first method is using a shaping filter to extend the two dimensional dynamical system to a higher order system by increasing the number of state space filter variables. The second is using the stochastic averaging of the energy envelope of the response by reducing the dimension of the stochastic system. Both methods are based on Markov process.

The shaping filter method was introduced in chapter III. Numerical solution of the FPE for high dimensional stochastic dynamical system always involves convergence and accuracy issues. Even if it is possible, it will be difficult. As an alternative analytical method introduced in the third Chapter, the Moment equation, which governs the

response of statistical moments, can be solved after applying some reasonable assumptions and closure technique. There is no small perturbation parameters assumption in the shaping filter model. By increasing additional filter dimensions, the difficulty of the shaping filter model is how to accurately estimate the probability density function of the stochastic dynamical systems. Once the solution of the FPE is given, the reliability function, the first passage time distribution and the mean first passage time will be easily calculated based on the Kolmogorov backward equation(Lin and Cai, 2004).

4.2.1 Energy based stochastic averaging

Instead of increasing the dimensions, stochastic averaging of the energy envelope enables the two dimensional rolling model to be reduced to a one dimensional problems for the system energy, which can be modeled approximately as a continuous one dimensional Markov process. This approach has been applied to ship rolling analysis for decades (Roberts, 1982; Roberts, 1986; Roberts and Spanos, 1986; Roberts and Vasta, 2000; Roberts and Vasta, 2000; Roberts and Vasta, 2001; Roberts and Vasta, 2002). The capsizing phenomenon is considered as a first passage type problem. Mean first passage time to reach a critical energy level can be evaluated from the associated FPE of the Markov process.

4.2.1.1 Rescaling of the roll equation of motion

For analytical convenience, the single degree of freedom roll equation can be non-dimensionalized to (Roberts, 1986),

$$\ddot{x}(\tau) + b_1\dot{x}(\tau) + b_2\dot{x}(\tau)\left|\dot{x}(\tau)\right| + x(\tau) - x^3(\tau) = F(\tau) \tag{4.1}$$

where the non-dimensionalized coefficients are defined as below

$$\begin{aligned} &\phi^* = \sqrt{C_1 / C_3}, x = \phi / \phi^*, \tau = \omega_n t, \omega_n = \sqrt{\frac{\Delta C_1}{I_{44} + A_{44}(\omega)}} \\ &b_1 = \frac{B_{44}(\omega)}{\Delta C_1}\omega_n, b_2 = \frac{B_{44q}(\omega)}{I_{44} + A_{44}(\omega)}, F(\tau) = \frac{f(t)}{\Delta C_1 \phi^*} \end{aligned} \tag{4.2}$$

It is noted that the nonlinear coefficient of stiffness has been non-dimensionalized to unity for convenience, but it is not necessary. Also the wave excitation force can be assumed as a stationary Gaussian stochastic process with zero mean and its spectrum can be defined as

$$S_{FF}(\Omega) = S_{ff}(\omega) / (\Delta C_1 \phi^*)^2 = \frac{1}{2\pi}\int_{-\infty}^{\infty} R(v)\cos(\Omega v)dv \tag{4.3}$$

$$R(v) = \mathrm{E}[F(\tau)F(\tau + v)] \tag{4.4}$$

$R(v)$ is the auto covariance function of $F(\tau)$ and frequency $\Omega = \omega / \omega_n$ is the non-dimensional frequency. $\mathrm{E}[\bullet]$ is expectation operator. The physical meaning of $S_{ff}(\omega)$ and $F_{rolling}(\omega)$ are defined in chapter three. In this chapter, $S_{\eta\eta}(\omega)$ is represented by the ISSC (International Ship Structure Congress) two parameter spectral formula given by

$$S_{\eta\eta}(\omega) = 0.11 H_s^2 \frac{\omega_z^4}{\omega^5}\exp(-0.44(\frac{\omega_z}{\omega})^4) \tag{4.5}$$

In the non-dimensionalized rolling model, we have only four parameters, linear damping b_1, nonlinear damping b_2, significant wave height H_s and characteristic wave frequency

ω_z. Both the Markov and Melnikov based approaches will be applied to analyze the effects of these four parameters.

The damping coefficients for rolling are small compared with the stiffness coefficients. For convenience in the derivation of the theory, equation (4.1) is rescaled using the perturbation parameter ε as followed,

$$\ddot{x}(\tau) + \varepsilon^2 \dot{x}(\tau)(b_{1\varepsilon^2} + b_{2\varepsilon^2} \left|\dot{x}(\tau)\right|) + x(\tau) - x^3(\tau) = \varepsilon F_\varepsilon(\tau) \tag{4.6}$$

where $\varepsilon^2 b_{1\varepsilon^2} = b_1$, $\varepsilon^2 b_{2\varepsilon^2} = b_2$ and $\varepsilon F_\varepsilon(\tau) = F(\tau)$. The scaling parameters ε is used here help to indicate the order of magnitude of the damping and excitation terms. The scaling of the excitation ensures that the standard deviation of the response is of order ε^0 as $\varepsilon \to 0$ but this does not imply that the excitation is weak in an absolute sense (Roberts and Vasta, 2001).The total energy envelope process $E(\tau)$ of the oscillator is defined as:

$$E(\tau) = \frac{\dot{x}^2}{2} + V(x) \tag{4.7}$$

where $V(x) = \int_0^x k(\xi) d\xi$, and $k(x) = x - x^3$ is the softening stiffness and the total energy consists of the kinetic energy and the potential energy. In the absence of input noise excitation and dissipation, the quantity of $E(\tau)$ is conserved. This implies that the Hamiltonian system is integrable. It is possible to define $E(\tau)$ and phase angle $\Phi(\tau)$ to rewrite the rolling equation followings (Roberts and Vasta, 2002):

$$\operatorname{sgn}(x)\sqrt{V(x)} = \sqrt{E}\cos\Phi \tag{4.8}$$

$$\dot{x} = -\sqrt{2E}\sin\Phi \tag{4.9}$$

The variable transformation gives two first order ordinary differential equation for $E(\tau)$ and $\Phi(\tau)$ independently.

$$\begin{bmatrix} \dot{E}(\tau) \\ \dot{\Phi}(\tau) \end{bmatrix} = \begin{pmatrix} -\varepsilon^2 \alpha_1 \\ -\varepsilon^2 \alpha_2 + \gamma \end{pmatrix} + \begin{bmatrix} \varepsilon \beta_1 \\ \varepsilon \beta_2 \end{bmatrix} F_\varepsilon(\tau) \tag{4.10}$$

where,

$$\alpha_1 = 2Eh \sin^2 \Phi \tag{4.11}$$

$$\alpha_2 = -h \sin \Phi \cos \Phi \tag{4.12}$$

$$\beta_1 = -\sqrt{2E} \sin \Phi \tag{4.13}$$

$$\beta_2 = -\cos \Phi \, / \, \sqrt{2E} \tag{4.14}$$

$$\gamma = \left| k(E, \Phi) \right| / \, V(E, \Phi) \tag{4.15}$$

$$h = b_{1\varepsilon^2} + b_{2\varepsilon^2} \left| \dot{x}(\tau) \right| \tag{4.16}$$

4.2.1.2 The Markov process approximation

The Markov process of the energy $E(\tau)$ is approximated by a one dimensional stochastic Itô differential equation:

$$dE(\tau) = m(E)dt + \sqrt{D(E)}dB \tag{4.17}$$

$dB \, / \, d\tau = W(\tau)$ and $W(\tau)$ is the Gaussian white noise excitation. $B(\tau)$ is defined as a Wiener or Brownian process. $m(E)$ and $D(E)$ are defined as the drift and diffusion coefficients and are estimated from the known coefficients in equation(4.1). The FPE equation associated with (4.17) is given by:

$$\frac{\partial p(E,\tau \mid E_0,\tau_0)}{\partial \tau} = -\frac{\partial}{\partial E}(m(E)p(E,\tau \mid E_0,\tau_0)) + \frac{1}{2}\frac{\partial^2}{\partial E^2}(D(E)p(E,\tau \mid E_0,\tau_0)) \quad (4.18)$$

$p(E \mid E_0,\tau)$ is the transition probability density function of the oscillator energy. For this one dimensional partial differential equation, a numerical solution is possible to be calculated. Also an analytical solution of stationary response is given in (Roberts and Vasta, 2000).

There are two alternative ways to derive the drift and diffusion coefficients and they are explained by Roberts in two separate papers (Roberts, 1982; Roberts and Vasta, 2000). The old theory is based on Stratonovich-Khasminskii (SK) limit theorem (Stratonovich, 1963; Khasminskii, 1966). The new derivation is based on physical reasoning, which gives a correction term to the drift coefficients. A fundamental assumption of the Markov model is $\Delta\tau > \tau_{corr}$, where τ_{corr} is the correlation time scale of the excitation and $\Delta\tau$ is that the time step for energy increment. If the damping is sufficiently small, then this condition can be met. If the bandwidth of the excitation increases, and the correlation time reduces, then the restriction on the magnitude of damping reduces (Roberts and Vasta, 2000). Define $\Delta E(\tau) = E(\tau + \Delta\tau) - E(\tau)$,the drift coefficient $m(E)$ and drift coefficient $D(E)$ are given by

$$m(E) = \frac{1}{\Delta\tau}\mathrm{E}[\Delta E] \quad (4.19)$$

$$D(E) = \frac{1}{\Delta\tau}\mathrm{E}[(\Delta E)^2] \quad (4.20)$$

These two coefficients are approximated by a perturbation to the free and undamped oscillation. It is necessary to find the solution for the undamped, unforced oscillator:

$$\ddot{x}_0 + x_0 - x_0^{\,3} = 0 \tag{4.21}$$

Fig. 37 shows the phase plane of above equation, and the solution for equation (4.21) is given as

$$x_0(\tau) = A\,sn(\omega_1\tau + K(m) \mid m) \tag{4.22}$$

where $0 \le A < 1$ is the amplitude of the oscillator and sn is the Jacobian elliptic function. Where $\omega_1 = (1 - A^2 / 2)^{1/2}$ and $m = A^2 / (2 - A^2)$. $K(m)$ is the complete elliptic integral. The natural frequency of oscillator is $T(E_0)$,which is a constant for each amplitude A .

$$T(E_0) = 4K(m) / (1 - A^2 / 2)^{1/2} \tag{4.23}$$

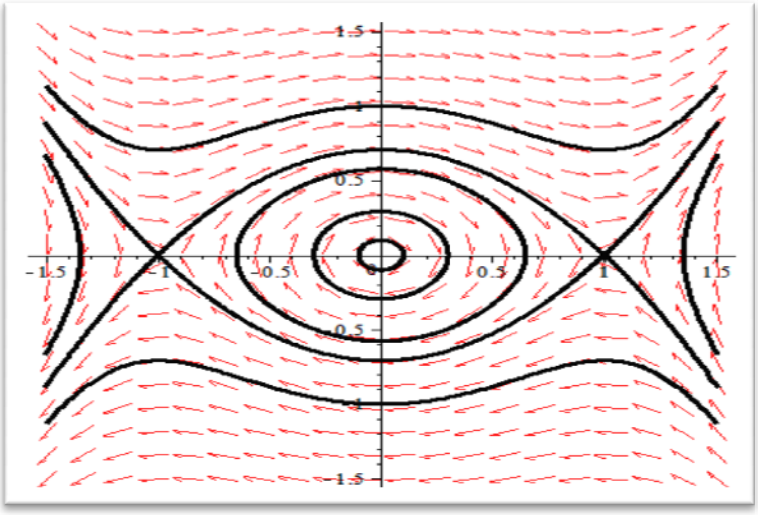

Fig. 37. Phase plane for undamped and unforced oscillator

The dissipation terms in equation (4.10) α_1 and α_2 can be averaged over the period of the unforced undamped oscillation $T(E_0)$ by treating E as a constant over one period and $\Phi = \Phi_0$.

$$\begin{bmatrix} \dot{E}(\tau) \\ \dot{\Phi}(\tau) \end{bmatrix} = \begin{pmatrix} -\varepsilon^2 \Lambda_1 \\ -\varepsilon^2 \Lambda_2 + \gamma \end{pmatrix} + \begin{bmatrix} \varepsilon \beta_1 \\ \varepsilon \beta_2 \end{bmatrix} F_\varepsilon(\tau) \tag{4.24}$$

$$\Lambda_1 = \frac{2E}{T(E_0)} \oint h \sin^2 \Phi_0 dt \tag{4.25}$$

$$\Lambda_2 = -\frac{1}{T(E_0)} \oint h \sin \Phi_0 \cos \Phi_0 dt \tag{4.26}$$

By using the drift and diffusion definitions given by equation (4.19) and (4.20), and the first row of equation (4.24), $m(E)$ and $D(E)$ can be obtained by following (Roberts and Vasta, 2000; Roberts and Vasta, 2002):

$$m(E) = -\varepsilon^2 \Lambda_1(E) + \frac{1}{2} \pi \sum_{n=1,2...}^{\infty} (s_n^{\ 2} + c_n^{\ 2}) S_{FF}(n\omega(E)) \tag{4.27}$$

$$D(E) = 2\pi E \sum_{n=1,2...}^{\infty} s_n^{\ 2} S_{FF}(n\omega(E)) \tag{4.28}$$

where,

$$\sin \Phi_0 = -\frac{\dot{x}_0(\tau)}{\sqrt{2E}} = \sum_{n=1}^{\infty} s_n \sin(n\omega(E)) \tag{4.29}$$

$$\cos \Phi_0 = \frac{\mathrm{sgn}(x_0)\sqrt{V(x_0)}}{\sqrt{E}} = \sum_{n=1}^{\infty} c_n \cos(n\omega(E)) \tag{4.30}$$

The derivation of drift and diffusion coefficients can be found in the Appendix B. Fig. 38 to Fig. 40 demonstrated the Fourier expansion of $\sin \Phi_0$ and $\cos \Phi_0$. At low energy

level, like Fig. 38, the coefficients of the expansion can be cut off at 1, which already gives a good approximation. However, when the system goes up to a higher energy orbit, Fig. 39 indicates the Fourier coefficients are not sufficient to provide a good approximation. While Fig. 40 gives an excellent estimation when the summation in equation (4.29) and (4.30) are truncated at n=5. A truncation order at n=5 will be adopted in the following computations.

The drift and diffusion coefficients are depicted in Fig. 41 and Fig. 42 with a varying excitation force and the same characteristic wave frequency $\omega_z = 2\pi / 9$. It is clear to see that both the drift and diffusion coefficients will increase with increasing of excitation force. Fig. 43 and Fig. 44 demonstrate the effect of the characteristic wave frequency ω_z on the drift and diffusion coefficients. It is interesting to observe that $\omega_z = 2\pi / 5$ gives a very large value of drift and diffusion coefficients at the low energy level. The reason is $\omega(E) \to 1$ as E_0 approach to zero, s_1 and c_1 is the dominant value for s_n and c_n, so $S_{FF}(\Omega = \omega / \omega_n = 1)$ will be dominant for $m(E)$ and $D(E)$. Based on the numerical testing, the frequency of the peak value of $S_{FF}(\Omega)$ will be close to 1, as $\omega_z \to 2\pi / 4$. This effect can be considered as kind of 'stochastic resonance'. The damping coefficients effect on the drift coefficient are demonstrated at Fig. 45 and Fig. 46, it is expected that the larger damping will give a larger negative effect on drift value. The diffusion coefficients are not affected by the damping coefficients based on equation(4.28).

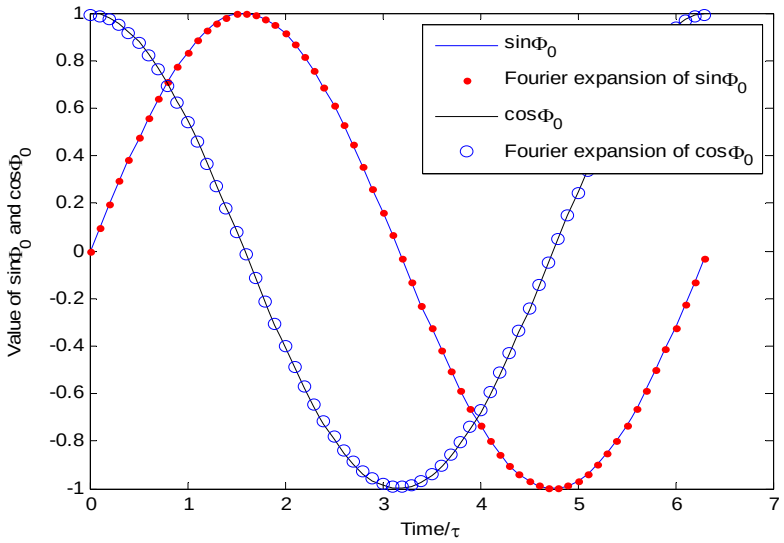

Fig. 38. Fourier expansion of $\sin\Phi_0$ and $\cos\Phi_0$ at E_0 =0.01 and n=1

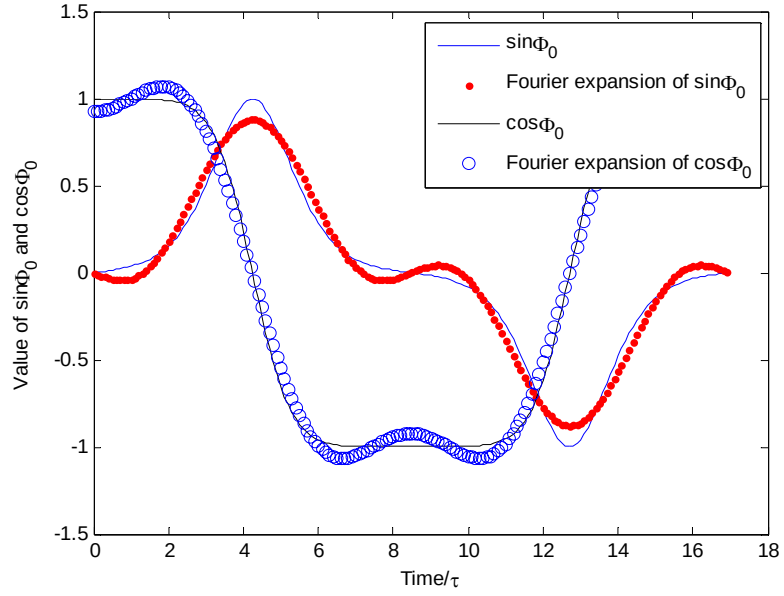

Fig. 39. Fourier expansion of $\sin\Phi_0$ and $\cos\Phi_0$ at E_0 =0.2499 and n=1...3

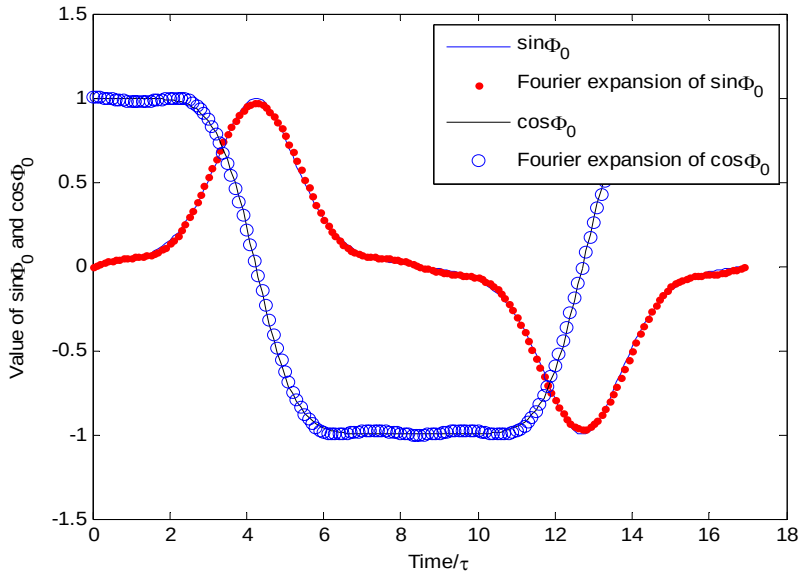

Fig. 40. Fourier expansion of $\sin\Phi_0$ and $\cos\Phi_0$ at E_0 =0.2499 and n=1...5

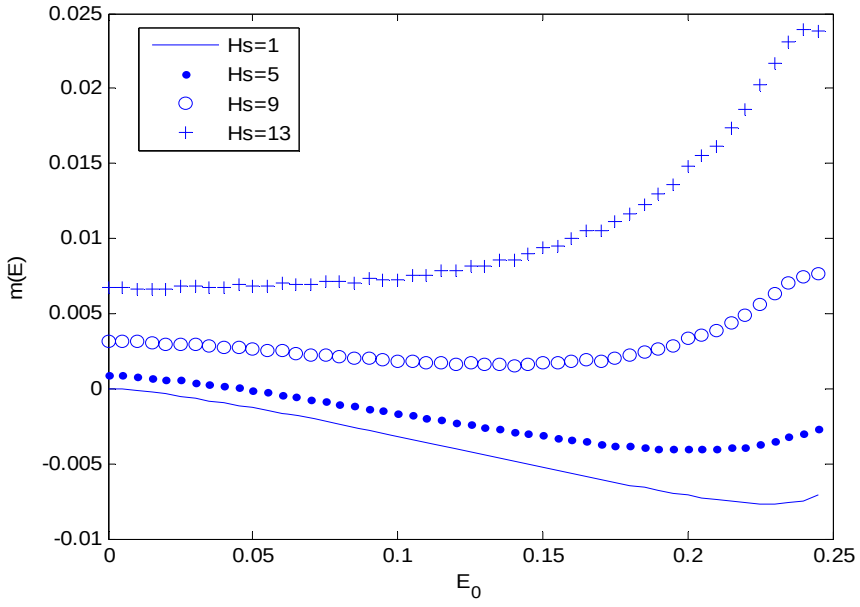

Fig. 41. Drift coefficients for various H_s, Unit: Meter

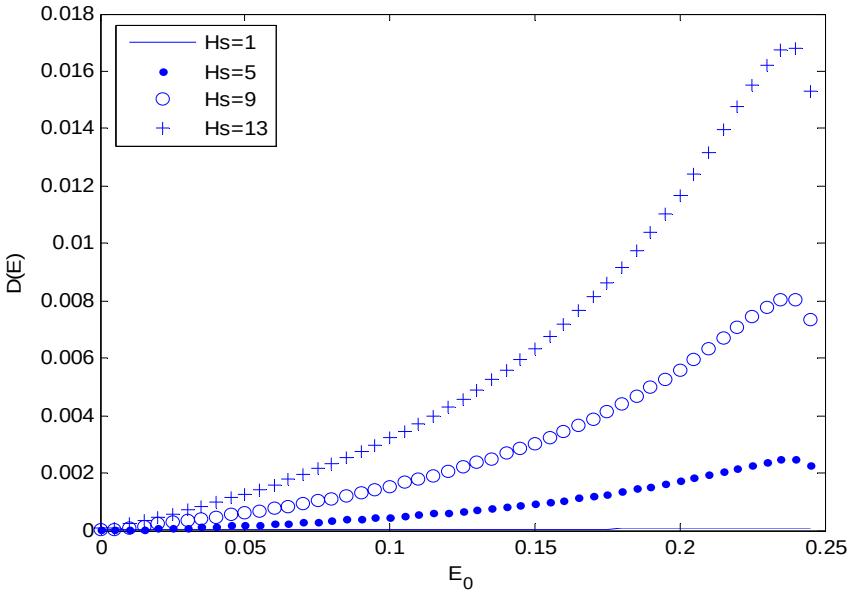

Fig. 42. Diffusion coefficients for various H_s, Unit: Meter

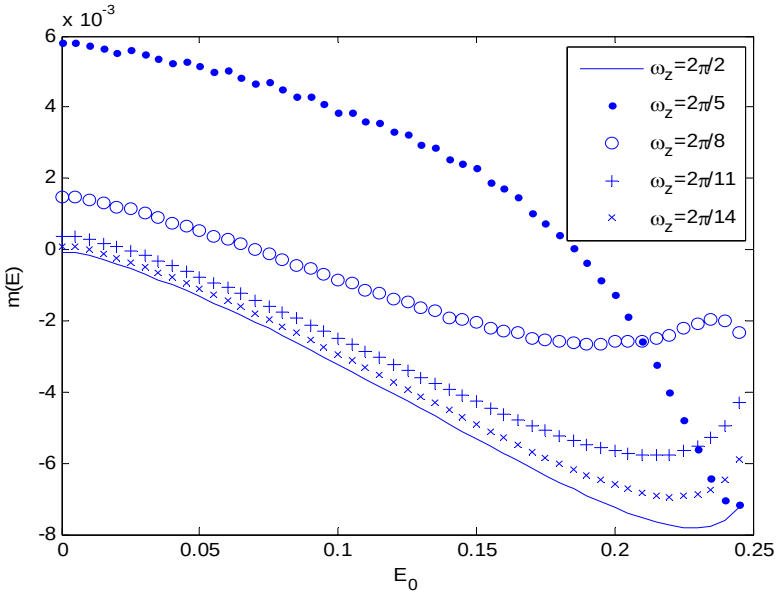

Fig. 43. Drift coefficients for various ω_z, H_s=5m

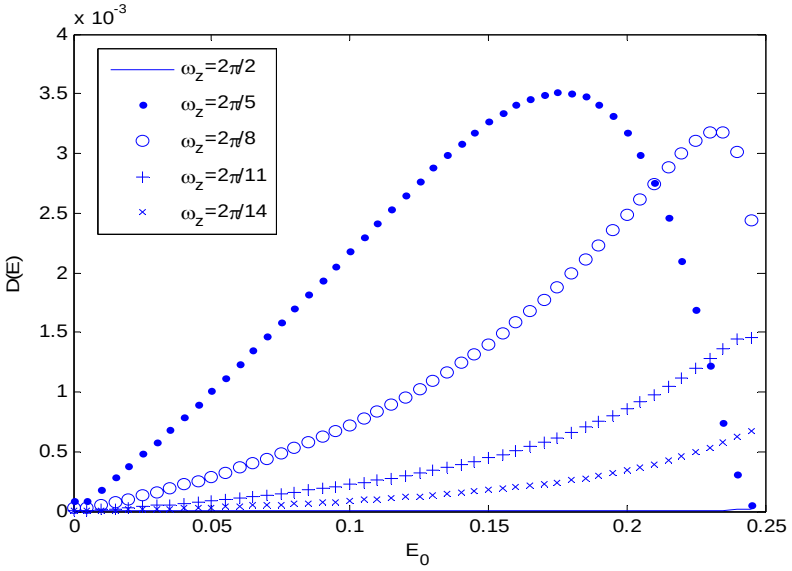

Fig. 44. Diffusion coefficients for various ω_z, H_s=5m

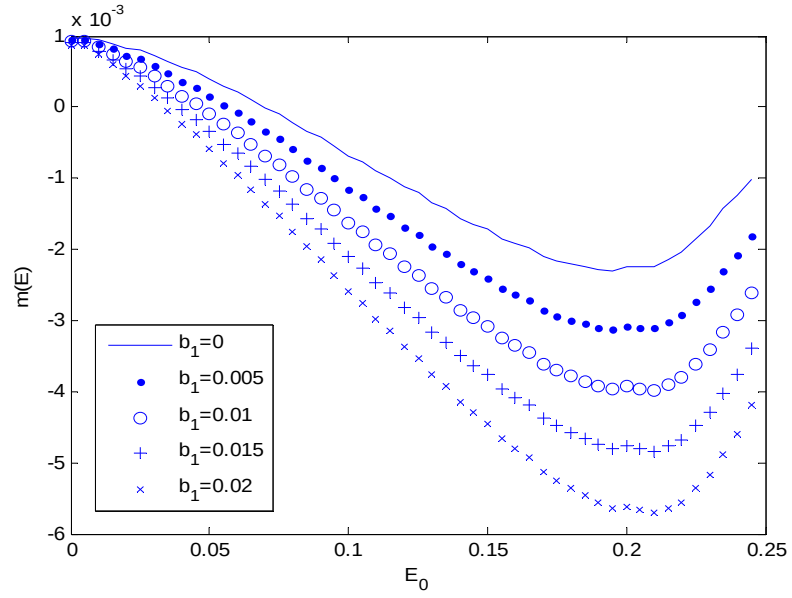

Fig. 45. Drift coefficients for various linear damping coefficients b_1, H_s=5m,

$\omega_z = 2\pi / 9$

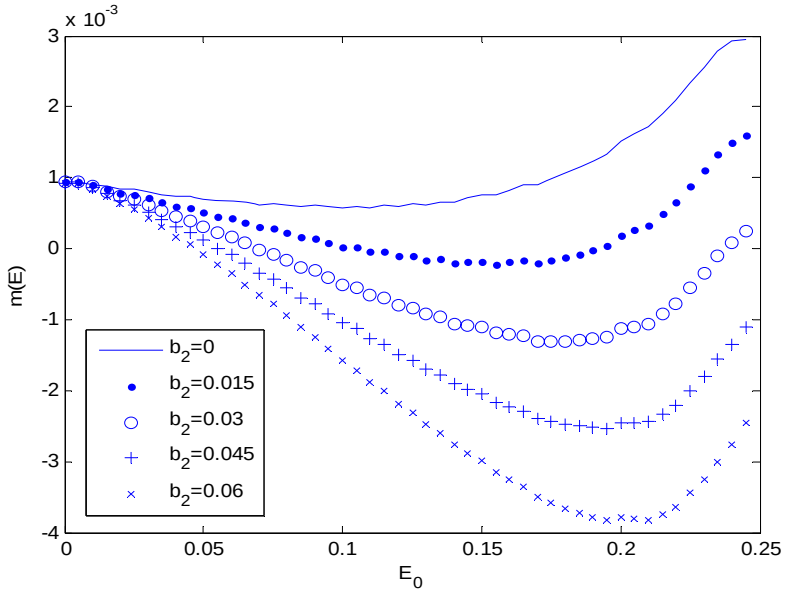

Fig. 46. Drift coefficients for various nonlinear damping coefficients b_2, H_s=5m

$\omega_z = 2\pi / 9$

4.2.2 First passage failures

The one dimensional Markov model equation (4.17) derived before can be easily applied to study the first passage problem. We are concerned with the random time T_{FPS} when the Markov process E first cross the critical boundary value E_c, given the condition that $E(\tau_0) = E_0$, where $E_0 < E_c$ and E_c corresponds to an absorbing boundary. We assume $p(E, \tau \mid E_0, \tau_0)$ to be the transition probability density of the Markov process $E(\tau)$. The reliability function $R(\tau, E_c; \tau_0, E_0)$, which is defined as the probability of $E_l \le E(\tau) < E_c$ at time τ, where E_l is the lower bound and is a non-critical boundary.

$$R(\tau, E_c; \tau_0, E_0) = \int_{E_l}^{E_c} p(E, \tau \mid E_0, \tau_0) d\tau = Prob[T_{FPS} > \tau - \tau_0 \mid E(\tau_0) = E_0] \quad (4.31)$$
$$E_l \le E(\tau) < E_c, \ \tau \ge \tau_0$$

If equation (4.18) can be solved for $p(E, \tau \mid E_0, \tau_0)$, the reliability function can be determined by integrating equation (4.31). Also, reliability function satisfies the Kolmogorov backward equation (Lin and Cai, 2004):

$$-\frac{\partial R}{\partial \tau_{FPS}} + m(E_0)\frac{\partial R}{\partial E_0} + \frac{1}{2} D(E_0)\frac{\partial^2 R}{\partial E_0^2} = 0 \quad (4.32)$$

where $\tau_{FPS} = \tau - \tau_0$ is the first passage time. Equation (4.32) can be solved given initial and boundary condition. Probability distribution function of first passage time T_{FPS} is given by

$$F_{T_{FPS}}(\tau_{FPS}) = Prob[T_{FPS} < \tau_{FPS} \mid E(\tau_0) = E_0] = 1 - R(\tau_{FPS}) \quad (4.33)$$

The probability density function of T_{FPS} is given by

$$p_{T_{FPS}}(\tau_{FPS}) = \frac{\partial}{\partial \tau_{FPS}} F_{T_{FPS}}(\tau_{FPS}) = -\frac{\partial}{\partial \tau_{FPS}} R(\tau_{FPS}) \quad (4.34)$$

The moments of first passage time T_{FPS} satisfy the generalized Pontryagin equation (Lin and Cai, 2004). M_n is the nth moment of the first passage time variable T_{FPS} and $M_n = \mathrm{E}[T_{FPS}^n]$

$$(n+1)M_n + m(E_0)\frac{d}{dE_0} M_{n+1} + \frac{1}{2} D(E_0)\frac{d^2}{dE_0^2} M_{n+1} = 0 \quad (4.35)$$

For the special cases, n=0, equation (4.35) is a two point boundary value problem for the mean first passage time $M_1(E_0)$, which represents the mean first passage time to cross the upper boundary given the initial value E_0.

$$M_0 + m(E_0)\frac{d}{dE_0}M_1(E_0) + \frac{1}{2}D(E_0)\frac{d^2}{dE_0^2}M_1(E_0) = 0 \tag{4.36}$$

where $M_0 = \int_0^\infty p_{T_{FPS}}(\tau_{FPS})\tau_{FPS}^0 d\tau_{FPS} = 1$. The appropriate boundary conditions have been given in (Roberts, 1986) as following:

$$M_1(E_c) = 0 \tag{4.37}$$

$$\frac{dM_1(0)}{dE_0} = -\frac{1}{\pi S_{FF}(1)} \tag{4.38}$$

For the non-dimensional rolling model (4.17), $E_c = 1/4$ is the heteroclinic boundary in Fig. 37. Equation (4.36)with boundary (4.37) and (4.38) can be solved by using the shooting method to determine $M_1(0)$. The mean first passage time $M_1(E_0)$ is given in Fig. 47 by the shooting method, with $H_s = 3m$. where the horizontal axis represents the initial energy level. In order to compare this result with the Melnikov criterion discussed in the next section, here we define R_e as the inverse of the mean first passage time, which will be adopted as the capsizing criterion as below,

$$R_e = 1 / M_1(0) \tag{4.39}$$

As denoted in Fig. 48, the mean first passage time decreases strongly with wave height increase. For a better understanding of the capsizing criterion, at higher wave excitation,

Fig. 49 illustrates the escape rate, which is defined as $1 / M_1(0)$. We will use the curve in Fig. 49 as one possible vessel capsizing criterion, and it will be directly compared with phase space flux determined from the Melnikov method described in next section. Note that there is a non-zero R_e for any non-zero significant wave height. However R_e starts to increase significantly beyond some critical wave height.

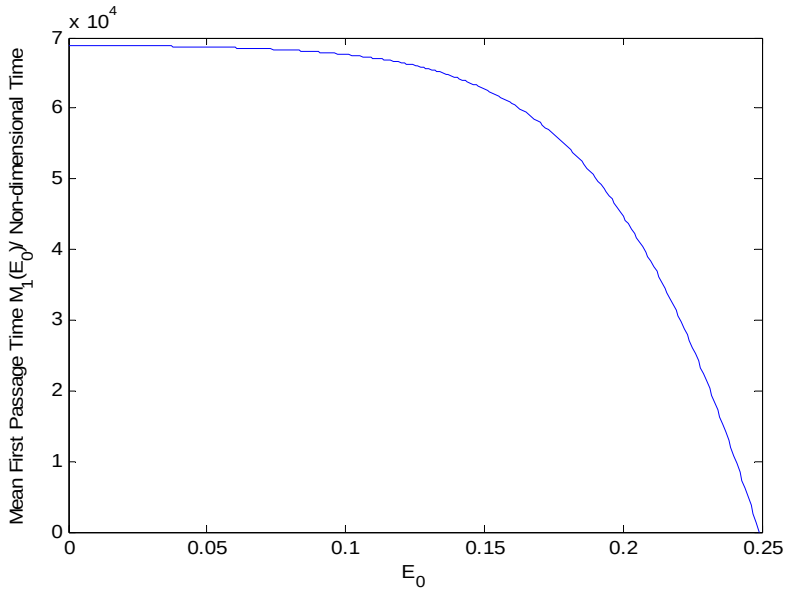

Fig. 47. Mean first passage time with initial condition E_0 , $H_s = 3m$

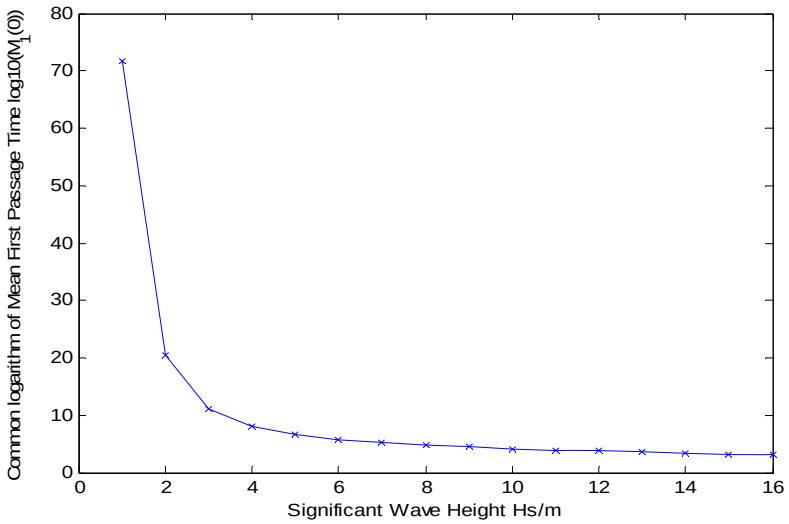

Fig. 48. Logarithm of mean first passage time $\log 10(M_1(0))$

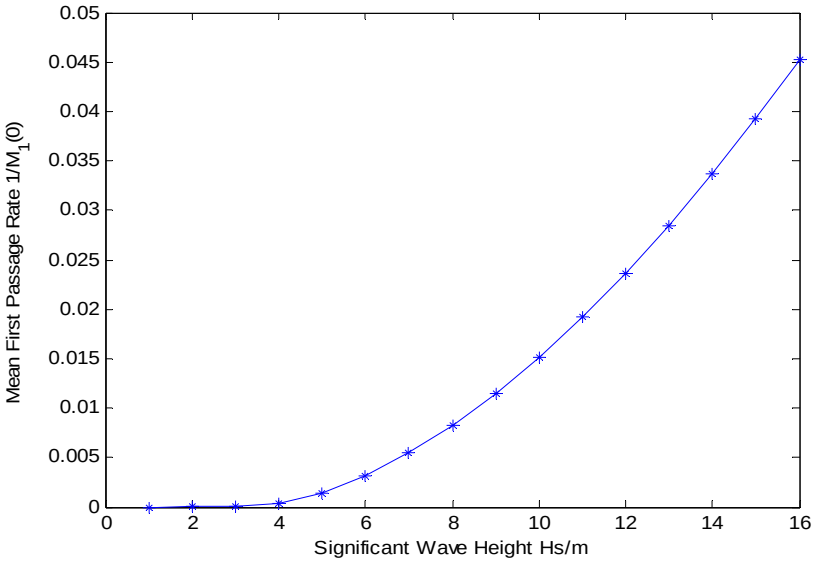

Fig. 49. Mean first passage rate $1/\mathrm{M}_1(0)$

4.3 The Melnikov Criterion for Capsizing Prediction

4.3.1 The fundamental background of the Melnikov function

Similar to the Markov model, given in equation(4.6), the rolling equation is rescaled by the perturbation parameter ε ,

$$\ddot{x}(\tau) + \varepsilon b_{1\varepsilon}\dot{x}(\tau) + b_{2\varepsilon}\dot{x}(\tau)\left|\dot{x}(\tau)\right| + x(\tau) - x^3(\tau) = \varepsilon F_{\varepsilon}(\tau) \tag{4.40}$$

where $\varepsilon b_{1\varepsilon} = b_1$, $\varepsilon b_{2\varepsilon} = b_2$ and $\varepsilon F_{\varepsilon}(\tau) = F(\tau)$. However, the scaling order for the damping is different with Markov model; the scaling parameter ε is just for the derivation of the theory and does not affect the final result. Equation (4.40) can be rewritten in the state space format as:

$$\begin{cases} \dot{x}(\tau) = y(\tau) \\ \dot{y}(\tau) = -x(\tau) + x(\tau)^3 + \varepsilon(-b_{1\varepsilon}y(\tau) - b_{2\varepsilon}y(\tau)\left|y(\tau)\right| + F_{\varepsilon}(\tau)) \end{cases} \tag{4.41}$$

Equation (4.41) becomes free undamped rolling motion when ε =0. The phase plane has a center at the origin and two saddles connected by heteroclinic orbits as shown in Fig. 37. The solution for $\varepsilon = 0$ is given by:

$$\begin{cases} x_0(\tau) = \pm\tanh(\dfrac{\tau}{\sqrt{2}}) \\ y_0(\tau) = \pm\sqrt{\dfrac{1}{2}}\operatorname{sec}h^2(\dfrac{\tau}{\sqrt{2}}) \end{cases} \tag{4.42}$$

The Melnikov function was first introduced to ship rolling research by Falzarano, see. e.g., (Falzarano et al., 1992), and its application to stochastic Melnikov method for constant coefficients was obtained by Hsieh, etc.(Hsieh et al., 1994). The memory effect was considered for hydrodynamics force by Jiang (Jiang et al., 2000). These analysis are

based on Melnikov function definition given by (Wiggins, 2003) and originally by (Guckenheimer and Holmes, 1983),

$$\begin{aligned} M(\tau_0) &= \int_{-\infty}^{\infty} y_0(\tau)(-b_{1\varepsilon} y_0(\tau) - b_{2\varepsilon} y_0(\tau)\left|y_0(\tau)\right| + F_\varepsilon(\tau+\tau_0))d\tau \\ &= \tilde{M}(\tau_0) - \bar{M} \end{aligned} \tag{4.43}$$

where $\tilde{M}(\tau_0)$ is the oscillatory part and $\bar{M}$ is the constant part of the Melnikov function, which are given by,

$$\tilde{M}(\tau_0) = \int_{-\infty}^{\infty} y_0(\tau) F_\varepsilon(\tau+\tau_0) d\tau \tag{4.44}$$

$$\bar{M} = \int_{-\infty}^{\infty} y_0(\tau)(b_{1\varepsilon} y_0(\tau) + b_{2\varepsilon} y_0(\tau)\left|y_0(\tau)\right|)d\tau = (\frac{2\sqrt{2}}{3} b_{1\varepsilon} + \frac{8}{15} b_{1\varepsilon}) \tag{4.45}$$

By setting $\tau_1 = \tau + \tau_0$ and noticing the evenness of $y_0(\tau)$, equation (4.44) can be transformed as follows:

$$\tilde{M}(\tau_0) = \int_{-\infty}^{\infty} y_0(\tau_1 - \tau_0) F_\varepsilon(\tau_1) d\tau_1 = \int_{-\infty}^{\infty} y_0(\tau - \tau_0) F_\varepsilon(\tau) d\tau = \int_{-\infty}^{\infty} y_0(\tau_0 - \tau) F_\varepsilon(\tau) d\tau \tag{4.46}$$

Equation (4.46) is the Duhamel convolution integral, $y_0(\tau_0 - \tau)$ which acts like an impulse response function of the linear system, $F_\varepsilon(\tau)$ is the random excitation and $\tilde{M}(\tau_0)$ is the system response. Assume that excitation force $F_\varepsilon(\tau)$ is stationary, the spectrum of $\tilde{M}(\tau_0)$ is given by:

$$S_{\tilde{M}\tilde{M}} = (2\pi)^2 \left|Y(\Omega)\right|^2 S_{F_\varepsilon F_\varepsilon}(\Omega) = 2\pi S_{y_0}(\Omega) S_{F_\varepsilon F_\varepsilon}(\Omega) \tag{4.47}$$

where $S_{\tilde{M}\tilde{M}}$ is the one sided spectral density function of the oscillatory part of the Melnikov function $\tilde{M}(\tau_0)$, and $S_{F_\varepsilon F_\varepsilon}(\Omega)$ is the one sided spectral density function of the force $F_\varepsilon(\tau)$. $Y(\Omega)$ and $S_{y_0}(\Omega)$ are respectively the Fourier transform and the spectral density function of $y_0(\tau)$.

$$Y(\Omega) = \frac{1}{2\pi}\int_{-\infty}^{\infty} y_0(\tau)e^{-i\Omega\tau}d\tau \tag{4.48}$$

$$S_{y_0}(\Omega) = \pi\left(\frac{\Omega}{\sinh(\Omega\pi\ /\ \sqrt{2})}\right)^2 \tag{4.49}$$

The mean and variance of the Gaussian distributed random variable $\tilde{M}(\tau_0)$ are to be determined for phase space flux calculations.

$$\mathrm{E}[\bar{M}(\tau_0)] = \mathrm{E}[\int_{-\infty}^{\infty} y_0(\tau)F_\varepsilon(\tau+\tau_0)d\tau] = \int_{-\infty}^{\infty} y_0(\tau)\mathrm{E}[F_\varepsilon(\tau+\tau_0)]d\tau = 0 \tag{4.50}$$

$$\mathrm{E}[\tilde{M}(\tau_0)^2] = \int_0^{\infty} S_{\tilde{M}\tilde{M}}(\Omega)d\Omega = \int_0^{\infty} 2\pi S_{y_0}(\Omega)S_{F_\varepsilon F_\varepsilon}(\Omega)d\Omega \tag{4.51}$$

4.3.2 The rate of phase space flux

The amount of phase space transported out of the safe basin is related to the areas of lobes formed when the stable manifold is inside of the unstable manifold (Jiang et al., 2000). If the Melnikov function is negative all the time, the stable manifold will be outside of unstable manifold all the time. This means the response will be bounded if they start from inside of safe basin. Fig. 50 is the Melnikov function time series, equation(4.43). With low excitation force $H_s = 1m$, all values are below zero, which

indicates that there is no phase transport. Fig. 51 starts to have some positive value, but still very little. For higher excitation force $H_s = 5m$, Fig. 52 clearly indicates relatively stronger phase transport flux, which means more probability of capsizing even if the vessel starts from the safe basin. The quantity of phase space flux up to first order is measured by the average rate of phase space flux given by (Hsieh et al., 1994):

$$\begin{aligned}\Phi_{flux} &= 2\lim_{T\to\infty}\frac{\varepsilon}{2T}\int_{-T}^{T} M^{+}(\tau_0)d\tau_0 + O(\varepsilon^2) \\ &= 2\lim_{T\to\infty}\frac{\varepsilon}{2T}\int_{-T}^{T} (\tilde{M}(\tau_0)-\bar{M})^{+}d\tau_0 + O(\varepsilon^2)\end{aligned} \tag{4.52}$$

where $M^{+}(\tau_0)$ represents the positive part of Melnikov function. Φ_{flux} is the rate of phase space flux through both upper and lower bound of the heteroclinic orbits. This is because the Melnikov process is an ergodic stationary Gaussian process. The time average in (4.52) is equal to the ensemble average given by

$$\begin{aligned}\Phi_{flux} &= 2\varepsilon \mathrm{E}[(\tilde{M}(\tau_0)-\bar{M})^{+}] = 2\varepsilon\int_{\bar{M}}^{+\infty}(z-\bar{M})\frac{1}{\sqrt{2\pi}\sigma}\exp(-\frac{z^2}{2\sigma^2})dz \\ &= 2\varepsilon\sigma\int_{\bar{M}/\sigma}^{+\infty}(x-\bar{M})\frac{1}{\sqrt{2\pi}}\exp(-\frac{x^2}{2})dx \\ &= 2\varepsilon(\sigma p(\bar{M}\ /\ \sigma)+\bar{M}P(\bar{M}\ /\ \sigma)-\bar{M}) \\ &= 2\varepsilon(H_s\sigma_0 p(\bar{M}\ /\ (H_s\sigma_0))+\bar{M}P(\bar{M}\ /\ (H_s\sigma_0))-\bar{M})\end{aligned} \tag{4.53}$$

where σ is the root mean square of $\tilde{M}(\tau_0)$, and σ is a linear function of the significant wave height, which is $\sigma = \sigma_0 H_s$, σ_0 is the RMS of $\tilde{M}(\tau_0)$ for unit significant wave height. $p(z)$ is the probability density function (PDF) of the standard Gaussian

distributed variable z and $P(z)$ is the Cumulative distribution function (CDF) of z as given by:

$$p(z) = \frac{1}{\sqrt{2\pi}} \exp(-\frac{1}{2} z^2) \tag{4.54}$$

$$P(z) = \int_{-\infty}^{z} p(x)dx \tag{4.55}$$

Φ_{flux} can be normalized by the area of the unperturbed safe basin $A_h = 4\sqrt{2} / 3$ for non dimensionalized oscillators in Fig. 37 as follows:

$$\Phi_{flux} = 2\varepsilon(H_s\sigma_0 p(\bar{M} / (H_s\sigma_0)) + \bar{M}P(\bar{M} / (H_s\sigma_0)) - \bar{M}) \tag{4.56}$$

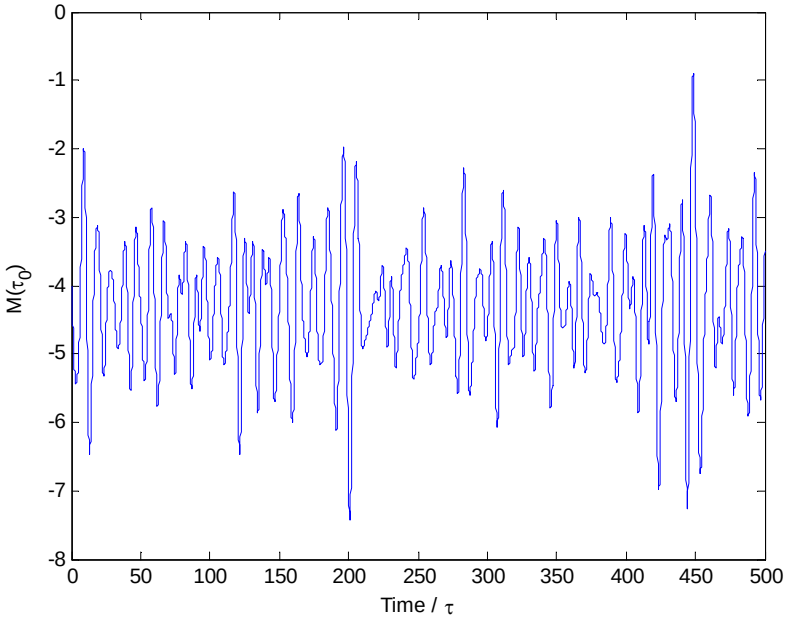

Fig. 50. Melnikov function for $H_s = 1m$

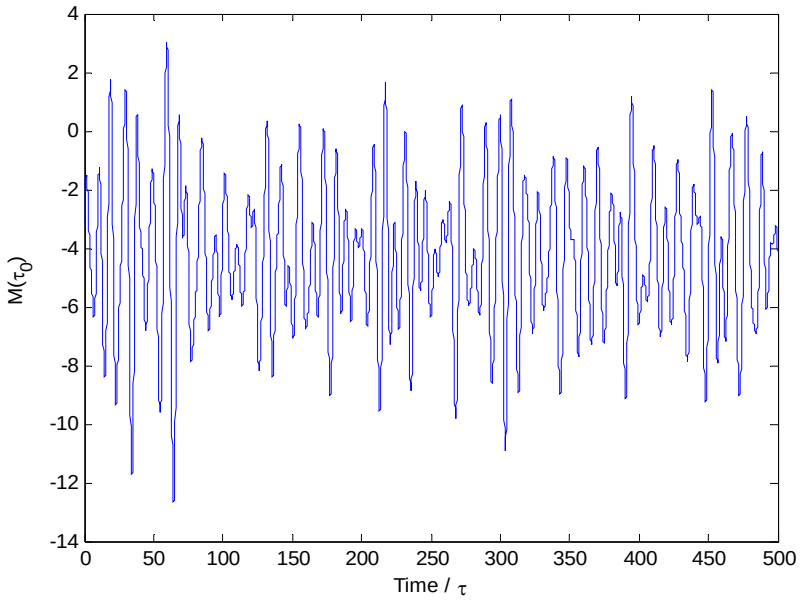

Fig. 51. Melnikov function for $H_s = 3m$

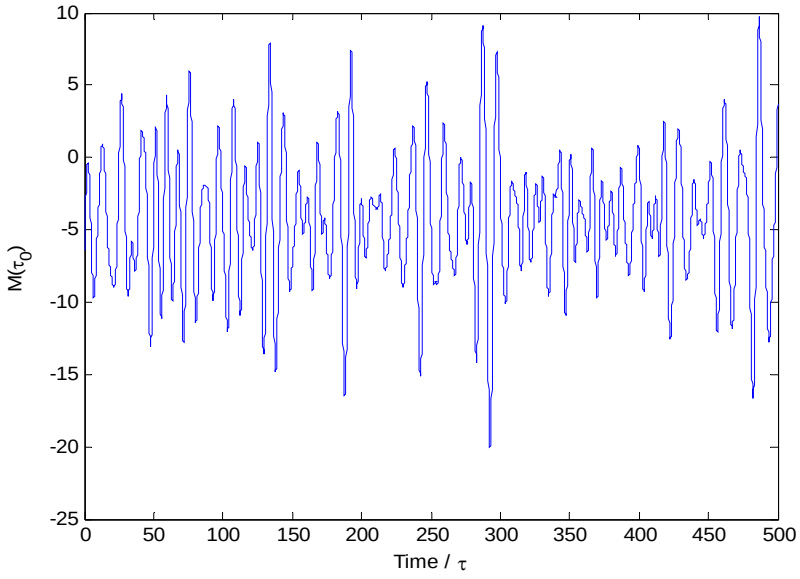

Fig. 52. Melnikov function for $H_s = 5m$

As $H_s \to +\infty$, the normalized phase space flux in equation (4.56) has an asymptotic form given by

$$\frac{\Phi_{flux}}{A_h} = \frac{2\varepsilon}{A_h}\left(\frac{1}{\sqrt{2\pi}} H_s \sigma_0 - \frac{1}{2}\bar{M}\right) \tag{4.57}$$

The asymptotic line intersects with H_s axis at a value

$$H_s^* = \frac{\sqrt{2\pi}\bar{M}}{2\sigma_0} \tag{4.58}$$

In the Melnikov analysis for vessel capsizing criterion, H_s^* is defined as the critical wave height at which substantial phase space flux starts to occur, which indicates higher probability of vessel capsizing.

4.4 Comparison of Two Methods for Analysis of Vessel Capsizing

To compare these two different approaches for vessel capsizing prediction, the inverse of the mean first passage time, which is defined as the escape rate $R_e = 1 / M_1(0)$, based on Markov model is defined as a measurement of capsizing criterion(Roberts and Vasta, 2000), here $M_1(0)$ is the mean first passage time given initial condition $E_0 = 0$. Also normalized phase space flux rate, given in equation (4.56), based on stochastic Melnikov theory was defined as another kind of capsizing criterion in (Hsieh et al., 1994; Jiang et al., 2000). We calculated both mean first passage rate and phase space flux rate in this section to analyze the effects of linear damping coefficients, nonlinear damping coefficients, characteristic wave frequency and significant wave height on both criteria. The purpose of this section is to find some differences and

similarities of capsizing analysis between these two criteria. Equation (4.58) provides a very convenient asymptote of significant wave height for capsizing criterion, which can be estimated that phase space flux will start to significantly occur after this critical value. However, the first passage theory cannot provide such analytical value at which escape will start to significantly occur. The plots given below indicate that both the escape rate and the phase transport rate have similar trends with increasing wave height, the question then become: is there any mathematical connection that can explain these similar trends?

4.4.1 Effects of linear and nonlinear damping coefficients

Both derivations of the Markov and the Melnikov methods mentioned above require very small linear and nonlinear damping coefficients for perturbation analysis, b_1 and b_2 are defined in equation(4.1) and scaled by perturbation parameters. Fig. 53 and Fig. 54 both indicate that the possibility of capsizing from two criteria will increase with significant wave height increasing and linear damping decreasing. This is easily understood when the dynamical system is excited only by additive noise given the same system coefficients (e.g. same mass, stiffness coefficients, etc). The interesting part of Fig. 55 is that both values for escape rate and phase transport rate are of the same order of magnitude, thus it is therefore expected that these two factors can be determined from the other in an approximate sense. The nonlinear damping coefficient for Fig. 53 to Fig. 55 is $b_2 = 0.06$, and wave characteristic frequency $\omega_z = 2\pi / 9$ .Fig. 56 to Fig. 58 demonstrate the nonlinear damping effects on both factors with $b_1 = 0.01$ and

$\omega_z = 2\pi / 9$. They provide similar conclusion as linear damping's effect. However, strong dependence of phase space transport rate on nonlinear damping in Fig. 57 is different with Fig. 56 for the mean escape rate, which has very limited dependency on the nonlinear damping coefficients.

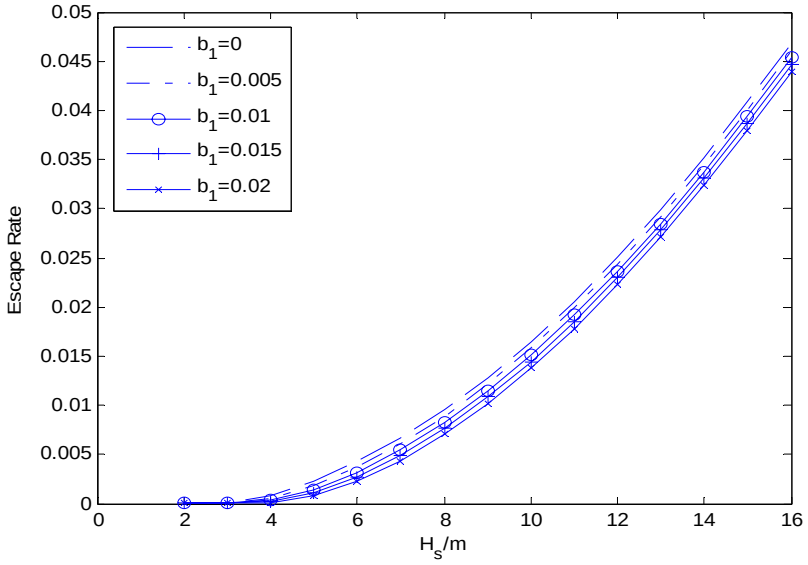

Fig. 53. Mean first passage rate for various linear damping coefficients and H_s

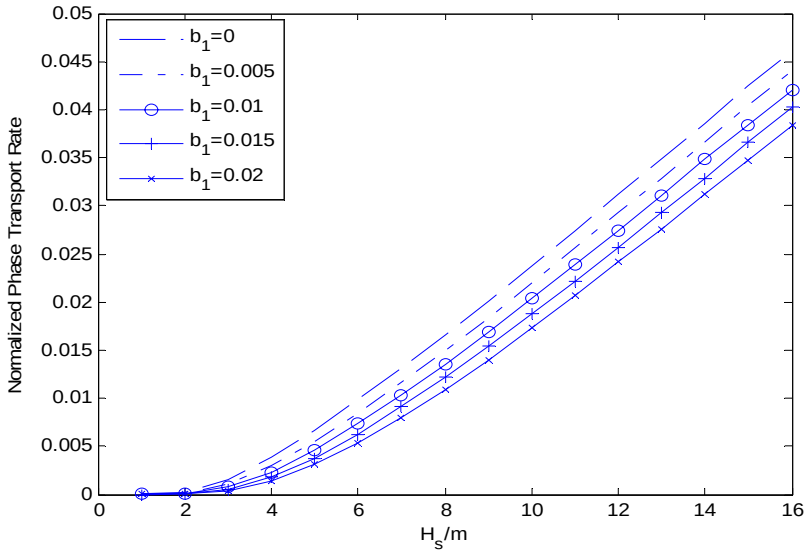

Fig. 54. Normalized phase transport rate for various linear damping coefficients and H_s

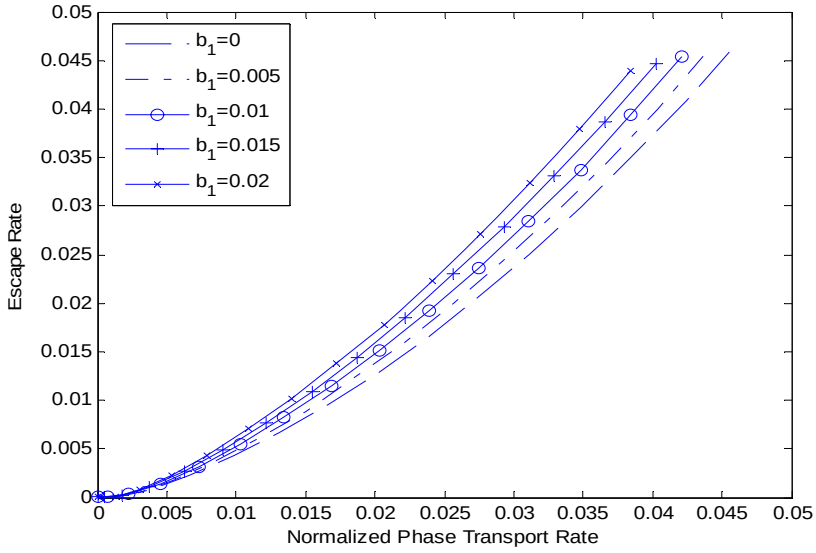

Fig. 55. Relation between normalized phase transport rate and mean first passage rate with different linear damping coefficients

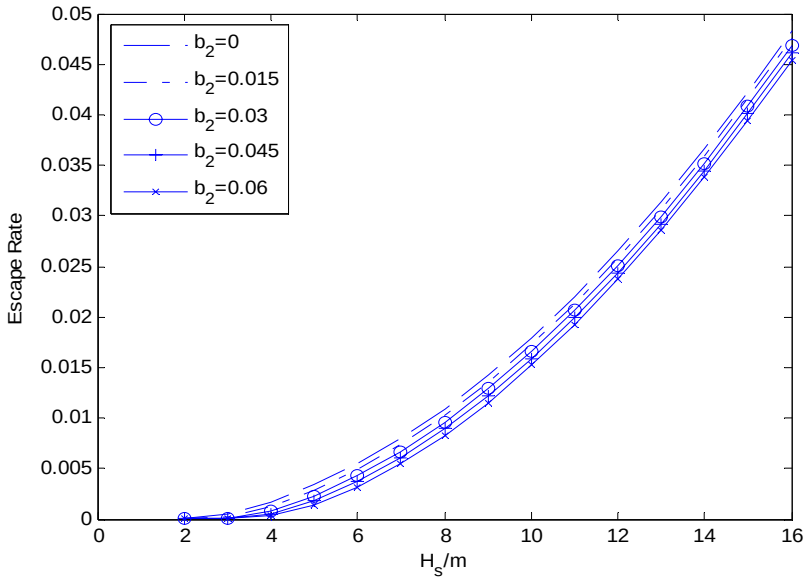

Fig. 56. Mean first passage rate for various nonlinear damping coefficients and H_s

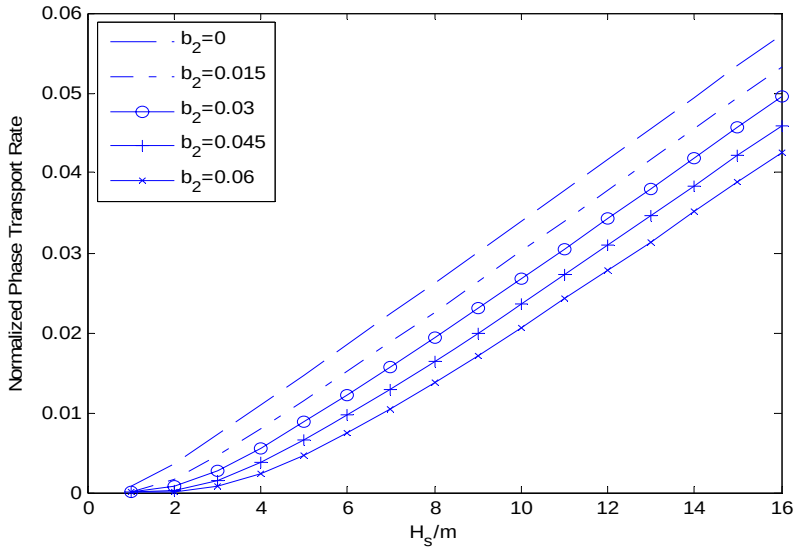

Fig. 57. Normalized phase transport rate for various nonlinear damping coefficients and H_s

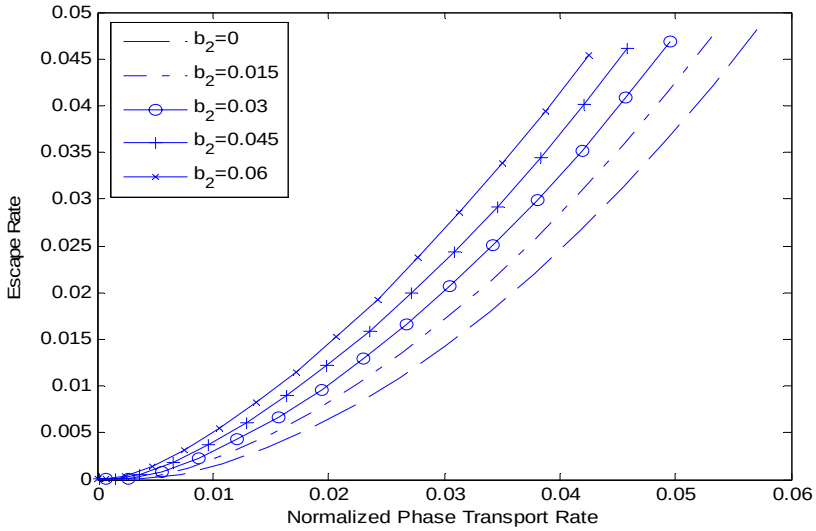

Fig. 58. Relation between normalized phase transport rate and mean first passage rate with different nonlinear damping coefficients

4.4.2 The effect of characteristic wave frequency

The effect of ω_z on the mean escape rate and phase space transport rate are different as compared to the damping effect. For the Markov modeling in Fig. 59, $\omega_z = 2\pi / 5$ gives a larger escape rate than any other characteristic wave frequency. This is consistent with the result from Fig. 43 and Fig. 44, both drift and diffusion coefficients are larger, which means the system will be more easily moved to the critical boundary. However, the Melnikov based phase transport rate has its maximum for $\omega_z = 2\pi / 8$ as displayed in Fig. 60. This can be explained by equation (4.57), the larger

variance σ_0^2 for $\tilde{M}(\tau_0)$ will give larger phase space transport. The variance for different characteristic wave frequency is given in Fig. 61.

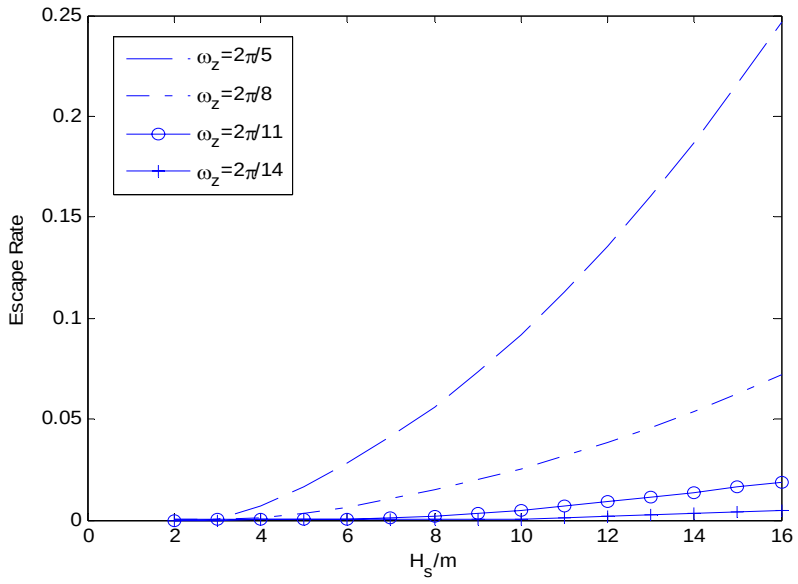

Fig. 59. Mean first passage rate for various characteristic wave frequency and H_s

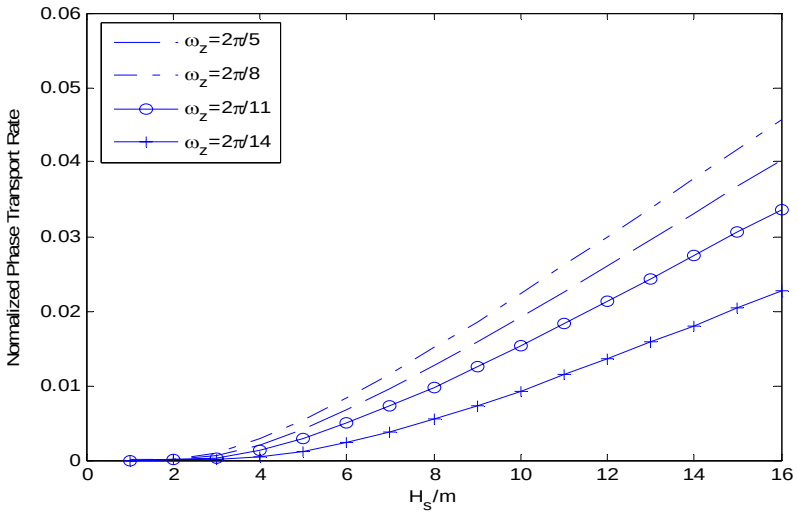

Fig. 60. Normalized phase transport rate for various characteristic wave frequency and H_s

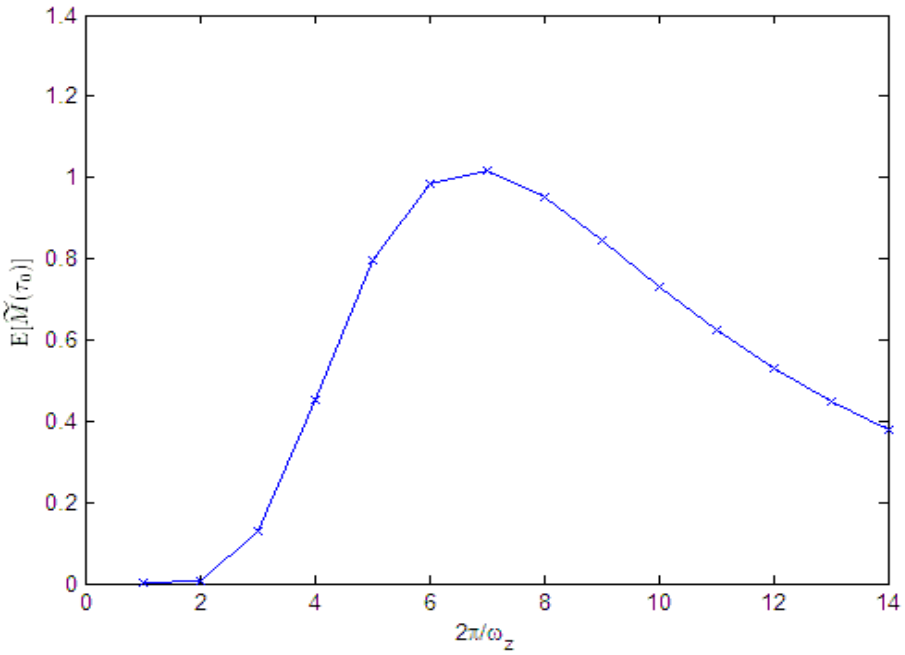

Fig. 61. Variance of $\tilde{M}(\tau_0)$ of unit significant wave height

CHAPTER V

CONCLUSIONS AND FUTURE EXTENSIONS

5.1 Conclusions

The purpose of this research is to understand the strongly nonlinear large amplitude rolling motion response and stability analysis using stochastic analytical techniques. In Chapter I, we first introduced the background and motivation of this dissertation. The next generation of stability criteria will be based on stochastic and probability approaches instead of just considering the static aspects. It is expected that the analytical methods studied and developed in this dissertation will contribute to the next generation of stability criterion. Fundamentals of stochastic dynamics are introduced in the Chapter II, including the history of the Fokker Planck Equation (FPE), fundamentals of Brownian motion and stochastic differential equation, and the derivation of FPE.

In Chapter III and IV, we studied two Markov based method and one Melnikov based method for capsizing criteria. For the shaping filter Markov model in Chapter III, there is no scaling limitation for damping and excitation and no assumption of stationary response process. However, the higher dimensions of the extended system generate more difficulties for the FPE solutions. Instead of solving the FPE directly, an automatic cumulant neglect tool was developed in (Su and Falzarano, 2011) to analyze the higher order dimensional nonlinear roll systems. To verify the algorithm developed in the

dissertation, several dynamical systems, with analytical PDF stationary solution, are tested with the automatic tool, efficiency and limitation of the cumulant neglect method is discussed.

To avoid the difficulty of increasing dimension, stochastic averaging of the energy envelope reduces the dimension to two uncoupled energy and phase first order differential equations, which have an analytical solution for the related stationary FPE and allows us to obtain the mean first passage time easily. The inverse of the mean first passage time is defined as a capsizing criterion. Compared with the shaping filter technique, the stochastic averaging of energy envelope has a more strict limitation on damping and excitation magnitudes.

Instead of studying the energy process of the response, the Melnikov analytical method directly analyzes the energy of the heteroclinic separatrix and the phase space transport rate is defined as a capsizing criterion. The Markov based stochastic averaging method does not have an analytical formula to find the critical wave height for the mean first passage time like Melnikov method in equation (4.58).

5.2 Future Recommendations

The energy Markov process has the same expression as the integral part of the Melnikov function in (4.43). The Melnikov function could be considered as the gained energy through the heteroclinic orbit. When the wave energy input is larger than the damping dissipation energy, the Melnikov function will have positive values and leads to the capsizing region. So stochastic averaging of the energy envelope based on the

Markov process provides information on the mean time to reach the stability boundary which is the heteroclinic orbit. The Melnikov function will predict the dynamical stabilities on the heteroclinic orbit. To relate these two methods, the Melnikov function for suborbit (Wiggins, 2003) of the oscillation has to be considered for the low level of oscillation as the Markov method does.

The shaping filter technique seems to have no assumption on damping and excitation magnitude, the mathematical difficulty is solving the high dimensional stochastic dynamical system. Numerical solution for high dimensional systems, especially high dimensional Fokker Planck Equation, is still a challenge for engineers and scientists, and also a very popular research topic in the field of stochastic dynamics. Also considering the Gaussian property of the filter variables, the number of moment equations could be reduced significantly for the cumulant neglect method. The automatic cumulant neglect tool need to be adjusted to consider the Gaussian property of filter variables.

The moment statistics information from this analytical moment equations could possibly be used to guide the real engineering design problem, e.g., model testing data statistics and numerical simulations. And reversely, the numerical simulation or model testing could also be used to refine and validate the methodology derived in the moment equation method.

Monte Carlo simulation of stochastic dynamical system is the most fundamental method to verify the true response distribution and extreme statistics. The challenge of applying the Monte Carlo method is the long computation time and the difficulty of

predicting the extreme or rare event. With the development of computational capacity and efficient simulation algorithm, the obstacle could be possibly avoided in the future.

Modeling of vessel rolling dynamics in beam waves is simplified to a single degree freedom system in this dissertation, multiple degree of freedom modeling with the time domain convolution term in random seas and also the random parametric rolling dynamics in following and heading seas should be considered as next research direction.

REFERENCES

Abkowitz, M. A., 1969. Stability and Motion Control of Ocean Vehicles, MIT Press, Cambridge, MA

Andronov, A., Pontryagin, L. and Vitt, A., 1933. On the statistical investigation of dynamical systems. Journal of Experimental and Theoretical Physics 3(3), 165-180.

ANSYS, 2010. ANSYS Aqwa User's Manual, ANSYS Inc, Canonsburg, PA

Bachelier, L., 1900. Théorie de la spéculation. English Translation: In: Cootner P.H., 1965. The Random Character of Stock Market Prices, MIT Press, Cambridge, MA, 17-78.

Beck, F. B. and Troesch, A. W., 1990. Documentation and user's manual for the computer program Shipmo, Department of Naval Architecture and Marine Engineering, The University of Michigan, Ann Arbor.

Belenky, V., de Kat, J. O. and Umeda, N., 2008. Toward performance-based criteria for intact stability. Marine Technology, 45(2), 101-120.

Belenky, V. and Sevastianov, N. B., 2007. Stability and Safety of Ships - Risk of Capsizing (2nd Edition), Society of Naval Architects and Marine Engineers (SNAME), Jersey City, NJ.

Belenky, V., Yu, H. C. and Weems, K., 2006. Numerical procedures and practical experience of assessment of parametric roll of container carriers. In: Proceeding of International Conference on Stability of Ships and Ocean Vehicles (STAB-2006). Rio de Janeiro, Brazil, September 22-29, 2006.

Beran, M., 1965. Statistical continuum theories. Transactions of the Society of Rheology, 9(1): 339-355.

Bikdash, M., Balachandran, B. and Navfeh, A., 1994. Melnikov analysis for a ship with a general roll-damping model. Nonlinear Dynamics, 6(1), 101-124.

Boltzmann, L., 1868. Studien über das Gleichgewicht der lebendigen Kraft zwischen bewegten materiellen Punkten [in German].Wiener Berichte, 58, 517-560.

Cardo, A., 1981. Ultraharmonics and subharmonics in the rolling motion of a ship: steady-state solution. International Shipbuilding Progress, 28(326), 234-251.

Cardo, A., Francescutto, A. and Nabergoj, R., 1984. Subharmonic oscillations in nonlinear rolling. Ocean Engineering, 11(6), 663-669.

Caughey, T. K., 1963a. Derivation and application of the fokker-planck equation to discrete nonlinear dynamic systems subjected to white random excitation. The Journal of the Acoustical Society of America, 35(11), 1683-1692.

Caughey, T. K., 1963b. Equivalent linearization techniques. The Journal of the Acoustical Society of America, 35(11), 1706-1711.

Caughey, T. K. and Dienes, J. K., 1961. Analysis of a nonlinear first-order system with a white noise input. Journal of Applied Physics, 32(11), 2476-2479.

Chen, S. L., 1999. A systematic approach to modeling nonlinear multi-DOF ship motions in regular seas. Journal of Ship Research, 43(1), 25-37.

Cottone, G., Di Paola, M., Ibrahim, R., Pirrotta, A. and Santoro, R., 2009. Ship roll motion under stochastic agencies using path integral method. Editor: R. Ibrahim, V. Babitsky and M. Okuma, Vibro-Impact Dynamics of Ocean Systems and Related Problems. Springer, Berlin, 44, 29-40.

Crandall, S. H. and Mark, W. D., 1963. Random Vibration in Mechanical Systems. Academic Press, New York.

Cummins, W. E., 1962. The Impulse Response Function and Ship Motions. Report 1661, Dept. of the Navy, David Taylor Model Basin, Washington, D.C .

Dalzell, J. F., 1978. A note on the form of ship roll damping. Journal of Ship Research, 22, 178-185.

Di Paola, M. and Sofi, A., 2002. Approximate solution of the Fokker-Planck-Kolmogorov equation. Probabilistic Engineering Mechanics, 17(4), 369-384.

Einstein, A., 1905. Über die von der molekularkinetischen Theorie der Wärme geforderte Bewegung von in ruhenden Flüssigkeiten suspendierten Teilchen [in German]. Annalen Der Physik, 322(8), 549-560.

Er, G. K., 1998. An improved closure method for analysis of nonlinear stochastic systems. Nonlinear Dynamics, 17(3), 285-297.

Er, G.-K., 2000a. Exponential closure method for some randomly excited non-linear systems. International Journal of Non-Linear Mechanics, 35(1), 69-78.

Er, G. K., 2000b. The probabilistic solutions to nonlinear random vibrations of multi-

degree-of-freedom systems. Journal of Applied Mechanics-Transactions of the ASME, 67(2), 355-359.

Er, G. K., 2011. Methodology for the solutions of some reduced Fokker-Planck equations in high dimensions. Annalen Der Physik. 523(3), 247-258.

Falzarano, J., 1990. Predicting Complicated Dynamics Leading To Vessel Capsizing. Ph.D. dissertation, Department of Naval Architecture, University of Michigan, Ann Arbor.

Falzarano, J., Shaw, S. W. and Troesch, A. W., 1992. Application of global methods for analyzing dynamical systems to ship rolling motion and capsizing. International Journal of Bifurcation and Chaos, 2(1), 101-115.

Falzarano, J., Vishnubhotla, S. and Cheng, J., 2004. Nonlinear dynamic analysis of ship capsizing in random waves. In: Proceedings of the Fourteenth International Offshore and Polar Engineering Conference, Vol 3, 479-484.

Falzarano, J. and Zhang, F., 1993. Multiple degree of freedom global analysis of transient ship rolling motion. Symposium on Nonlinear Dynamics of Marine Vehicles. In: Proceedings of the ASME Winter Annual Meeting, New Orleans, LA, 57-72

Falzarano, J. M., Vishnubhotla, S. and Juckett, S. E., 2005. Combined steady state and transient analysis of a patrol vessel as affected by varying amounts of damping and periodic and random wave excitation. in: Proceedings of the 24th International Conference on Offshore Mechanics and Arctic Engineering, Vol 1, Pts A and B, 1081-1085.

Fokker, A. D., 1913. Over Brown'sche bewegingen in het stralingsveld [in German], Ph.D. Dissertation, Leiden Unversity, Netherlands.

Fokker, A. D., 1914. Die mittlere Energie rotierender elektrischer Dipole im Strahlungsfeld [in German]. Ann. Phys. Annalen der Physik, 348(5), 810-820.

Francescutto, A., 1990. On the nonlinear motions of ships and structures in narrow band sea. In: Proceedings of the IUTAM Symp. on Dynamics of Marine Vehicles and Structures in Waves, London, Elsevier Publishing, 291-304.

Francescutto, A. and Naito, S., 2004. Large amplitude rolling in a realistic sea. International Shipbuilding Progress, 51(2), 221-235.

Frey, M. and Simiu, E., 1993. Noise-induced chaos and phase space flux. Physica D, Nonlinear Phenomena, 63(3–4), 321-340.

Froude, W., 1861. On the rolling of ships. Institution of Naval Architects Transactions, 11, 180-229.

Fuller, A. T., 1969. Analysis of nonlinear stochastic systems by means of Fokker-Planck equation. International Journal of Control, 9(6), 603-655.

Guckenheimer, J. and Holmes, P., 1983. Nonlinear Oscillations, Dynamical Systems, and Bifurcations of Vector Fields, Springer Verlag, New York.

Holappa, K. W. and Falzarano, J. M., 1999. Application of extended state space to nonlinear ship rolling. Ocean Engineering, 26(3), 227-240.

Hsieh, S.-R., Troesch, A. W. and Shaw, S. W., 1994. A nonlinear probabilistic method for predicting vessel capsizing in random beam seas. Transactions of the Royal Society of London Series A-Mathematical and Physical Sciences, 446(1926), 195-211.

Huang, X., 2003. The invesitigation of the safe basin erosion under the action of irregular waves. In: Proceedings of the 8th International Conference on Stability of Ship and Ocean Vehicles (STAB), Madrid, Spain, September, 2003, 539-549.

Huang, X., 2004. The study of ship capsize on random beam waves. In: Proceedings of the 7th International Ship Stability Workshop, Shanghai, China, November 2004, 330-338.

Ibrahim, R. A., 2007. Parametric Random Vibration. Dover Publications, Mineola, NY.

Ibrahim, R. A. and Grace, I. M., 2010. Modeling of ship roll dynamics and its coupling with heave and pitch. Mathematical Problems in Engineering,Vol 2010, 1-32.

Itô, K., 1951. On a formula concerning stochastic differentials. Nagoya Math Journal, 3, 55-65.

Jamnongpipatkul, A., Su, Z. and Falzarano, J. M., 2011. Nonlinear ship rolling motion subjected to noise excitation. Ocean Systems Engineering, 1(3), 33-43.

Jiang, C., Troesch, A. W. and Shaw, S. W., 2000. Capsize criteria for ship models with memory-dependent hydrodynamics and random excitation. Philosophical Transactions of the Royal Society of London Series A-Mathematical Physical and Engineering Sciences, 358(1771),1761-1791.

Jiang, C. B., Troesch, A. W. and Shaw, S. W., 1996. Highly nonlinear rolling motion of biased ships in random beam seas. Journal of Ship Research, 40(2), 125-135.

Khasminskii, R. Z., 1966. A limit theorem for the solutions of differential equations with random right-hand sides. Theory of Probability and its Applications, 11(3), 390-406.

Kim, C. H., 2008. Nonlinear Waves and Offshore Structures, World Scientific Publishing Company, Hackensack, NJ.

Kolmogoroff, A., 1931. Über die analytischen methoden in der wahrscheinlichkeitsrechnung. English Translation: On analytical methods in probability theory, Mathematische Annalen [in German]. 104(1), 415-458.

Kolmogorov, A. N., 1933. Grundbegriffe der wahrscheinlichkeitsrechnung, English Translation: Foundations of the Theory of Probability. Springer, Berlin.

Kumar, M., Chakravorty, S. and Junkins, J. L., 2010. A semianalytic meshless approach to the transient Fokker-Planck equation. Probabilistic Engineering Mechanics, 25(3), 323-331.

Kumar, P. and Narayanan, S., 2006. Solution of Fokker-Planck equation by finite element and finite difference methods for nonlinear systems. Sadhana-Academy Proceedings in Engineering Sciences, 31, 445-461.

Lee, C.-H. and Newman, J. N., 2009. WAMIT Theory Manual, Massachusetts Institute of Technology.

Lewandowski, E. M., 2004. The Dynamics of Marine Craft : Maneuvering and Seakeeping. World Scientific Publishing Company, Hackensack, NJ.

Lewis, E. V.,1989. Principles of Naval Architecture, Society of Naval Architects and Marine Engineers, Jersey City, NJ.

Lin, H. and Yim, S. C. S., 1995. Chaotic roll motion and capsize of ships under periodic excitation with random noise. Applied Ocean Research, 17(3), 185-204.

Lin, H. A. and Yim, S. C. S., 1995. Chaotic roll motion and capsize of ships under periodic excitation with random noise. Applied Ocean Research, 17(3), 185-204.

Lin, Y. K. and Cai, G. Q., 2004. Probabilistic Structural Dynamics: Advanced Theory and Applications. McGraw-Hill, New York.

Liqin, L. and Yougang, T., 2007. Stability of ships with water on deck in random beam waves. Journal of Vibration and Control, 13(3), 269-280.

Lutes, L. D., 1970. Approximate technique for treating random vibration of hysteretic systems. The Journal of the Acoustical Society of America, 48(1B), 299-306.

Lutes, L. D. and Sarkani, S., 2004. Random Vibrations: Analysis of Structural and Mechanical Systems. Elsevier, Boston, MA.

Martens, W. and Wagner, U. v., 2011. Advances in solving high dimensional Fokker-Planck equations. In: Proceedings of the European Nonlinear Oscillations Conferences, 2011, Rome, Italy.

Maxwell, J. C., 1860. Illustrations of the dynamical theory of gases. Philosophical Magazine, 20 (130), 21-37.

Maxwell, J. C., 1867. On the dynamical theory of gases. Philosophical Transactions of the Royal Society of London, 157, 49-88.

Moe, V., 1997. Nonlinear Random Vibrations - Numerical Analysis by Path Integration Methods. Ph.D. dissertation, Norwegian University of Science and Technology, Norway.

Moseley, H., 1850. On the dynamical stability and on the oscillations of floating bodies. Philosophical Transactions of the Royal Society of London, 140, 609-643.

Naess, A. and Moe, V., 2000. Efficient path integration methods for nonlinear dynamic systems. Probabilistic Engineering Mechanics, 15(2), 221-231.

Nayfeh, A. H., 1986a. Nonlinear rolling of biased ships in regular beam waves. International Shipbuilding Progress, 33(381), 84-93.

Nayfeh, A. H., 1986b. Nonlinear rolling of ships in regular beam seas. International Shipbuilding Progress. 33(379), 40-49.

Nayfeh, A. H., 1990. Stability and complicated rolling responses of ships in regular beam seas. International Shipbuilding Progress. 37(412), 331-352.

Ness, O. B., McHenry, G., Mathisen, J. and Winterstein, S. R., 1989. Nonlinear analysis of ship rolling in random beam waves. In: Proceedings of SNAME STAR Symposium, New Orleans,LA, 49-66.

Ogilvie, T., 1964. Recent progress towards the understanding and prediction of ship motions. In: Proceedings of the 5th Symposium on Naval Hydrodynamics, Bergen, Norway, 3-79.

Planck, M., 1917. Zur theorie des rotationsspektrums [in German]. Ann. Phys. Annalen der Physik, 358(11), 241-256.

Rahola, J., 1939. The judging of the stability of ships and the determination of the

minimum amount of stability, especially considering the vessels navigating Finnish waters, Ph.D. dissertation, University of Finland, Finland.

Rayleigh, L., 1880. On the resultant of a large number of vibrations of the same pitch and of arbitrary phase. Philosophical Magazine, 10, 73-78.

Rayleigh, L., 1891. Dynamical problems in illustration of the theory of gases. Philosophical Magazine, 32(5), 424.

Risken, H., 1996. The Fokker-Planck Equation: Methods of Solution and Applications, Springer, New York.

Roberts, J. B., 1982. Effect of parametric-excitation on ship rolling motion in random waves. Journal of Ship Research, 26(4), 246-253.

Roberts, J. B., 1982. A stochastic-theory for non-linear ship rolling in irregular seas. Journal of Ship Research, 26(4), 229-245.

Roberts, J. B., 1986. Response of an oscillator with non-linear damping and a softening spring to non-white random excitation. Probabilistic Engineering Mechanics, 1(1), 40-48.

Roberts, J. B., Dunne, J. F. and Debonos, A., 1994. Stochastic estimation methods for nonlinear ship roll motion. Probabilistic Engineering Mechanics, 9(1-2), 83-93.

Roberts, J. B. and Spanos, P. D., 1986. Stochastic averaging - an approximate method of solving random vibration problems. International Journal of Non-Linear Mechanics, 21(2), 111-134.

Roberts, J. B. and Spanos, P. D., 2003. Random Vibration and Statistical Linearization. Dover Publications, Mineola, NY.

Roberts, J. B. and Vasta, M., 2000. Markov modelling and stochastic identification for nonlinear ship rolling in random waves. Philosophical Transactions of the Royal Society of London Series A-Mathematical Physical and Engineering Sciences, 358(1771), 1917-1941.

Roberts, J. B. and Vasta, M., 2000. Parametric identification of systems with non-Gaussian excitation using measured response spectra. Probabilistic Engineering Mechanics, 15(1), 59-71.

Roberts, J. B. and Vasta, M., 2001. Response of non-linear oscillators to non-white random excitation using an energy based method. In: the Proceedings of the IUTAM Symposium on Nonlinearity and Stochastic Structural Dynamics, 85, 221-231.

Roberts, J. B. and Vasta, M., 2002. Energy based stochastic estimation of nonlinear oscillators with parametric random excitation. Meccanica, 37(1-2), 33-49.

Scheurkogel, A. and Elishakoff, I., 1988. Non-linear random vibration of a two-degree-of-freedom system. In: the proceedings IUTAM Symposium on Non Linear Stochastic Engineering Systems, Springer-Verlag, Berlin. 285-299.

SLF50/4, 2006. Revision of the intact stability code. Report of the working group on intact stability at SLF49 (part 2). Submitted by the chairman of the working group. 50st session of IMO Sub-Committee on Stability and Load Lines and on Fishing Vessels Safety.

SLF51/4, 2008. Revision of the intact stability code. report of the working group (part 2). Submitted by the chairman of the working group. 51st session of IMO Sub-Committee on Stability and Load Lines and on Fishing Vessels Safety.

SLF52/3, 2009. Revision of the intact stability code. report of the working group (part 2). Submitted by the chairman of the working grou. 52st session of IMO Sub-Committee on Stability and Load Lines and on Fishing Vessels Safety.

Sobczyk, K. and Trcebicki, J., 1999. Approximate probability distributions for stochastic systems, maximum entropy method. Computer Methods in Applied Mechanics and Engineering, 168(1-4), 91-111.

Soize, C., 1994. The Fokker-Planck Equation for Stochastic Dynamical Systems and Its Explicit Steady State Solutions. World Scientific, Teaneck, NJ.

Soong, T. T. and Grigoriu, M., 1993. Random Vibration of Mechanical and Structural Systems. PTR Prentice Hall, Englewood Cliffs, NJ.

Spanos, P. T. D., 1983. ARMA algorithms for ocean wave modeling. Journal of Energy Resources Technology, 105(3), 300-309.

Spanos, P. T. D., 1986. Filter approaches to wave kinematics approximation. Applied Ocean Research, 8(1), 2-7.

Spencer, B. F. and Bergman, L. A., 1993. On the numerical solution of the Fokker-Planck equation for nonlinear stochastic systems. Nonlinear Dynamics, 4(4), 357-372.

Spyrou, K. J., 1996a. Dynamic instability in quartering seas: The behavior of a ship during broaching. Journal of Ship Research, 40(1), 46-59.

Spyrou, K. J., 1996b. Dynamic instability in quartering seas: Analysis of ship roll and

capsize for broaching. Journal of Ship Research, 40(4), 326-336.

Spyrou, K. J., 1997. Dynamic instability in quartering seas: Nonlinear effects on periodic motions. Journal of Ship Research, 41(3), 210-223.

Stark, H. and Woods, J. W., 2002. Probability and Random Processes with Applications to Signal Processing. Prentice Hall, Upper Saddle River, NJ.

Stratonovich, R. L., 1963. Topics in the Theory of Random Noise. Gordon and Breach, New York.

Su, Z. and Falzarano, J. M., 2011. Gaussian and non-Gaussian cumulant neglect application to large amplitude rolling in random waves. International Shipbuilding Progress, 58(2), 97-113.

Su, Z. and Falzarano, J. M., 2011. Gaussian and non Gaussian response of ship rolling in random beam waves. In: Proceedings of the12th International Ship Stability Workshop, Washington D.C., USA, June 12-15, 2011. 189-193.

Thampi, S. K. and Niedzwecki, J. M., 1992. Filter approach to ocean structure response prediction. Applied Ocean Research, 14(4), 259-271.

Thompson, J. M. T., 1990. Ship stability criteria based on chaotic transients from incursive fractals. Philosophical Transactions of the Royal Society of London Series A-Mathematical Physical and Engineering Sciences, 332(1624), 149-167.

Thompson, J. M. T., 1992. Mechanics of ship capsize under direct and parametric wave excitation. Philosophical Transactions of the Royal Society of London Series A-Mathematical Physical and Engineering Sciences, 338(1651), 471-490.

To, C. W. S., 2000. Nonlinear Random Vibration: Analytical Techniques and Applications, Swets & Zeitlinger Publishers, London, UK.

Uhlenbeck, G. E. and Ornstein, L. S., 1930. On the theory of the brownian motion. Physical Review, 36(5), 823-841.

Ultramarine, 2010. Reference Manual for MOSES.Ultramarine, Inc, Houston,TX.

Virgin, L. N., 1987. The nonlinear rolling response of a vessel including chaotic motions leading to capsize in regular seas. Applied Ocean Research, 9(2), 89-95.

Vishnubhotla, S. and Falzarano, J., 2009. Effect of more accurate hydrodynamic modeling on calculating critical nonlinear ship rolling response. Vibro-Impact Dynamics of Ocean Systems and Related Problems, 44, 269-274.

Vishnubhotla, S., Falzarano, J. and Vakakis, A., 2000. A new method to predict vessel/platform critical dynamics in a realistic seaway. Philosophical Transactions of the Royal Society of London Series A-Mathematical Physical and Engineering Sciences, 358(1771), 1967-1981.

Vugts, J. H., 1970. The hydrodynamic forces and ship motions in waves. Ph.D. dissertation, University of Waltman, Delft.

Wang, M. C. and Uhlenbeck, G. E., 1945. On the theory of the brownian motion II. Reviews of Modern Physics. 17(2-3), 323-342.

Wiggins, S., 2003. Introduction to Applied Nonlinear Dynamical Systems and Chaos, Springer-Verlag, New York.

Winterstein, S. R., 1988. Nonlinear vibration models for extremes and fatigue. Journal of Engineering Mechanics, 114(10), 1772-1790.

Wojtkiewicz, S. F., 2000. Contributions to the Computational Analysis of Multi-Dimensional Stochastic Dynamical Systems. Ph.D. dissertation, Aeronautical and Astronautical Engineering, University of Illinois at Urbana-Champaign.

Wong, E. and Zakai, M., 1964. On the relation between ordinary and stochastic differential equations. International Journal of Engineering, 3, 213-229.

Wu, W. and McCue, L., 2008. Application of the extended Melnikov's method for single-degree-of-freedom vessel roll motion. Ocean Engineering, 35(17-18), 1739-1746.

Yim, S. C. S., Nakhata, T. and Huang, E. T., 2005. Coupled nonlinear barge motions, Part II, Stochastic models and stability analysis. Journal of Offshore Mechanics and Arctic Engineering, Transactions of the ASME, 127(2), 83-95.

Zhang, F. and Falzarano, J., 1994. Multiple degree of freedom global transient ship rolling motion: large amplitude forcing. In: The proceedings of Stochastic Dynamics and Reliability of Nonlinear Ocean Systems, Chicago, Illinois, 99-108.

Zhu, W. Q., 1988. Stochastic averaging methods in random vibration. Applied Mechanics Reviews, 41(5), 189-199.

APPENDIX A

DERIVATION OF NONLINEAR COUPLED EQUATIONS OF MOTION

Equations (1.1) to (1.6) are derived in this Appendix following (Abkowitz, 1969). Newton's law for a particle can be directly applied to the "rigid body" ship for both linear momentum and angular momentum equations:

$$\vec{F} = \frac{d(Momentum)}{dt} = \frac{d(m\vec{U}_G)}{dt} \tag{A.1}$$

$$\vec{\mathrm{M}}_G = \frac{d(Angular\ momentum)}{dt} = \frac{d(\vec{I}\vec{\Omega})_G}{dt} \tag{A.2}$$

where $\vec{F}$ is the resultant of all external force; m is the mass of ship; $\vec{U}_G$ is the velocity of the center of gravity; $\vec{\mathrm{M}}_G$ is the resultant of the applied moments; $\vec{I}$ is moment of inertial about the body fixed coordination system.

For the origin not at the center of the gravity and in a system of axes fixed in and moving with the vehicle.

$$\vec{U}_G = \vec{U} + \Omega \times \vec{R}_G \tag{A.3}$$

Ω is the angular velocity of the body about the origin of body fixed system; $\vec{R}_G$ is the vector distance of the gravity from the origin of body fixed system; $\vec{U}$ is the velocity of the origin; $\times$ is the cross product.

The definitions of above qualities are given as follows,

$$\vec{U} = u\vec{i} + v\vec{j} + w\vec{k} \tag{A.4}$$

$$\vec{\Omega} = p\vec{i} + q\vec{j} + r\vec{k} \tag{A.5}$$

$$\vec{R}_G = x_G\vec{i} + y_G\vec{j} + z_G\vec{k} \tag{A.6}$$

$$\vec{F} = X\vec{i} + Y\vec{j} + Z\vec{k} \tag{A.7}$$

$$\vec{\mathrm{M}} = K\vec{i} + M\vec{j} + N\vec{k} \tag{A.8}$$

Substituting the above expressions back to (A.1), we get,

$$\begin{aligned} X\vec{i} + Y\vec{j} + Z\vec{k} &= m\frac{d\vec{U}}{dt} + m\frac{d(\Omega \times \vec{R}_G)}{dt} \\ &= m\dot{\vec{U}} + m(\dot{\Omega} \times \vec{R}_G) + m(\Omega \times \dot{\vec{R}}_G) \end{aligned} \tag{A.9}$$

Considering the unit vector derivative with respect to time, we have following expressions,

$$\frac{d\vec{i}}{dt} = r\vec{j} - q\vec{k} \tag{A.10}$$

$$\frac{d\vec{j}}{dt} = p\vec{k} - r\vec{i} \tag{A.11}$$

$$\frac{d\vec{k}}{dt} = q\vec{i} - p\vec{j} \tag{A.12}$$

$$\begin{aligned} \dot{\vec{U}} &= \frac{d}{dt}(u\vec{i} + v\vec{j} + w\vec{k}) = \dot{u}\vec{i} + u\frac{d\vec{i}}{dt} + \dot{v}\vec{j} + v\frac{d\vec{j}}{dt} + \dot{w}\vec{k} + w\frac{d\vec{k}}{dt} \\ &= (\dot{u} + qw - rv)\vec{i} + (\dot{v} + ru - pw)\vec{j} + (\dot{w} + pv - qu)\vec{k} \end{aligned} \tag{A.13}$$

$$\begin{aligned} \dot{\vec{R}}_G &= \frac{d}{dt}(x_G\vec{i} + y_G\vec{j} + z_G\vec{k}) = x_G\frac{d\vec{i}}{dt} + y_G\frac{d\vec{j}}{dt} + z_G\frac{d\vec{k}}{dt} \\ &= (z_Gq - y_Gr)\vec{i} + (x_Gr - z_Gp)\vec{j} + (y_Gp - x_Gq)\vec{k} \end{aligned} \tag{A.14}$$

$$\dot{\Omega} = \frac{d}{dt}(p\vec{i} + q\vec{j} + r\vec{k}) = \dot{p}\vec{i} + \dot{q}\vec{j} + \dot{r}\vec{k} \tag{A.15}$$

Substituting the equations (A.10) to (A.15) back to the force expression (A.9), we get,

$$X = m[\dot{u} + qw - rv - x_G(q^2 + r^2) + y_G(pq - \dot{r}) + z_G(pr + \dot{q})] \tag{A.16}$$

$$Y = m[\dot{v} + ru - pw + x_G(pq + \dot{r}) - y_G(r^2 + p^2) + z_G(qr - \dot{p})] \tag{A.17}$$

$$Z = m[\dot{w} + pv - qu + x_G(rp - \dot{q}) + y_G(rq + \dot{p}) - z_G(p^2 + q^2)] \tag{A.18}$$

The above equations for X Y Z components are for an origin not at the center of gravity. Practically, $y_G = 0$ for most ships and offshore structures, therefore we get the equations (1.1) ,(1.2) and (1.3) in Chapter I.

For the origin not at the center of gravity, the moment expression becomes,

$$\vec{\mathrm{M}} = \vec{\mathrm{M}}_G + \vec{R}_G \times \vec{F} \tag{A.19}$$

Following equation (A.2),

$$\begin{aligned}(\vec{I}\vec{\Omega})_G &= \begin{pmatrix} I_{G44} & -I_{G45} & -I_{G46} \\ -I_{G54} & I_{G55} & -I_{G56} \\ -I_{G64} & -I_{G65} & I_{G66} \end{pmatrix}\begin{pmatrix} p \\ q \\ r \end{pmatrix} \\ &= (I_{G44}p - I_{G45}q - I_{G46}r)\vec{i} + (-I_{G54}p + I_{G55}q - I_{G56}r)\vec{j} \\ &\quad + (-I_{G64}p - I_{G65}q + I_{G66}r)\vec{k}\end{aligned} \tag{A.20}$$

where $I_{G..}$ indicates the inertial moments are refer to the origin at the center of gravity. The relationship between different local coordination systems for moment of inertial are given by equation (A.20). The I_{44}, I_{55} and I_{66}, refer to the moment of inertia about the body fixed coordination system with origin at arbitrary point.

$$\begin{cases} I_{G44} = I_{44} - m(y_G^2 + z_G^2) \\ I_{G55} = I_{55} - m(z_G^2 + x_G^2) \\ I_{G66} = I_{66} - m(x_G^2 + y_G^2) \\ I_{G45} = I_{45} - mx_G y_G \\ I_{G56} = I_{56} - my_G z_G \\ I_{G64} = I_{64} - mz_G x_G \end{cases} \tag{A.21}$$

Substituting the equation (A.21) back into (A.20), and using the angular moment equation (A.2), we will be able to get the moments expressions,

$$\vec{\mathrm{M}}_G = K_G\vec{i} + M_G\vec{j} + N_G\vec{k} \tag{A.22}$$

The second term in the equation (A.19) is given by,

$$\vec{R}_G \times \vec{F} = (y_G Z - z_G Y)\vec{i} + (z_G X - x_G Z)\vec{j} + (x_G Z - y_G Y)\vec{k} \tag{A.23}$$

Substituting the equation (A.23) back to (A.19), moments about the body fixed system can be calculated by,

$$\begin{cases} K = K_G + (y_G Z - z_G Y) \\ M = M_G + (z_G X - x_G Z) \\ N = N_G + (x_G Z - y_G Y) \end{cases} \tag{A.24}$$

Equation (A.24) is totally same with the equation (1.4), (1.5) and (1.6) Chapter I, after considering the symmetry property of ships, y_G=0; $I_{45} = I_{56}$=0.

APPENDIX B

DERIVATION OF THE DRIFT AND DIFFUSION COEFFICIENTS FOR STOCHASTIC AVERAGING

Deriving the drift and diffusion coefficients in the equation (4.27) and (4.28) is the most important step to apply Markov assumption to the rolling process of the energy envelope. Following (Lin and Cai, 2004) and (Roberts and Vasta, 2000; Roberts and Vasta, 2002), evaluation of the Markov coefficients are introduced in this Appendix. The first row of equation (4.24) can be re written as below with integration from τ to $\tau + \Delta\tau$:

$$\Delta E(\tau) = -\varepsilon^2 \Lambda_1 \Delta\tau + \int_{\tau}^{\tau+\Delta\tau} \varepsilon \beta_1 F_{\varepsilon}(\tau) du \tag{B.1}$$

The drift coefficient is given by equation (4.19) and can be written as,

$$\begin{aligned} m(E) = \frac{1}{\Delta\tau} \mathrm{E}[\Delta E] &= \frac{1}{\Delta\tau} \mathrm{E}[-\varepsilon^2 \Lambda_1 \Delta\tau + \int_{\tau}^{\tau+\Delta\tau} \varepsilon \beta_1 F_{\varepsilon}(u) du] \\ &= -\varepsilon^2 \Lambda_1 + \frac{\varepsilon}{\Delta\tau} \int_{\tau}^{\tau+\Delta\tau} \mathrm{E}[\beta_1 F_{\varepsilon}(u)] du \end{aligned} \tag{B.2}$$

β_1 could be expanded by its deterministic evolution with ε=0, for $\tau < u < \tau + \Delta\tau$

$$\beta_1(u) = \beta_{1,0}(u) + \left(\frac{\partial \beta_1}{\partial E}\right)_0^u e(u) + \left(\frac{\partial \beta_1}{\partial \Phi}\right)_0^u \theta(u) + \ldots \tag{B.3}$$

Where $\beta_{1,0}(u) = \beta_1(E_0, \Phi_0)$, and $e(u) = E(u) - E_0$, $\theta(u) = \Phi(u) - \Phi_0$ are the perturbation terms about the free undamped solution E_0 and Φ_0; higher order expansion

terms are neglected. So the expansion order is ε. Substituting equation (B.3) back into (B.2), and notice that the first term in equation (B.3) does not contribute to the expectation operator, we obtain,

$$m(E) = -\varepsilon^2 \Lambda_1(E) + I_1 + I_2 \tag{B.4}$$

where

$$I_1 = \frac{\varepsilon}{\Delta\tau} \int_{\tau}^{\tau+\Delta\tau} \left(\frac{\partial \beta_1}{\partial E} \right)_0^u \mathrm{E}[e(u) F_\varepsilon(u)] du \tag{B.5}$$

$$I_2 = \frac{\varepsilon}{\Delta\tau} \int_{\tau}^{\tau+\Delta\tau} \left(\frac{\partial \beta_1}{\partial \Phi} \right)_0^u \mathrm{E}[\theta(u) F_\varepsilon(u)] du \tag{B.6}$$

To evaluate the integral of I_1, $e(u)$ corresponding to the undamped oscillator needs to be obtained by first integrating the energy of the system from τ to u,

$$e(u) = -\varepsilon^2 \int_\tau^u \Lambda_1 dv + \varepsilon \int_\tau^u \beta_{1,0} F_\varepsilon(v) dv \tag{B.7}$$

Considering the order up to ε, the first term on the RHS can be neglected. Combining equations (B.7) and (B.5), and considering the expression for β_1 in (4.13), we get

$$I_1 = \frac{\varepsilon^2}{\Delta\tau} \int_{\tau}^{\tau+\Delta\tau} \int_{\tau}^{u} \left(\frac{\partial \beta_1}{\partial E} \right)_0^u \beta_{1,0}(v) \mathrm{E}[F_\varepsilon(u) F_\varepsilon(v)] dv du \tag{B.8}$$

Considering the correlation function of $F_\varepsilon(u)$, equation (4.3) and the Fourier expansion in (4.29). Refer to (Roberts and Vasta, 2002; Lin and Cai, 2004) for more details of the derivation of the transformation of variables,

$$I_1 = \frac{1}{2} \varepsilon^2 \pi \sum_{n=1,2}^{\infty} {s_n}^2 S_{FF}(n\omega(E)) \tag{B.9}$$

The second integration I_2 could be analyzed in a similar way as the integration I_1. It is necessary to obtain the expressions for the phase increment $\theta(u)$ corresponding to the undamped oscillator by integrating the second row of equation(4.24). Noticed that the variable γ can be substituted by γ_0 based on some approximation proved by Roberts (Roberts and Vasta, 2000).

$$\theta(u) = -\varepsilon^2 \int_{\tau}^{u} \Lambda_2 dv + \varepsilon \int_{\tau}^{u} \beta_{2,0} F_{\varepsilon}(v) dv \tag{B.10}$$

Following the same rule of I_1, I_2 is given by,

$$I_2 = \frac{1}{2}\varepsilon^2 \pi \sum_{n=1,2}^{\infty} {c_n}^2 S_{FF}(n\omega(E)) \tag{B.11}$$

Collecting (B.4), (B.8) and (B.11) and correct to the order ε^2, the drift coefficient is given by,

$$m(E) = -\varepsilon^2 \Lambda_1(E) + \frac{1}{2}\pi \sum_{n=1,2...}^{\infty} ({s_n}^2 + {c_n}^2) S_{FF}(n\omega(E)) \tag{B.12}$$

The diffusion coefficient is given by equation (4.20),

$$\begin{aligned} D(E) = \frac{1}{\Delta\tau}\mathrm{E}[\Delta E^2] &= \frac{1}{\Delta\tau}\int_{\tau}^{\tau+\Delta\tau}\int_{\tau}^{\tau+\Delta\tau} \beta_{1,0}(u)\beta_{1,0}(v)R(u-v)dvdu \\ &= \frac{2E}{\Delta\tau}\int_{\tau}^{\tau+\Delta\tau}\int_{\tau}^{\tau+\Delta\tau} \sin\Phi_0(u)\sin\Phi_0(v)R(u-v)dvdu \end{aligned} \tag{B.13}$$

Combining the Fourier expansion of the $\sin\Phi_0$, the diffusion coefficient can be evaluated as:

$$D(E) = 2\pi E \sum_{n=1,2...}^{\infty} {s_n}^2 S_{FF}(n\omega(E)) \tag{B.14}$$

The rolling motion process under non-white noise can be considered as a Markov process with the drift and diffusion coefficients derived above.

VITA

ZHIYONG SU

The author was born in Handan, Hebei, China. He graduated from Shanghai Jiao Tong University with B.S. and M.S. degree in naval architecture and ocean engineering in 2006 and 2009. After that, he entered the graduate program of Ocean Engineering at Texas A&M University in 2009 for PhD degree with Professor Falzarano. He can be reached at: louder024@gmail.com or through Prof. Falzarano.

Department Address:

Coastal and Ocean Engineering Division

Department of Civil Engineering

Texas A&M University

3136 TAMU

College Station, TX 77843-3136